2006

The role of Src homology 2 domain containing 5' inositol phosphatase 1 (SHIP) in hematopoietic cells

Caroline Desponts
University of South Florida

The Role of Src Homology 2 Domain Containing Inositol-5'-Phosphatase 1 (SHIP) in Hematopoietic Cells

by

Caroline Desponts

A dissertation submitted in partial fulfillment
of the requirements for the degree of
Doctor of Philosophy
Department of Biochemistry and Molecular Biology
College of Medicine
University of South Florida

Major Professor: William G. Kerr, Ph.D.
Huntington Potter Ph.D.
Gary W. Reuther Ph.D.
Kenneth L. Wright Ph.D.

Date of Approval:
June 2, 2006

Keywords: embryonic stem cell, hematopoietic stem cell, NK cells, megakaryocytes, hematopoiesis, s-SHIP

Dedication

In loving memory of Joseph McIntosh MD, who touched everybody's life with his generosity, talent, and simplicity.

Acknowledgements

Thanks to my husband, Luc Aubin, and my parents, Francine and Gaston who always were believing in me, encouraging me, and giving me the strength to pursue my dream.

I express sincere appreciation to
John Ninos M.D., Amy L Hazen, Kim HT Paraiso M.S., Joseph Wahle, Amy Costello, Jia-Wang Wang Ph.D., Steve L. Highfill, Tomar Ghansah Ph.D., Daniela Wood, Davina Ramos and Sarah L. Highfill for their help and for making the lab an enjoyable place to work.

Thanks to Lia E. Perez M.D. and Nancy Parquet for collaboration on the megakaryocyte project.

I thank the members of my committee for their support.

I express my deepest gratitude to William G. Kerr Ph.D. for his mentorship, patience, and resourcefulness.

Note to Reader

The original of this document contains color that is necessary for understanding the data. The original is on file with the USF library in Tampa, Florida.

TABLE OF CONTENTS

Table of Contents i

List of Tables viii

List of Figures ix

Abstract xii

Introduction on SH2 Domain Containing 5' Inositol Phosphatase 1 (SHIP) 1

SHIP Structure and Cell Signaling 5

SH2 Domain 5

5' Inositol Phosphatase 8

NPXY Motifs 9

Proline Rich (PxxP) Region 10

SHIP Isoforms 10

Inositol Phosphatases with a Redundant Function to SHIP 12

SHIP2 12

Phosphatase and Tensin Homolog Deleted on Chromosome Ten 14

Study of SHIP Function Using SHIP Knock-Out Models 15

Results 18

Section I SHIP-Deficiency Enhances HSC Proliferation and Survival but Compromises Homing and Repopulation 18

Introduction 18
HSC Development 18
Cytokines Impacting HSC Self-Renewal 20
BM Homing and Retention of HSC 21
SHIP in HSC Biology 22
Aims: 26
Results 26
SHIP$^{-/-}$ Mice Have an Expanded HSC Compartment 26
Induced Deletion of SHIP During Adulthood Leads to an Increase in KFLS Numbers in Hematopoietic Organs 31
SHIP$^{-/-}$ BM Cells Show Decreased Ability to Reconstitute the Hematopoietic Compartment of Lethally Irradiated Recipients 35
SHIP$^{-/-}$ HSC do not Exhibit Characteristics of Premature Differentiation 39
SHIP$^{-/-}$ HSC Self-Renew to a Lesser Extent than WT HSC in Transplanted Mice 43
SHIP$^{-/-}$ HSC Have a Lower Rate of Spontaneous Apoptosis 46
In vivo Homing of SHIP$^{-/-}$ Stem/Progenitors to the BM is Significantly Reduced as Compared to WT 48

Reduced Surface Expression of CXCR4 and VCAM-1^{+} on KTLS Cells in SHIP$^{-/-}$ BM 50
Elevated Levels of Soluble VCAM-1 Levels in SHIP$^{-/-}$ Mice Sera 56
Discussion 57
Materials and Methods 61
Mice 61
Cell Isolation 62
HSC Phenotype 62
Cell Cycle Analysis 64
CRU Assay 65
DC Assay 65
Assessment of Multi-Lineage Reconstitution 66
Annexin V Assay and TUNEL Assay 67
In Vivo Homing Assay 67
Measurement Cytokines and Growth Factors Levels in Mice Sera 68
Section II: Influence of SHIP on Megakaryocytes and Megakaryocyte Progenitors 69
Introduction 69
Megakaryocytes 69
The Involvement of SHIP in MK Signaling Pathway 72

Aims: 76
Results 76
MKP and MK are Increased in BM and Spleen of SHIP-Ablated Mice 80
Platelet Levels are Lower in SHIP-Deficient Mice as Compared to WT Mice 82
SHIP-Deficient MK are Morphologically Different than WT MK 83
Comparable Ploidy Distribution in SHIP$^{-/-}$ MK as Compared to WT 84
TPO Levels are Increased in SHIP$^{-/-}$ Plasma as Compared to WT 86
Discussion 88
Materials and Methods 92
Mice Strains 92
Cell Isolation 93
Flow Cytometry Analysis and Antibodies 93
Platelet Analysis 94
Histopathology 94
Ploidy assay 94
Measurement of Cytokines and Growth Factors Levels in the Sera of Experimental Mice 95

Section III: Natural Killer Cells and SHIP 96
Introduction to Natural Killer Cells 96
NK Cell Receptors 98
SHIP and NK Cell Development 104
Results 105
Spleen of SHIP$^{-/-}$ Have Increased Number of NK Cells 105
SHIP is found associated with Ly49 receptors where it may control the level of $PI_{(3,4,5)}P3$ generated by PI3K and negatively regulate Akt phosphorylation 110
DAP12 is Expressed by SHIP$^{-/-}$ BM Cells and NK Cells 112
SHIP but not Shp-1 is Found Associated with Ly49A under Physiological Conditions 114
Discussion 117
Materials and Methods 118
FACS Analysis of the NK Cell Compartment and their Receptors 118
Protein Lysis Buffers 119
Radioimmunoprecipitation (RIPA) buffer. 119
Digitonin cell lysis buffer. 120
Biochemical Analysis of SHIP and Akt 121
RT-PCR for DAP10 and DAP12 123

Western Blot for Shp-1 124
Section IV: Murine ES Cells and s-SHIP 126
Introduction to ES Cells 126
ES Cells Signaling Pathways 127
LIF and ES cells 127
STAT3 stimulates ES cell self-renewal. 129
ERKs antagonize ES cell self-renewal. 129
PI3K signaling in ES cells. 131
s-SHIP 132
s-SHIP and ES Cell 133
Aims: 135
Results 135
MEF Cells Express Full-Length SHIP, but Only ES Cells Express the s-SHIP Isoforms 135
$SHIP^{-/-}$ Murine BM Cells Express s-SHIP 137
s-SHIP Does Not Become Phosphorylated Following LIF Stimulation 138
s-SHIP Associates with gp130 In Vivo 140
Discussion 142
Materials and methods 144
Propagation of mES Cells 144

Preparation of mES Cell Lysates for Biochemical Analysis 144
Nested Reverse-Transcription Polymerase Chain Reaction Assay for Detection of s-SHIP Expression 145
Western blot antibodies and techniques 146
Cell stimulation 147
Western blot analysis of gp130 immunoprecipitates 148
Final Discussion 150
Bibliography 154
About the Author ..... End Page

LIST OF TABLES

Table 1. Increased numbers of HSC cells in the BM and spleen of SHIP$^{-/-}$ mice compared to WT littermates. 27

Table 2. Platelet and Hematocrit counts in SHIP-deficient mice..... 82

Table 3. Functions and ligands of Ly49 NK cell receptors..... 99

LIST OF FIGURES

Figure 1. Signaling pathways influenced by SHIP. 4

Figure 2. Schematic representing different SHIP isoforms structure..... 7

Figure 3. Two SHIP KO models, $SHIP^{-/-}$ and $SHIP^{\Delta IP/\Delta IP}$. 17

Figure 4. Hematopoietic compartment. 19

Figure 5. Significant increase in the percentage and absolute number of $KLSCD48^{-}$ cells in $SHIP^{-/-}$ BM. 30

Figure 6. Significant increase in the percentage and absolute number of HSC in SHIP-ablated BM, spleen and PB. 34

Figure 7. $SHIP^{-/-}$ WBM cells have compromised reconstituting activity. 36

Figure 8. $SHIP^{-/-}$ purified HSC have compromised reconstituting activity. 38

Figure 9. More $SHIP^{-/-}$ TLS cells express high levels of c-Kit as compared to WT. 40

Figure 10. $SHIP^{-/-}$ KTLS express similar levels of Mac1 as compared to WT KTLS. 42

Figure 11. $SHIP^{-/-}$ HSC do not engraft and self-renew as well as WT HSC, although transplanted in equal numbers. 44

Figure 12. $SHIP^{-/-}$ HSC exhibit decreased apoptotic rate. 47

Figure 13. $SHIP^{-/-}$ $Sca1^{+}Lin^{-}$ cells do not home to the BM as efficiently as WT $Sca1^{+}Lin^{-}$. 49

Figure 14. SHIP$^{-/-}$ HSC express lower levels of CXCR4 and VCAM-1 molecules as assessed by flow cytometry. 52

Figure 15. SHIP$^{-/-}$ late progenitor and differentiated cells express the same levels of homing molecules as assessed by flow cytometry. 53

Figure 16. SHIP$^{-/-}$ early progenitors express the same levels of CXCR4 and have a reduced percentage of VCAM-1+ cells. 54

Figure 17. SHIP$^{-/-}$ early progenitors express the same levels of CXCR4 and have a reduced percentage of VCAM-1^{+} cells. 55

Figure 18. sVCAM-1 levels are significantly increased in SHIP$^{-/-}$ sera as compared to WT littermates. 56

Figure 19. Megakaryocytopoiesis and cytokines that influence the process. 71

Figure 20. Increased number of MKP in SHIP-deficient BM. 77

Figure 21. Total MKP but not total MK numbers are increased in SHIP-deficient mice are compared to WT. 79

Figure 22. Significant increase in the percentage of MKP cells in SHIP-ablated BM and spleen. 81

Figure 23. Hematoxylin-eosin staining of SHIP-deficient WT BM and spleen. 83

Figure 24. SHIP$^{-/-}$ MK undergo endocytosis with the same efficiency as WT MK. 85

Figure 25. TPO levels are significantly increased in SHIP$^{-/-}$ sera as compared to WT littermates. 87
Figure 26. Missing-self hypothesis. 103
Figure 27. Increased NK cell numbers in SHIP$^{-/-}$. 106
Figure 28. MHC class I receptors on peripheral NK cells in SHIP$^{-/-}$ mice. 109
Figure 29. SHIP is recruited to NK inhibitory receptors in vivo to oppose activation of Akt. 111
Figure 30. DAP12 is expressed in SHIP$^{-/-}$ and WT BM cells and NK cells. 113
Figure 31. DAP10 is expressed in SHIP$^{-/-}$ and WT BM cells. 113
Figure 32. SHIP but not Shp-1 is recruited to NK inhibitory receptor Ly49A in vivo. 115
Figure 33. Signaling pathways downstream of Ly49A and C that can be influenced by SHIP in NK cells. 116
Figure 34. LIFR/gp130 receptor complex signal transduction pathways and how s-SHIP may impact them in pluripotent stem cells. 128
Figure 35. MEF cells express full-length SHIP, while ES cells express only s-SHIP. 136
Figure 36. Nested RT-PCR detection of s-SHIP expression in SHIP$^{-/-}$ BM. 137
Figure 37. ES cells express the s-SHIP protein isoform that does not become phosphorylated following growth factor stimulation..... 139
Figure 38. s-SHIP is associated with gp130 in ES cells. 141

The Role of Src Homology 2 Domain Containing Inositol-5'-Phosphatase 1 (SHIP) in Hematopoietic Cells

Caroline Desponts

ABSTRACT

The principal isoform of Src homology (SH) 2-domain containing 5' inositol phosphatase protein 1 (SHIP) is a 145kDa protein primarily expressed by cells of the hematopoietic compartment. The enzymatic activity of SHIP is responsible for hydrolyzing the 5' phosphate of phosphatidylinositol-3,4,5-trisphosphate ($PI_{(3,4,5)}P3$), and thereby preventing the recruitment of pleckstrin homology domain containing effector proteins. Furthermore, SHIP contains protein-protein interaction domains, such as an SH2 domain, two NPXY and several proline-rich motifs. All of these different domains endow SHIP with the capacity to impact signaling pathways important for proliferation, survival, differentiation and activation. Therefore, we hypothesized that SHIP-deficiency could result in the loss of hematopoietic cell homeostasis and function

To this verify this hypothesis, we first studied the effect of SHIP ablation on hematopoietic stem cell (HSC) proliferation, survival, function and homing. Most interestingly we observed that SHIP impacts HSC homeostasis and their

ability to home appropriately to the bone marrow. Then, since SHIP was shown to be activated after engagement of the *c-mpl* receptor by its ligand, thrombopoietin, we studied the impact of SHIP deletion on the function of megakaryocytes, the major target cell of that cytokine. We found that SHIP is also important for homeostasis of the megakaryocyte compartment. Thirdly, we studied the role of SHIP in natural killer (NK) cells biology. We observed that F4 generation $SHIP^{-/-}$ mice have increased NK cells in their spleen and that these cells exhibit a disrupted receptor repertoire. We verified the hypothesis that SHIP helps shape the receptor repertoire of NK cells, mainly through regulation of cell survival and proliferation. Also included, is a study on the role of a SHIP isoform lacking the SH2-domain, called stem cell-SHIP (s-SHIP) in the biology of embryonic stem (ES) cells. To date, this isoform is expressed by stem/progenitor cells and not by normal differentiated cells. Due to its specific expression pattern, s-SHIP has the potential to have an important role in stem cell biology.

INTRODUCTION ON SH2 DOMAIN CONTAINING 5' INOSITOL PHOSPHATASE 1 (SHIP)

SHIP stands for Src homology (SH) 2 domain containing 5' inositol phosphatase 1 and is a protein primarily expressed by cells of the hematopoietic compartment.[1-4] In 1996, five independent groups cloned murine SHIP using its ability to bind; 1) the SH3 domain of growth factor receptor-bound protein 2 (Grb2),[2] 2-3) the protein-tyrosine binding domain (PTB) of SH2-containing sequence protein (Shc) (also called SH and collagen gene or SH2-containing oncogene src homology protein),[3,4] 4) the FcγRIIB,[5] and 5) by gene trap assay.[6]

SHIP is known to hydrolyze the 5'phosphate of phosphatidylinositol-3,4,5-phosphate ($PI_{(3,4,5)}P3$) *in vivo* and inositol-1,3,4,5–tetrakisphosphate ($I_{(1,3,4,5)}P4$) *in vitro,*[2,4] two inositides phosphates important for cell signaling (Figure 1).[7-10] Since SHIP appears to require the presence of a phosphate on the 3' position to exert its effect, it was proposed that it opposes the activity of phosphatidyl inositol 3' kinase (PI3K), and by doing so, regulates several cellular signaling pathways important for proliferation, differentiation, apoptosis and migration.

SHIP was first observed as a 145kDa protein that becomes tyrosine-phosphorylated after stimulation of hematopoietic human DA-ER and MO7-ER cell lines with erythropoietin (Epo).[11] In this particular model, stimulation of these cells with Epo resulted in SHIP tyrosine-phosphorylation and association with Shc.[11] Shc being implicated in several mitogenic signaling transduction pathways,[12] it became essential to determine the role of SHIP in hematopoietic cell function. It was then determined that stimulation of several receptors resulted in SHIP tyrosine-phosphorylation and/or SHIP association with other signaling molecules such as SH2-containing tyrosine phosphatase (Shp-2),[13] and Grb2.[14,15] SHIP becomes activated after engagement of cytokines, chemokine and immunological receptors. The cytokines that have been identify to stimulate SHIP consist of interleukin (IL)-3,[13,16-18] IL-4,[19,20] macrophage colony stimulating factor (M-CSF or c-FMS),[21] granulocyte-macrophage-CSF (GM-CSF),[16,18] granulocyte-CSF(G-CSF),[22,23] Stem Cell Factor (c-KitL or SCF),[1,16] thrombopoietin (TPO),[24,25] Fms-like tyrosine kinase 3 ligand (Flt3L).[26] The major chemokine known to induce SHIP recruitment is stromal cell derived factor-1/CXCL12 (SDF-1) which binds to the CXCR4 receptors on multiple hematopoietic cells.[27,28] The immunological receptors known to recruit SHIP are the Fc receptor,[5,29,30] the T cell receptor,[31] and B-cell-receptor Ig-α and Ig-β chains.[32-34] Once SHIP is activated or recruited by these receptors, it can dampen the levels of $PI_{(3,4,5)}P3$, phosphorylation of Protein Kinase B (Akt or PKB), accumulation of intracellular calcium, the formation of the protein complex,

composed of Shc, Grb2, and Son of Sevenless (SOS), and by doing so, SHIP negatively regulates the activation of the mitogen-activated protein kinase (MAPK or Erk) pathway (Figure 1). For example, SHIP impacts pathways downstream of G-CSF receptors that tightly regulate proliferation and survival of neutrophils.[22,23] The cytoplasmic tail of the G-CSF receptor contains a region that is responsible for recruiting PI3K and stimulating proliferation and survival signaling pathways.[22] On the other hand, this same receptor has another region on its cytoplasmic tail that can recruit the SHIP/Shc complex, this region is associated with negative regulation of proliferative signaling.[22] This demonstrates the great balancing act in which these molecules are involved.

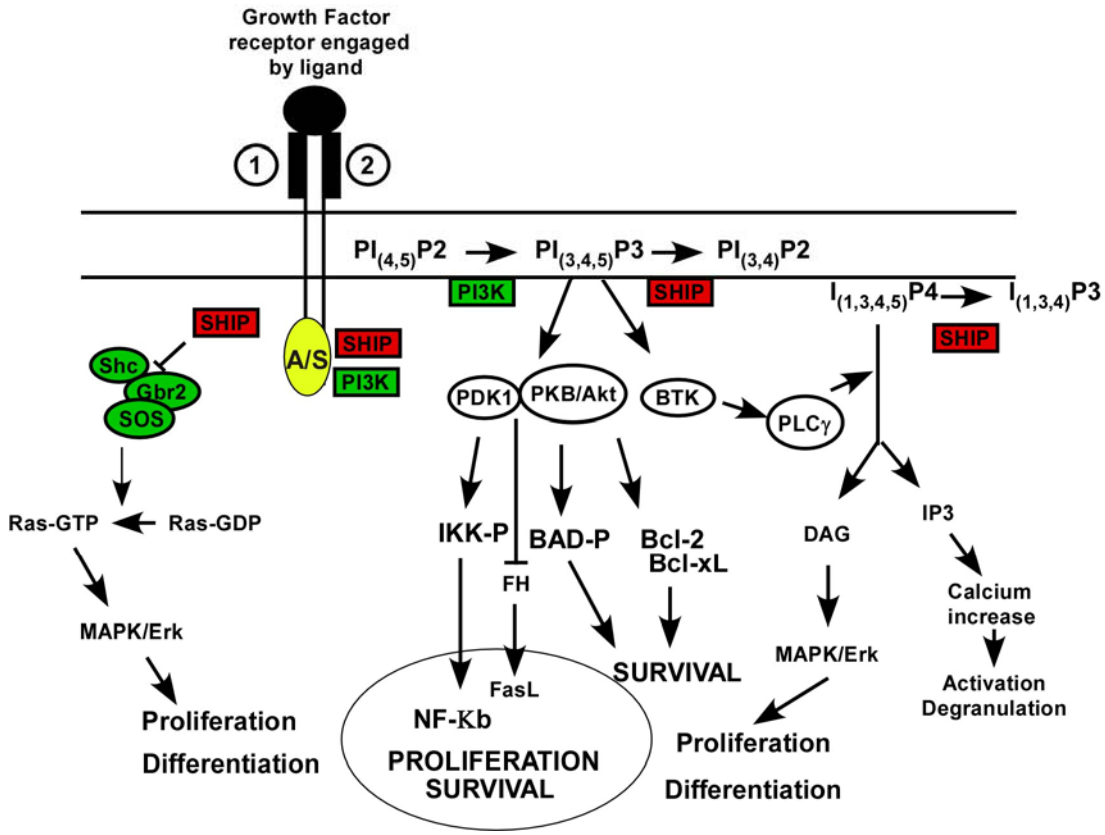

Figure 1. Signaling pathways influenced by SHIP. Engagement of receptor by its ligand leads to recruitment of SHIP with can impact different signaling pathway. 1) SHIP can prevent the Grb2/SOS from binding to Shc, thus preventing the activation of RAS and the downstream MAPK pathway. 2) Alternatively, SHIP can hydrolyze the 5' phosphate of $PI_{(3,4,5)}P3$ generating $PI_{(4,5)}P2$. This prevents the recruitment of pleckstrin homology (PH) containing protein to the membrane and their activation. In this manner, SHIP prevents activation of Bruton's tyrosine kinase (Btk), which is responsible for phospholipase Cγ (PLCγ) activation, leading calcium entry and MAPK activation. SHIP also dampens the recruitment and activation of Akt, which leads to phosphorylation of proteins in the Bcl family, such as BAD, Bcl-2, BclXL, preventing apoptosis. Furthermore Akt can phosphorylate Forkhead (FH) and prevent its translocation to the nucleus.[35,36] Consequently, FH is prevented from inducing transcription of cell death related genes such as Fas ligand (FasL).[35]

SHIP Structure and Cell Signaling

The SHIP protein sequence contains several interaction domains including an SH2 domain, a 5'inositol phosphatase, several proline-rich domain, and two NPXY motifs (Figure 2A). Full length SHIP is a 145kDa protein,[11] which has several isoforms that have different molecular weight including an 130kDa or 135kDa isoform in human and murine cells, respectively, and an 110kDa isoform found in both human and murine cells (Figure 2).[4,37] All of these isoforms appear to have lost a specific protein domain when compared to full length SHIP, which could lead to having a different function in the cell.

SH2 Domain

The SH2 domain of SHIP, stands for Src homology domain 2, a structure that has the potential to bind to phosphotyrosine.[38,39] Using this domain SHIP can bind to phosphorylated immuno-receptor tyrosine based activation or inhibition motifs (ITAMs or ITIMs)[5,40] present in the cytoplasmic tail of several receptors, such as FcγRIIB (ITIM) on B cells,[5,41] Ly49A and C receptors on natural killer (NK) cells,[42,43] and FcRεI (ITAM) on mast cells.[40,44] The SH2 domain of SHIP was also shown to interact with the Src kinase Lyn,[45] which can phosphorylate SHIP.[46] This stabilizes SHIP near the membrane and enhances

its capacity to regulate the Akt signaling pathway.[45] It is important to note that location more than phosphorylation contributes to SHIP phosphatase activity.[46] Furthermore, it was shown that the SH2 domain of SHIP interacts with tyrosine-phosphorylated Shp-2.[13,17] Since a SHIP mutant, with a deleted SH2 domain, can not be phosphorylated or bind to Shc nor Shp-2 after stimulation with IL-3, it was suggested that this domain is crucial for SHIP function.[13,47,48] Consistent with this observation, we found that a SHIP isoform lacking the SH2 domain called stem cell-SHIP (s-SHIP) (Figure 2) can not get phosphorylated and is unable to associate with Shc after stimulation of embryonic stem (ES) cells with leukemia inhibitory factor (LIF).[49] The SH2 domain of full-length SHIP appears to compete with Grb2 for interaction with the same phosphorylated tyrosine on Shc.[1] Interaction of Shc with Grb2 would lead to the recruitment of a protein complex including SOS, which catalyzes the exchange of GDP to GTP on RAS, resulting in the activation of the MAPK/Erk pathway.[1] Thus, SHIP prevents formation of this complex and negatively regulates MAPK activation (Figure 1). Although this hypothesis is compelling, it is important to keep in mind that Shc could associate with SHIP through a different mechanism. For example, it has been proposed that Shc PTB domain can bind the phosphorylated tyrosine Y917 and Y1020 on the NPXY motifs of SHIP.[50] Studies using a SH2 domain deleted SHIP mutant revealed that this domain is necessary for the NPXY motifs to become phosphorylated[48] and for SHIP to interact with Shc.[50] Therefore, it becomes difficult to exactly determine which domain between the SH2 and NPXY domain is used by SHIP to bind to Shc. Another protein with which SHIP

interacts through its SH2 domain is Gab1.[51] However, in this case it is impossible to rule out if SHIP and Gab1 associate directly or through intermediary molecules, since they are found in a multi-protein complex involving phosphorylated Shp-2, PI3K, and Shc.[51,52]

Figure 2. Schematic representing different SHIP isoforms structure. (A) Full-length SHIP, is SHIP and 145kDa. (B)SHIPβ is app. 130kDa and lacks 183 amino acids between the NPXY motifs, resulting in the deletion of a proline-rich domain and the amino acids adjacent to the first NPXY motif, IGM, which would be important for p85 subunit binding. (C) SHIPδ is the result of the deletion of all the proline-rich regions and the last NPXY motifs. The last 62 amino acids at the c-terminal are changed from the full length SHIP, caused by an out-of-frame 230 amino acids deletion. Depending on the reports the SHIPβ and SHIPδ are either the result of proteolytic cleavage[37] or alternative splicing.[53,54] (D) Stem cell-SHIP (s-SHIP) is expressed from the same chromosomal region but has an alternative promoter/start site than the SHIPα, situated in the intron5/6 of SHIPα. This was first proposed in a paper we published in 2001[49] and then confirmed by Rohrschneider *et al*.[55] A 125kDa isoform that is probably generated through truncation of the 145 full-length SHIP c-terminal exists, however this isoform has not been sequenced, thus the structure is not available.

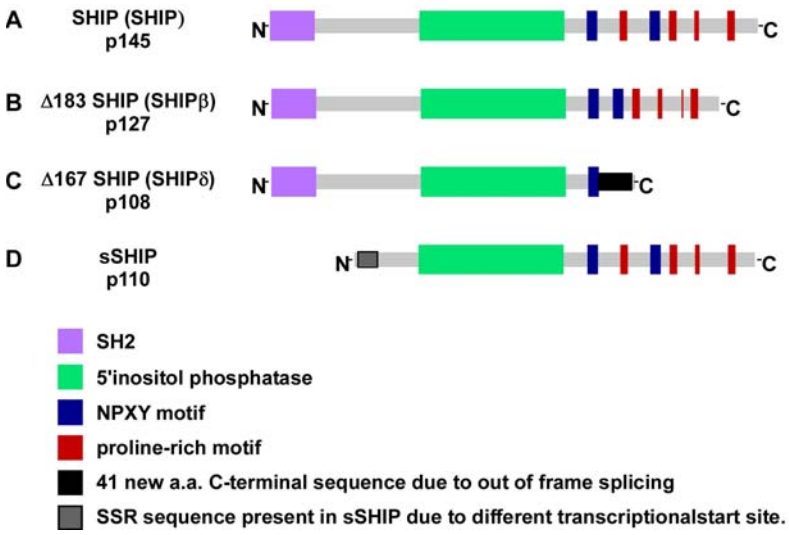

5' Inositol Phosphatase

PI3K catalyzes the addition of a phosphate at the 3' position on Phosphatidyl Inositol(4,5) Phosphate ($PI_{(4,5)}P2$), creating $PI_{(3,4,5)}P3$, this molecule allows the recruitment of pleckstrin homology (PH) domain containing proteins (e.g.: Akt, phosphoinositide dependent kinase 1 (PDK1), Bruton's tyrosine kinase (Btk)), which can then stimulate proliferation, survival, and activation pathways.[10,56-59] SHIP, by removing the 5' phosphate of $PI_{(3,4,5)}P3$, can prevent the recruitment of these effector molecules and negatively regulate some of PI3K downstream signaling pathways.[10,56-59] In particular, SHIP has been shown to decrease Akt recruitment and phosphorylation, leading to a decrease in survival and proliferation signaling.[60,61] Furthermore, the degradation of $PI_{(3,4,5)}P3$ by SHIP after it is recruited to co-ligated B cell receptor (BCR) and FcγRIIB1 can lead to a reduction in Btk membrane localization, which would prevent its activation, resulting in a subsequent decrease in PLCγ2 activity and stopping of calcium flux.[62,63] On the other hand, the ability of SHIP to remove the 5' phosphate of $I_{(1,3,4,5)}P4$ could limit the extracellular entry of calcium and negatively control cell activation.[64-66] There is no requirement for SHIP to be phosphorylated before it can hydrolyze the 5' phosphate of $PI_{(4,3,5)}P3$ or $I_{(1,3,4,5)}P4$, suggesting that localization of SHIP in proximity to the target molecule is the determining mechanism of activation.[54]

NPXY Motifs

NPXY stands for arginine (N), proline (P), any amino acid (X), and tyrosine (Y), and there are two on the carboxyl-terminus of SHIP (Figure 2). This motif can become tyrosine phosphorylated upon activation, which becomes a potential binding site for some PTB domain containing protein.[67-69] In this manner, it was proposed that the PTB domain of Shc could interact with the phosphorylated tyrosines of the NPXY motifs on SHIP, in particular Y917 and Y1020.[2,50] Furthermore, a SHIP isoform, SHIPδ, in which the 2nd NPXY motif and all the poly-proline rich stretch has been deleted can not bind to Shc.[52] However, as mentioned earlier, depending on the cell context, it appears that SHIP can also interact with Shc, through its SH2 domain binding to the phosphorylated Y187 on Shc, a site for which SHIP and Grb2 are competing in order to exert opposite effects on the Ras/MAPK pathway.[1] Although the nature of these conflicting results will not be further discussed in this dissertation, they are worth mentioning to emphasize that more work needs to be done to fully understand the function of SHIP in the different cell context.

Another protein that has been found to interact with the NPXY motifs of SHIP is the p85 subunit of PI3K.[14,70,71] Of the two NPXY motifs present on the carboxyl terminal region of SHIP, the first one is followed by a consensus sequence for the binding of the p85 subunit of PI3K, isoleucine-glycine-

methionine (IGM).[53,71,72] It was shown that p85 PI3K subunit interacts with SHIP only when the first NPXY region is tyrosine-phosphorylated.[53,71]

Proline Rich (PxxP) Region

PxxP motifs are spread between the 1st and 2nd and after the 2nd NPXY motifs within the carboxyl terminus of SHIP (Figure 2). PxxP motifs are known to interact with SH3 motifs,[73] To this effect, SHIP can associate with Grb2, a protein containing two SH3 domains flanking an SH2 domain on each side. Immunoprecipitation assays have shown that Grb2 can associate with SHIP and s-SHIP.[2,4,49]

SHIP Isoforms

As mentioned above, several SHIP isoforms have been identified, mostly through immunoblots. In humans it was shown that peripheral blood (PB) cells expressed a 100kDa version of SHIP, while CD34+ acute myeloblastic leukemia cells expressed 130kDa and 145kDa.[74] In the murine system, most of the lower molecular weight isoforms, the 110, 124, and 135kDa isoforms bear a deletion in the c-terminus region, and appear to be generated from the full-length 145kDa SHIP,[3,5,53] either by proteolytic cleavage[37,75,76] or alternative splicing.[52] Importantly, the 110kDa SHIPδ isoform (Figure 2C), which lacks the proline-rich

region and the 2nd NPXY motifs at the carboxyl terminus, exhibit reduced phosphorylation and interaction with Shc after stimulation of FD-FMS cells by M-CSF.[52] Lucas and Rohrschneider (1999) reported the co-expression of a 135kDa and 145kDa SHIP isoforms in a series of macrophage, B cell progenitor, and T-cell cell lines.[53] This 135kDa isoform results from the internal deletion of a PxxP containing stretch between the 2 NPXY motifs due to alternative splicing. This isoform, which was called SHIPΔ183, can still bind to Shc and Grb2 but has reduced affinity for the p85 subunit of PI3K.[53] This is explained by the deletion of an important consensus sequence after the first NPXY motif, leading to a change in the following amino acids from YIGM to YIAN. The elimination of the methionine at the +3 position after the tyrosine reduces the ability of p85 PI3K subunit to bind SHIPΔ183.[53]

Even though most of the isoforms isolated seem to involve cleavage or alternative splicing in the carboxyl-terminal of SHIP, another 110kDa isoform lacking the SH2 domain was identified in human[4] and in mice.[49] The human 110kDa isoform, called SIP-110, isolated by Kavanaugh *et al* lacks 214 amino acids at the amino-terminus, resulting in the absence of the SH2 domain.[4] It was proposed at the time that SIP-110 isoform resulted from alternative splicing of the full length SIP-145 mRNA.[4] In 2001, our laboratory published that murine ES cells express a 110kDa SHIP isoform (calculated MW 104kDa), called s-SHIP. This isoform lacks 263 amino acids at the amino-terminus.[49] In that study, we

proposed that s-SHIP and SIP-110 were homologues, and were both the result of an alternative start site. The promoter region of that isoform being present in the in the intron 5/6.[49] This was confirmed in a study by Rohrschneider *et al*, which showed that intron 5/6 had promoter activity able to drive the expression of a reporter gene in stem/early progenitor cells *in vivo*.[55] Importantly, s-SHIP is expressed in ES cell and hematopoietic stem cells (HSC) but not in normal lineage differentiated cells.[49,55] This characteristic makes it a very important isoform that certainly should be investigated further for its possible role in stem cell biology.

Inositol Phosphatases with a Redundant Function to SHIP

SHIP2

A 150-155kDa protein with 38% amino acid sequence homology to SHIP1 was identified by Pasesse et al (1997), and was named SHIP2.[77] It was later found that this protein had already been isolated as 51C protein also called inositol polyphosphate-like-protein1 (INPPL-1), which is an inositol phosphatase with the potential to complement the Fanconi anemia group A gene defect.[78] While murine SHIP1 is expressed from chromosome 1 and its human homologue from chromosome 2, SHIP2 is expressed from Chromosome 7 in mouse and 8 in human. [79] However, although SHIP2 reside on a different chromosome, it

contains most of the hallmark domains of SHIP1. For example, SHIP2 has an amino-terminal SH2-domain with 54% identity and a 5'inositol phosphatase with 64% homology to the one found in SHIP1.[77] SHIP2 also has several poly-proline rich stretches in its carboxyl terminal (up to 8), where SH3-domain containing protein can bind and one NPXY motif, a site where PTB domain can bind. This could account for SHIP2 ability to interact with Shc.[80] Whereas SHIP1 expression appears to be restricted to hematopoietic cells, it was reported that SHIP2 is ubiquitously expressed, being observed in hematopoietic cells, such as T cells, B cells, thymus and spleen[81] and in non-hematopoietic tissues such as brain and skeletal muscle.[77,82] Like SHIP1, SHIP2 has the potential to influence many signaling pathways. For example, like SHIP1, SHIP2 has been shown to associate with the ITIM domain of FcγRIIB in B cells under negative signaling.[83] Furthermore, IL-3, c-KitL, and GM-CSF stimulated the phosphorylation and interaction of SHIP2 with Shc in hematopoietic cells.[80]. Another example of the importance of SHIP2, is its ability to be recruited to epidermal growth factor (EGF) receptor where it hydrolyzes the 5' phosphate of $PI_{(3,4,5)}P3$ after EGF stimulation of COS-7 cells. More importantly, SHIP2 has been shown to control insulin receptor signaling *in vitro*[84-87] and *in vivo*, in a knock-out model.[88] Different groups have shown that SHIP2 over-expression led to a decrease in insulin signaling whereas a SHIP2 deficiency led to an increase in insulin sensitivity.[84-89] It is important to mention that since SHIP2 interacts with different molecules than SHIP1 and that it can not hydrolyze the 5' phosphate of

$I_{(1,3,4,5)}P4$, even though these molecules have great homology they are not simply redundant molecules, but have defined purpose in the cells.

Phosphatase and Tensin Homolog Deleted on Chromosome Ten

The defect observed in $SHIP^{-/-}$ mice is severe, but at the same time is probably compensated for by different phosphates such as SHIP2, s-SHIP or phosphatase and tensin homolog deleted on chromosome ten (PTEN). PTEN is a 54kDa ubiquitously expressed tumor suppressor inositol phosphatase that can hydrolyze the 3' phosphate of $PI_{(3,4,5)}P3$, thus, counteract PI3K activity and contribute to the control of Akt activation.[90] PTEN also has a modest capacity to dephosphorylate tyrosine phosphorylated proteins.[91] *PTEN* is one of the most commonly inactivated genes in several type of cancers[92] and a key regulator of cell growth and apoptosis.[93] The major function of PTEN appears to be the reduction of basal $PI_{(3,4,5)}P3$ levels and Akt activity in a constitutive manner,[90] and not upon stimulation by growth factor like SHIP. Therefore, its ablation leads to a more severe phenotype than in $SHIP^{-/-}$ mice, in fact $PTEN^{-/-}$ are embryonic lethal,[94] further suggesting that PTEN is important for normal development. Interestingly, $PTEN^{+/-}$ and $SHIP^{-/-}$ mice share many characteristics, suggesting that the phenotype observed in both mice result mainly from the accumulation of $PI_{(3,4,5)}P3$.[95,96]

Study of SHIP Function Using SHIP Knock-Out Models

The study of SHIP knock-out (KO) mouse models has given great insight into SHIP function in the hematopoietic system.[43,95,97] Although SHIP expression is detectable during embryogenesis at day 7.5 post-coitus,[98] SHIP KO mice are viable.[43,95,97] However, they suffer from a myeloproliferative disorder, that causes an increase in macrophage progenitor and mature macrophage numbers in the BM, spleen and periphery.[95] These macrophages infiltrate the lung of $SHIP^{-/-}$ mice, and this is the suspected cause for their demise at 8 to 12 weeks of age.[95] Using SHIP KO mouse model, it was shown that SHIP negatively regulates the phosphorylation and activation of Akt through downregulation of $PI_{(3,4,5)}P3$ in B cells,[61] in myeloid cells,[18] and NK cells.[43] Huber *et al* also showed that through binding to FcεRI in mast cells,[40,44] SHIP can downregulate their degranulation after stimulation of c-Kit receptor with its ligand.[99] The stimulation of mast cells leads to the activation of PI3K and the production of $PI_{(3,4,5)}P3$, which can then stimulate the entry of extracellular calcium,[99,100] and the release of granule content. Interestingly, SHIP KO mice were also shown to suffer from osteoporosis caused by hyper-resorptive osteoclasts.[101] This could disrupt the BM matrix and perturb the HSC niche.

Most of our studies were done using the SHIP-deficient mouse model generated in our laboratory. These mice were created by targeting the promoter

and exon 1 of the SHIP gene using the Cre-*lox*P strategy and we refer to it as $SHIP^{-/-}$ (Figure 3).[43] In this model, the region to be deleted is flanked (floxed) by two recombinase (Cre) recognition sites, called *lox*P, which were introduced by homologous recombination in ES cells.[102] In order to get deletion of the targeted region, the 34 base pair *lox*P sites need to be inserted in the same orientation.[103] Once a germline flox/flox or flox/+ animal is obtained, it is crossed with a $Cre^{+/+}$ mouse, which result in the deletion of the targeted region. The resulting mice can then be used to generate germline knockout mice. This system allows deleting or targeting the gene of interest either in the entire animal or specific cell type dependent on the promoter that is used for Cre expression. The other SHIP KO model used in our laboratory was a kind gift from Dr. Ravetch at the Rockefeller University in New York. His team produced that model by targeting the region that encodes part of the inositol phosphatase region using the CRE-*lox*P strategy (Figure 3).[97] Consequently, this mouse model will be referred to as $SHIP^{\Delta IP/\Delta IP}$. The $SHIP^{\Delta IP/\Delta IP}$ mice were mainly used less frequently and mainly to confirm the results obtained with $SHIP^{-/-}$ mice to ensure that different mutations of the same gene lead to the same phenotype.

Figure 3. Two SHIP KO models, SHIP$^{-/-}$ and SHIP$^{\Delta IP/\Delta IP}$. (A) Our laboratory created the SHIP$^{-/-}$ model using 129SvJ ES cells, Cre-*lox*P recombinant technology. The promoter region and the exon 1 of SHIP were targeted.[43] The SHIP$^{\Delta IP/\Delta IP}$ model was created using the same technology but targeting the exon 10 and 11, which form part of the inositol phosphatase region.[97] (B) Both of these knockout mice do not express SHIP.

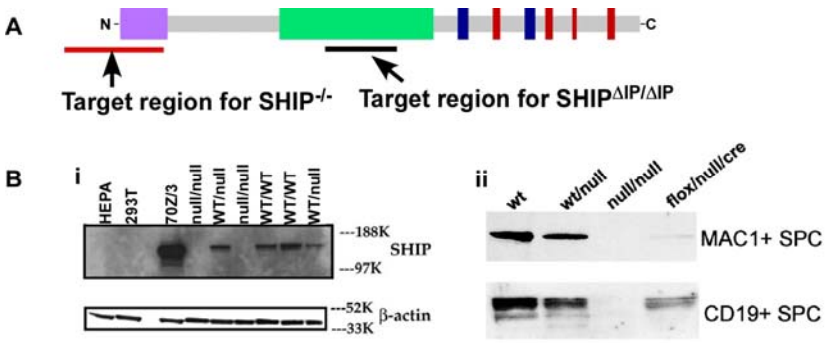

(i) Western blot done on littermates of a mating between heterozygote male and female, harboring a deletion of the promoter and first exon, SHIP$^{-/-}$.[43] (ii) Western blot done on littermates of a mating between a heterozygote male and female, harboring a deletion of exon 10 and 11, SHIP$^{\Delta IP/\Delta IP}$.[97] The later mouse model was generated in the laboratory of Dr. Ravetch at Rockefeller University, New York, USA.[97]

RESULTS

Section I SHIP-Deficiency Enhances HSC Proliferation and Survival but Compromises Homing and Repopulation

Introduction

HSC Development

HSC are responsible for the maintenance of the hematopoietic compartment throughout an organism's lifespan (Figure 4). These cells have the ability to self-renew, differentiate into all hematopoietic lineage and to reconstitute a lethally irradiated host. In the mouse, the embryonic or primitive HSC appear in the yolk sac at day E7 of embryonic development.[104,105] These cells participate in transient hematopoiesis during embryogenesis giving rise mainly to nucleated erythrocytes,[106] although some studies have shown that putative yolk sac HSC have long-term multilineage repopulation capacity,[107] suggesting that they have he potential to differentiate into several hematopoietic lineage. At day E10, the definitive HSC is found in the aorta-gonad-mesonephros (AGM).[108,109] Only these HSC will have the ability to establish definitive hematopoiesis and to reconstitute a lethally irradiated adult host.[104,108-110] Later during fetal development the definitive HSC migrate to the fetal liver, to the spleen and shortly thereafter birth all hematopoiesis is concentrated mainly in

the BM.[104] The maintenance of the hematopoietic compartment depends on HSC homeostasis, the balance between self-renewal, proliferation, apoptosis, and migration (i.e. homing and mobilization) of HSC. Several factors responsible for HSC homeostasis have been identified, nevertheless more information is needed.

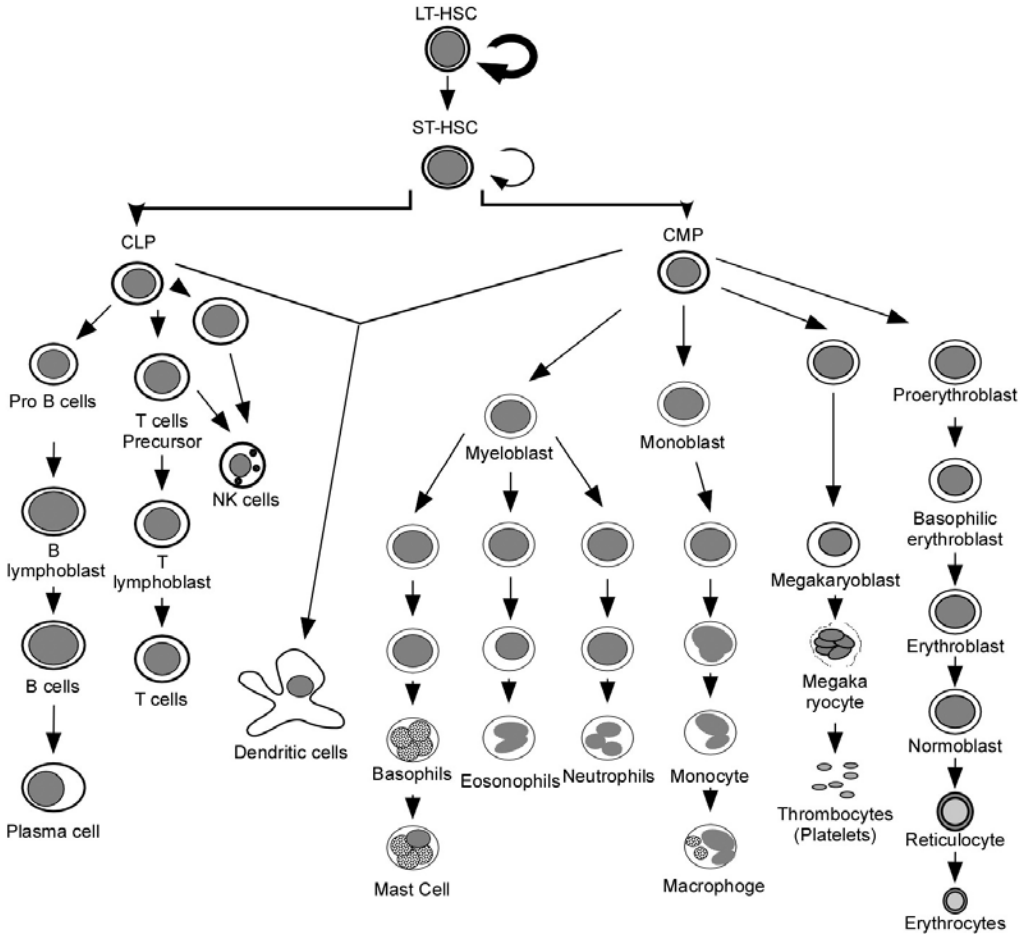

Figure 4. Hematopoietic compartment. HSC have the potential to self-renew without limits, differentiate and produce all the cells necessary for a functional hematopoietic compartment. This differentiation occurs through a series of intermediaries (often called progenitors), which usually have the potential to self-renew with limitations and to differentiate into a defined cell type.

Cytokines Impacting HSC Self-Renewal

It is well accepted that the niche in which the HSC reside in the BM is responsible for the retention of HSC and their ability to self-renew, differentiate, or apoptose. Cell-to-cell contact and external signaling plays a major role in that process. Several cytokines have been shown to influence HSC proliferation and self-renewal *in vitro* and *in vivo*. In fact, several *in vitro* studies have shown that TPO alone or in combination with c-KitL, IL-3, or Flt3L[111-115] can stimulate the proliferation of early human and murine hematopoietic progenitors.[116-127] Most importantly, expansion of early progenitor cells in the presence of TPO with c-KitL or Flt3L confer these cells with the ability to self-renew, to retain a primitive phenotype and maintain the capacity for multilineage differentiation for a defined number of cell division.[116,119-121,123-125] It was also shown that tumor necrosis factor-α (TNF-α) can stimulate the self-renewal and proliferation of human CD34++CD38- *in vitro* in the presence of IL-3, potentially in a synergistic manner.[128] Most importantly, maintenance of hematopoiesis *in vivo* depends on the presence of osteoblast and stromal cells that will form the niche. This microenvironment will promote HSC homeostasis. Furthermore, several factors that are important for maintenance of HSC have also been shown to impact homing and retention of HSC to the BM niche.

BM Homing and Retention of HSC

The homing process was characterized as a 3 step process; 1) Loose or rolling interaction of cells with vascular endothelium, 2) Firm adhesion to the vessel or sinus, 3) Diapedesis through the endothelial layer.[129] This process first requires the presence of specific cytokines and of cell adhesion molecule (CAM) that will mediate the associate of HSC with the stromal cells and osteoblasts that compose the niche in the endosteal region in the BM that support HSC homeostasis.[130-135] To this effect, HSC can interact with a series of molecules produced by the BM stroma such as extracellular matrix (ECM) components, CAM mediating cell-cell adhesions, and endothelial selectins. The ECM components are fibronectin,[136,137] hyaluronic acid,[138] laminins,[139] collagen, and thrombospondin.[140] The CAM mediating cell-cell adhesions include the intracellular cell adhesion molecule-1 (ICAM-1/CD54) and vascular cell endothelial molecule-1 (VCAM-1 or CD107).[141,142] The endothelial selectins are P-selectin/CD62P and E-selectin/CD62E.[143,144] All of these molecules are ligands for receptors present on HSC. These receptors, once engaged will lead to HSC attachment and establishment in the BM niche and thus, contribute to HSC homeostasis. For example, very-late-antigen 4 ($\alpha_4\beta_1$, CD49d/CD29 (VLA-4)) is expressed by hematopoietic cells including HSC and can bind fibronectin and VCAM-1 present on endothelial cells. VLA-4 can promote initial capture, rolling and firm cell adhesion to the endothelial cells.[145] In previous studies, *in vitro* stimulation of murine BM stem/progenitor cells with different cytokines was

shown to induce cell cycle, decrease VLA-4 expression and resulting in compromised engraftment.[146,147] Most importantly it was shown that engagement of VLA-4 an VLA-5 receptors can lead to HSC quiescence,[148] an important aspect of HSC biology. Most importantly, HSC quiescence protects the compartment against external insult and insure the organism that the hematopoietic compartment will be replenish once the insult is cleared.

Proper homing of the HSC to the BM also depends on the presence of a chemokine, SDF-1 also called CXCL-12 and the engagement of its receptor on HSC, CXCR4. The CXCR4 receptor induces cell migration towards an increasing gradient of SDF-1.[149] Treatment of NOD/SCID mice with SDF-1 leads to the mobilization of HSC to PB[150] and treatment of human HSC with anti-CXCR4 antibody prior to transplantation in NOD/SCID mice results in HSC engraftment failure.[151] Furthermore, CXCR4 and SDF-1-deficient mice are embryonic lethal since HSC fail to migrate from the fetal liver to the BM, where definitive hematopoiesis would take place. Interestingly, SHIP$^{-/-}$ myeloid progenitor cells have been shown to migrate more efficiently towards SDF-1 compared to WT myeloid progenitors.[152] Furthermore, SHIP appears to be recruited to the membrane upon CXCR4 engagement by SDF-1.[27]

SHIP in HSC Biology

As mentioned earlier, the survival of an organism is dependent upon the ability of HSC to replenish the blood compartment on a daily basis (Figure 4). To accomplish this task, HSC must maintain a fine balance between three possible fates: self-renewal, differentiation or senescence. Although the decision process that determines the fate of an HSC clone remains to be completely defined, several molecules are already known to play a role in this process, including components of the HSC microenvironment or niche. This niche consists of both extra-cellular matrix molecules and cells, such as osteoblasts and stromal cells that produce cytokines and chemokines important for the maintenance of the HSC pool.[131-135]

These microenvironmental or external cues engage receptors on HSC, leading to the activation of signaling pathways governing cell proliferation, self-renewal, differentiation, mobilization and BM retention.[135] Some of these pathways, such as those initiated by c-KitL,[153] SDF-1,[154] IL-3,[155] Flt-3L,[111-115] and TPO,[17] result in the activation of PI3K and the formation of $PI_{(3,4,5)}P3$. Therefore, SHIP may influence these pathways in HSC.[47,152] SHIP is a 145kDa protein primarily expressed by cells of the hematopoietic system,[3] including HSC,[49] that can associate with various adapter proteins, scaffold proteins, or receptors following activation of hematopoietic cells.[18,152] Formation of these complexes enables SHIP to hydrolyze the 5'phosphate on $PI_{(3,4,5)}P3$,[2,3] thus preventing membrane recruitment and activation of pleckstrin homology domain containing kinases that serve as effectors of PI3K signaling. This activity permits SHIP to

limit the survival, activation, differentiation and/or proliferation of hematopoietic cells.[47] Thus, we hypothesized that SHIP might also influence these processes in the HSC compartment. Previous studies reported that SHIP$^{-/-}$ whole bone marrow (WBM) cells do not reconstitute lethally irradiated mice as well as wild-type (WT) WBM in a non competitive setting.[156] Furthermore it was reported that SHIP$^{-/-}$ WBM has comparable numbers of competitive-repopulating-units (CRU) relative to WT littermates in a limiting-dilution assay, which uses compromised competitor cells.[156] However, because these analyses were performed with WBM rather than purified HSC, they did not assess whether SHIP$^{-/-}$ HSC are defective for repopulation in a WT environment. Thus, it is not possible from these previous studies to conclude that SHIP plays a direct role in signaling pathways essential for HSC function.

To study the role of SHIP in HSC we used SHIP$^{-/-}$ mice generated by a Cre-*lox* mutation strategy.[43] We found that SHIP$^{-/-}$ mice contain significantly more HSC in their BM, spleen, and blood as measured by flow cytometry. We also observed that a greater proportion of SHIP$^{-/-}$ HSC enter the cell cycle compared to WT HSC. Since it was shown in previous studies that SHIP$^{-/-}$ BM contains reduced HSC activity relative to WT BM,[156] it became important to assess the function of SHIP$^{-/-}$ HSC in different assays. We found that when purified SHIP$^{-/-}$ HSC or WBM are transplanted into lethally irradiated mice, they failed to compete effectively with WT HSC or BM cells for long-term multi-lineage repopulation of the hematopoietic compartment. These results might have

suggested that the absence of SHIP causes accelerated senescence of the HSC compartment. However, we observed fewer apoptotic HSC in SHIP$^{-/-}$ BM as compared to WT BM. We then assessed the ability of SHIP$^{-/-}$ HSC to reach the BM niche, where they encounter the proper environment to support their function. *In vivo* homing studies performed using purified stem/progenitor cells suggest that SHIP$^{-/-}$ cells home to the BM with a decreased efficiency compared to WT cells. Most interestingly, we also observed that SHIP$^{-/-}$ HSC have significantly lower surface expression of CXCR4 and VCAM-1, key receptors for homing and retention of hematopoietic cells in the BM.[151,157,158] Therefore, SHIP plays an important role in regulating HSC proliferation, survival, self-renewal, as well as BM homing and retention.

Aims:

1) Quantitate the HSC compartment in different hematopoietic organs of SHIP-deficient mice as compared to WT by flow cytometry.
2) Assess if SHIP$^{-/-}$ HSC are functional in a transplant assay. This is the only *in vivo* assay to measure HSC ability to self-renew and differentiate into cells of the hematopoietic compartment.
3) Determine why SHIP$^{-/-}$ HSC do not engraft as efficiently as WT HSC; Are they short-term HSC?, do they lack the ability to differentiate in a transplant setting?, are they more prone to apoptosis due to the osteoporotic phenotype observed in SHIP$^{-/-}$ BM?, are they deficient in their ability to engraft?

Results

SHIP$^{-/-}$ Mice Have an Expanded HSC Compartment

We initially quantitated HSC numbers based on a phenotype established by Morrison *et al.,* Lin$^{-/low}$Thy1^{+}c-Kit^{+}Sca1^{+} (KTLS),[159] which are highly enriched for long-term repopulating HSC (LT-HSC) activity.[159] We found that SHIP$^{-/-}$ mice have an increased percentage and absolute number of KTLS cells in their BM, spleen (Table 1) and PB (data not shown).

Table 1. Increased numbers of HSC cells in the BM and spleen of SHIP$^{-/-}$ mice compared to WT littermates. *n* at least 3 for each genotype, ♦ spleen

Population		% over WBM cells			Abs. #/pair of femur + tibia or Abs#/spleen (x10^3)		
		SHIP$^{\Delta IP/\Delta IP}$	WT	*p*	SHIP$^{\Delta IP/\Delta IP}$	WT	*p*
Lin$^-$Sca1$^+$ c-Kit$^+$Thy1^{low}	BM	0.276±0.024	0.041±0.008	0.0005	46.24±8.01	16.95±4.18	0.0343
	spl♦	0.1767±0.0481	0.01±0.001	0.0255	89.2±28.2	2.93±0.282	0.0375
Population		**SHIP$^{-/-}$**	**WT**	***p***	**SHIP$^{-/-}$**	**WT**	***p***
Lin$^-$Sca1$^+$ c-Kit$^+$Thy1^{low}	BM	0.4114±0.0353	0.0725±0.025	<0.001	205.3±33.9	37.9±15.3	0.001
	spl	0.0957±0.0131	0.0142±0.0040	0.004	50.90±9.25	5.80±1.92	0.01
Lin$^-$Sca1$^+$c-Kit$^+$ Flk2$^-$	BM	0.2860±0.0398	0.1340±0.0202	0.01	221.4±45.9	103.0±72.2	0.03
	spl	0.0827±0.0141	0.027±0.002	0.02	52.10±7.89	13.58±0.75	0.008
Lin$^-$Sca1$^+$c-Kit$^+$ CD48$^-$	BM	0.019±0.002	0.0068±0.0006	0.001	7.84±0.95	2.76±0.30	0.001
	spl	0.0020±0.0003	0.0002±0.0001	0.005	5.53±0.073	0.289±0.087	0.002
Lin$^-$Sca1$^+$c-Kit$^+$ CD48$^-$CD150$^+$	BM	0.0008±0.0001	0.0004±0.0001	0.04	0.35±0.019	0.164±0.062	0.045
Side population (SP)	BM	0.0565±0.0044	0.0290±0.0044	0.004	26.7±4.7	12.5±2.4	0.035

BM of SHIP$^{-/-}$ mice contained 6-fold more KTLS cells than WT controls (Table 1). In the spleen of SHIP$^{-/-}$ mice, we observed a greater than 6-fold increase in the percentage and absolute numbers of KTLS cells (Table 1). A comparable scenario was seen in the PB, where KTLS cell percentage was increased by 2.5–fold as compared to WT littermates (data not shown). A similar expansion of the KTLS compartment was observed in SHIP$^{\Delta IP/\Delta IP}$ mice, another germline SHIP mutant model with a different genetic background.[97] As for the SHIP$^{-/-}$, SHIP$^{\Delta IP/\Delta IP}$ BM and spleen exhibited a significant increase in KTLS cells when compared to WT control (Table 1). The percentage of KTLS present in SHIP$^{\Delta IP/\Delta IP}$ BM and spleen were 6.7 and 2.7-fold higher than observed in WT

control. Furthermore, KTLS absolute numbers were increased 18.2-fold in the BM and 30.4-fold in spleen of $SHIP^{\Delta IP/\Delta IP}$ mice as compared to WT controls.

Although Thy1.2 expression can be detected on HSC from C57BL6/J mice, surface expression is lower, making negative and positive distinction more difficult than for the Thy1.1 allele.[160,161] Thus, we also quantified HSC numbers using different phenotypes, including the immunophenotype defined by Christensen *et al*:[160] $Lin^{-/low}Flk2^{-}c\text{-}Kit^{+}Sca1^{+}$ (KFLS). KFLS cells, as opposed to KTLS, can be used regardless of genetic background.[160] We found that $SHIP^{-/-}$ mice also exhibited an increased percentage and absolute number of KFLS cells in their BM and spleen (Table 1). KFLS cell numbers are expanded by 2-fold in the BM of $SHIP^{-/-}$ mice relative to WT mice. We also observed that both the percentage and absolute numbers of KFLS cells in $SHIP^{-/-}$ spleens were increased by more than 3-fold as compared to WT spleens (Table 1). In addition, Kiel *et al* recently published a new phenotype to identify HSC that relies on the differential expression of the SLAM family receptors, CD48 and CD150, by HSC and MPP.[162] We observe a 2.8-fold increase in the number of $KLSCD48^{-}$ cells in $SHIP^{-/-}$ BM compared to WT BM (Table 1, Figure 5A, B). Moreover, the percentage and absolute numbers of $KLSCD48^{-}$ cells are increased by 8.7 and 19-fold, respectively in $SHIP^{-/-}$ relative to WT spleen (Table 1, Figure. 5A, B). When using the $KLSCD48^{-}CD150^{+}$ immunophenotype we detect a 2-fold increase in the number of HSC in the BM of $SHIP^{-/-}$ BM as compared to WT

(Table1). In order to confirm our observations made using immunophenotypes relying on surface marker expression, we assessed the level of HSC using the side population (SP) phenotype. Identification of SP cells relies on the function of a transporter protein that exclude the dye Hoechst 33342,[163,164]-- these cells are enriched ~1000-fold for LT-HSC activity compared to WBM cells.[163] When comparing SHIP$^{-/-}$ vs. WT BM, we observed a 2-fold increase in the percentage and absolute number of SP cells in SHIP$^{-/-}$ BM (Table 1). Thus, analysis of five different HSC phenotypes[159,160,162,163] demonstrated a preferential expansion of the LT-HSC compartment in SHIP$^{-/-}$ mice. These observations implicate SHIP in the control of HSC compartment homeostasis.

Figure 5. Significant increase in the percentage and absolute number of KLSCD48$^-$ cells in SHIP$^{-/-}$ BM. (A) Representative FACS plots showing detection of KLSCD48$^-$ HSC in SHIP$^{-/-}$ and WT BM. (B) Percentage and absolute number of KLSCD48$^-$ cells in the BM (per femur and tibia pair) and spleen (Spl) of SHIP$^{-/-}$ (square) and WT (triangle) mice. Data acquired on a FACS Aria with DiVa (BD Biosciences, San Jose, CA) software, analyzed with FlowJo (Tree Star Inc., Ashland, Oregon). (C) Histogram of DNA content in SHIP$^{-/-}$ and WT KTLS cells. (D) Bar graph showing the percentage of SHIP$^{-/-}$ (black) or WT (grey) KTLS/KFLS cells in each stage of cell cycle as calculated using the Watson Pragmatic model in the FlowJo cell cycle platform. Data acquired on FACS Vantage with DiVa software (BD Biosciences). Significance was established using the unpaired student t test (Prism 4 (GraphPad Software, San Diego, CA, USA)). ***p<0.0001, **p<0.001, *p<0.01, and +++p<0.0005. (mean ± SEM, n≥3).

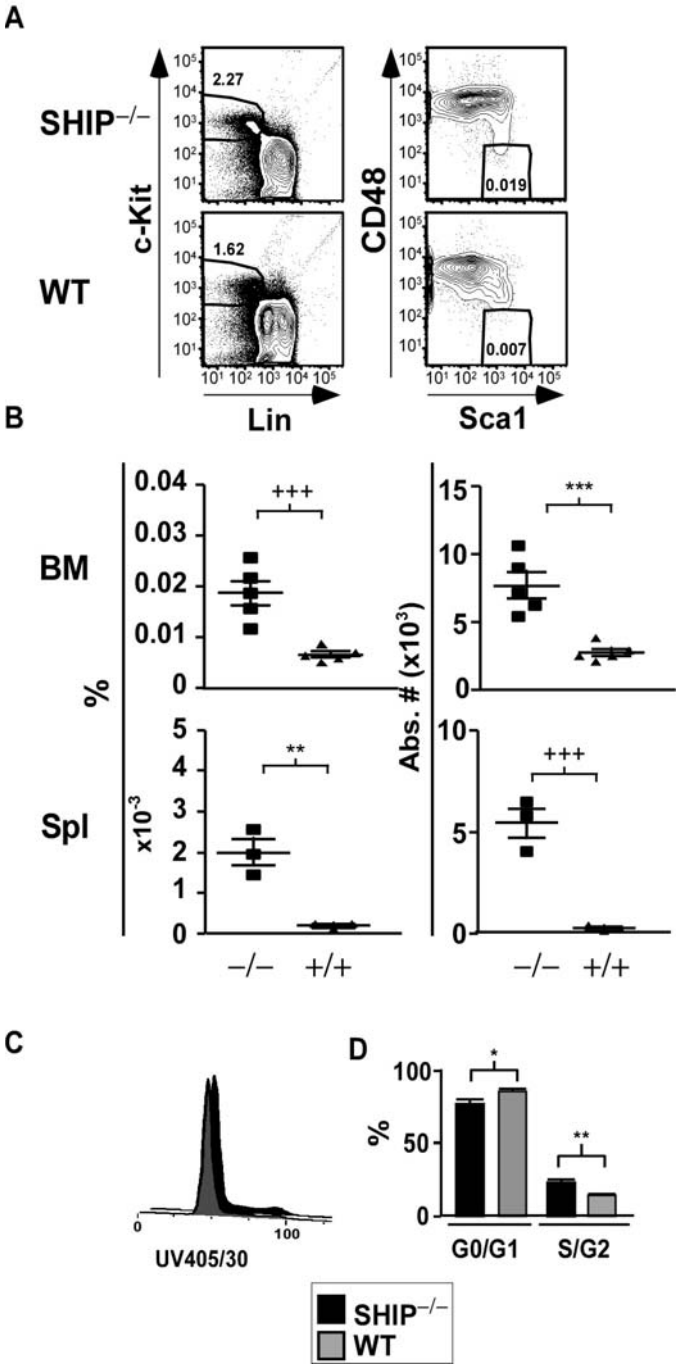

Since SHIP has been shown to negatively regulate proliferation of different cell types,[18] its deficiency could lead to an increase HSC cell cycle activity. In agreement with this, we observed that SHIP$^{-/-}$ BM contained a greater proportion of KTLS in the S/G2 phase, 23.2±1.5% as compared with 14.1±0.1% for WT BM (Figure 5C). This study directly demonstrates that SHIP$^{-/-}$ HSC themselves have increased cycling activity relative to WT. This is consistent with findings of Helgason *et al* that CRU in SHIP$^{-/-}$ BM are more sensitive to 5-fluorouracil treatment.[156] In SHIP$^{-/-}$ BM, we also observed a significant decrease in the proportion of HSC in the quiescent (G0/G1) stage: a subset of cells enriched for long-term multi-lineage engraftment relative to those that have entered the cell cycle.[147,165-167]

Induced Deletion of SHIP During Adulthood Leads to an Increase in KFLS Numbers in Hematopoietic Organs

In the previous section, we studied the impact of SHIP ablation in germline knockout mice. Although this model is very useful, SHIP is ablated during embryogenesis, which could lead to the disruption of cell function or signaling pathways necessary for normal development. Thus, we also assessed the levels of HSC in an inducible Mx1-Cre-*lox*P SHIP knockout model, where SHIP is deleted only during adulthood, allowing for the mice to develop normally. In this model, the region to be targeted is flanked by *lox*P sites, and the Cre expression is under the control of the Type 1 interferon-inducible Mx1 promoter.[43,102,103]

Treatment of these mice with a double stranded RNA homolog, polyinositolic polycytidylic acid (polyIC), leads to the induction of an endogenous anti-viral Type 1 interferon response, which results in Mx1 promoted Cre expression and Cre-mediated recombination of the target gene, in this case the *SHIP* promoter and first exon.[102,103]. This deletion results in the ablation of SHIP expression. Twenty-one days after polyIC treatment, the mice were euthanatized and HSC were quantitated by flow cytometry (Figure 6). As a negative control, we used MxCre- mice treated with polyIC, however, since the MxCre promoter/gene is missing, no rearrangement of the *lox*P site can take place. In the three hematopoietic organs examined, BM, PB and spleen, we observed a significant increase in the percentage of KFLS cells in MxCre+$^{fl/fl}$ mice as compared to MxCre-$^{fl/fl}$. In the BM of SHIP-ablated mice, we observed a subtle but statistically significant increase of 1.5-fold in the percentage and absolute number of KFLS cells as compared to MxCre- mice (Figure 6 a, b). Interestingly, the spleen and the PB of SHIP-ablated mice exhibited the greatest increase in the percentage of KFLS cells. Indeed, there was a 9.8 and 16.7-fold increase, respectively, in the percentage and in the absolute numbers of KFLS cells in SHIP-ablated spleen as compared to control (Figure 6 b). In the PB of SHIP-ablated mice, we observed a 12.6-fold increase in the percentage of KFLS cells (Figure 6 b). This result is consistent with these two organs being more dynamic than the BM, and therefore, responding more rapidly to the absence of SHIP. Furthermore, in another experiment, we determined that the percentage and absolute number of KLSCD48$^-$ cells were significantly increased 3.2-fold and 5.6-fold, respectively, in

SHIP-ablated BM. In these same mice, we observed a 3.9-fold augmentation in KLSCD48$^-$ cells in the PB. KLSCD48$^-$ cells were not increased to the same levels than KFLS in the PB, this might result from the fact that CD48 appears to be present on cycling HSC.[168] Since most of the HSC that are mobilized to the PB usually are proliferating, it is difficult to find the KLSCD48$^-$ cells in the PB. Nevertheless, we observed that SHIP ablation during adulthood results in an enlargement of the HSC compartment, suggesting that the HSC increase observed in SHIP$^{-/-}$ germline mice is not the result of a developmental defect. These results also suggest that the effect of SHIP ablation on the HSC compartment is intrinsic to the HSC.

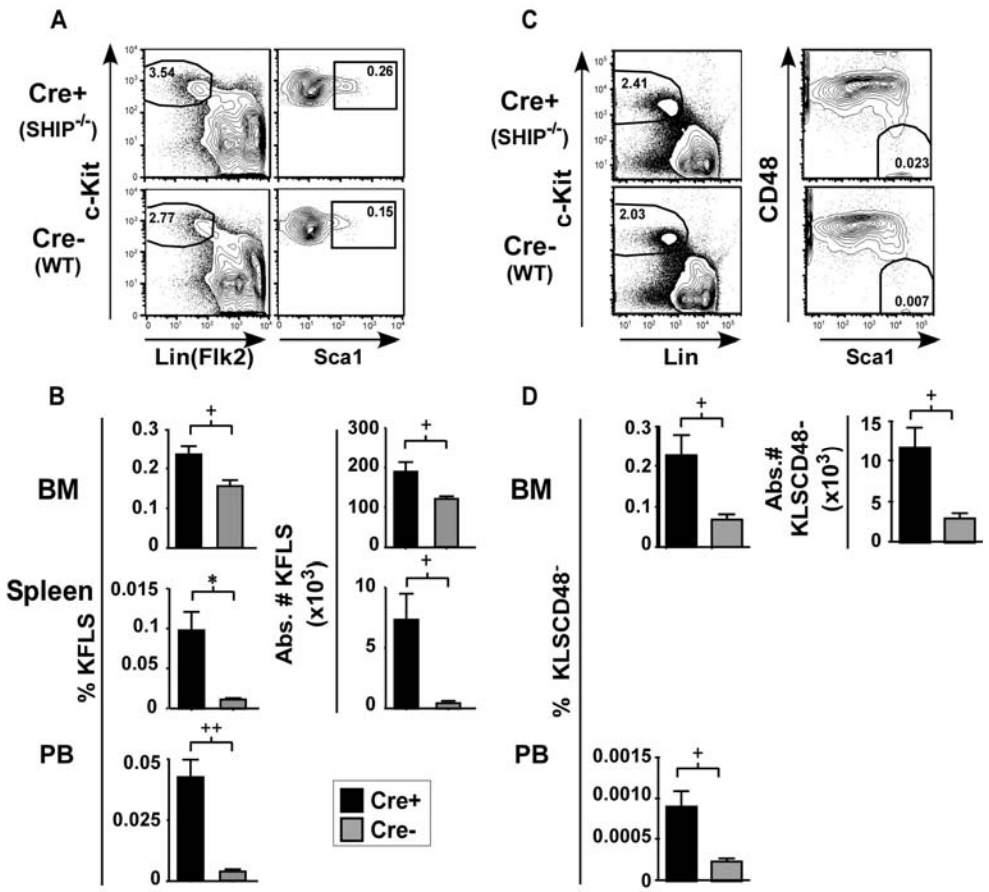

Figure 6. Significant increase in the percentage and absolute number of HSC in SHIP-ablated BM, spleen and PB. MxCre+ and MxCre- mice with floxed SHIP alleles were treated 3 times with 625 μg of polyIC in the course of a week, 21 days prior to being analyzed. (A) Representative FACS plots showing detection of KFLS HSC in SHIP-ablated and MxCre- BM. (B) Percentage of KFLS cells in the BM, spleen and PB of SHIP-ablated (black) and MxCre- (grey) mice, and absolute number of KFLS cells in BM (per femur and tibia pair) and spleen. (C) Representative FACS plots showing detection of KLSCD48$^-$ HSC in SHIP-ablated and MxCre- BM. (D) Percentage of KLSCD48$^-$ cells in the BM and PB of SHIP-ablated (black) and MxCre- (grey) mice, and absolute number of KLSCD48$^-$ cells in BM (per femur and tibia pair). Data acquired on a FACS Calibur with CellQuest software (BD Biosciences), analyzed with FlowJo. Significance was established using the unpaired student t test (Prism 4). *$p<0.01$, ++ $p<0.005$, and +$p<0.05$. (mean ± SEM, n≥3).

SHIP$^{-/-}$ BM Cells Show Decreased Ability to Reconstitute the Hematopoietic Compartment of Lethally Irradiated Recipients

It was previously reported that SHIP$^{-/-}$ BM cells have a lower ability to reconstitute irradiated mice after transplantation, but contains similar CRU activity as compared to WT BM when measured by limiting-dilution assay.[156] Since these results are inconsistent with our finding that SHIP$^{-/-}$ BM contains increased number of HSC (Table 1, Figure 5), we addressed this discrepancy by measuring the ability of SHIP$^{-/-}$ HSC to accomplish long-term multi-lineage repopulating activity. We first performed a well-defined CRU assay as described by Harrison[169] to assess the level of repopulation activity in WBM. WBM is used for the CRU assay and therefore is not dependent on isolation of HSC based on cell surface markers, whose expression can be altered by genetic mutation of unrelated loci.[170] Using this assay, we observed that SHIP$^{-/-}$ BM cells did not reconstitute recipients as efficiently as WT littermates, with a significant reduction of 4.4-fold in CRU numbers in primary transplant recipients (Figure 7A, B).

Figure 7. SHIP$^{-/-}$ WBM cells have compromised reconstituting activity. (A) CRU activity calculated based on the percentage of global repopulation in the PB by donor WBM cells (SHIP$^{-/-}$ (black); WT (grey)). (B) Percentage of global repopulation of PB by SHIP$^{-/-}$ (black) and WT (grey) donor in a CRU assay. (C) Percentage of lymphoid and myeloid PB cells derived from SHIP$^{-/-}$ (black) or WT (grey) WBM 16 weeks after transplantation in a CRU assay. Data acquired using FACS Calibur, CellQuest software (BD Biosciences) and analysis done with FlowJo. Significance was established using the unpaired student t test (Prism 4): ***p<0.0001, **p<0.001, and +p<0.05. (mean ± SEM).

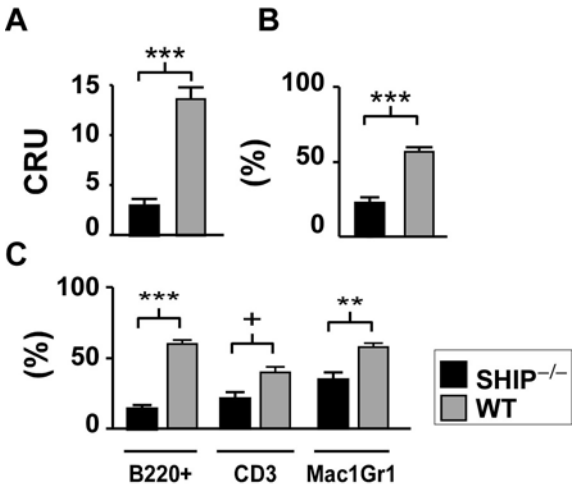

SHIP$^{-/-}$ BM cells showed a significant decrease in long-term reconstitution of both the lymphoid and myeloid cell lineages. For example, 16 weeks after transplantation only 13.2±2.7% of B cells were SHIP$^{-/-}$ derived (CD45.2^{+}) compared to 60.1±2.8% for WT (CD45.1^{+}) WBM, T cell repopulation were 21.2±4.7% SHIP$^{-/-}$ derived vs. 39.7±4.1 for WT and 34.7±5.2% of myeloid cells were SHIP$^{-/-}$ BM derived vs. 57.4±2.8% from WT (Figure 7C). The reduction in the SHIP$^{-/-}$ B cell representation observed in the CRU assay agrees with other studies showing that SHIP deficiency negatively impacts early B-lineage development.[171] We did not observe that SHIP$^{-/-}$ BM cells had enhanced myeloid repopulation relative to WT BM cells (Figure 7C). However, we did observe a bias toward myeloid differentiation within cells derived from SHIP$^{-/-}$ BM, where 59.7±2.7% of the CD45.2^{+} in the SHIP$^{-/-}$ WBM recipients were Mac1^{+}/Gr1^{+}

compared to 24.1±2% for WT BM recipients. This occurred at the expense of the B cell lineage, for which only 25.3±1.5% of CD45.2+ cells were $B220^{+}$ compared to 61.8±3.1% for WT (data not shown). The overall reduction in long-term multi-lineage repopulation by $SHIP^{-/-}$ BM cells demonstrates that despite the increase in HSC numbers observed (Table 1 and Figure 5A, B), HSC activity is significantly compromised in these mice (Figure 7A, C).

Measuring HSC activity by transplantation of WBM from mutant mice can be confounded by the fact that the mutation can endow lineage-committed progenitor cells with properties that may obscure the observation of compromised HSC function.[172] This is a concern when working with $SHIP^{-/-}$ BM as the SHIP mutation enhances myelopoiesis, causing an increase in myeloid progenitors, which have enhanced survival.[95] Therefore, analysis of HSC activity in $SHIP^{-/-}$ mice must also be assessed with purified HSC to rule out these potential experimental artifacts. To directly assess whether SHIP expression by HSC is required for long-term multi-lineage repopulation and self-renewal, we directly compared the repopulating potential of purified HSC from $SHIP^{-/-}$ and WT mice. Thus, CD45.2 $SHIP^{-/-}$ KTLS or KFLS cells were transplanted into lethally irradiated CD45.1/CD45.2 WT recipients with an equivalent number of CD45.1 WT KTLS or KFLS and $Sca1^{-}$ CD45.1/CD45.2 support cells. This assay, the direct competition (DC) assay,[173] directly compares the capacity of genetically-modified HSC to compete with WT HSC for engraftment and long-term multi-lineage repopulation. The level of repopulation in recipients PB was assessed at

regular intervals (Figure 8A), and at sixteen to twenty weeks post-transplant, we observed that global repopulation by SHIP$^{-/-}$ KTLS was reduced by 15-fold relative to WT KTLS (Figure 8B).

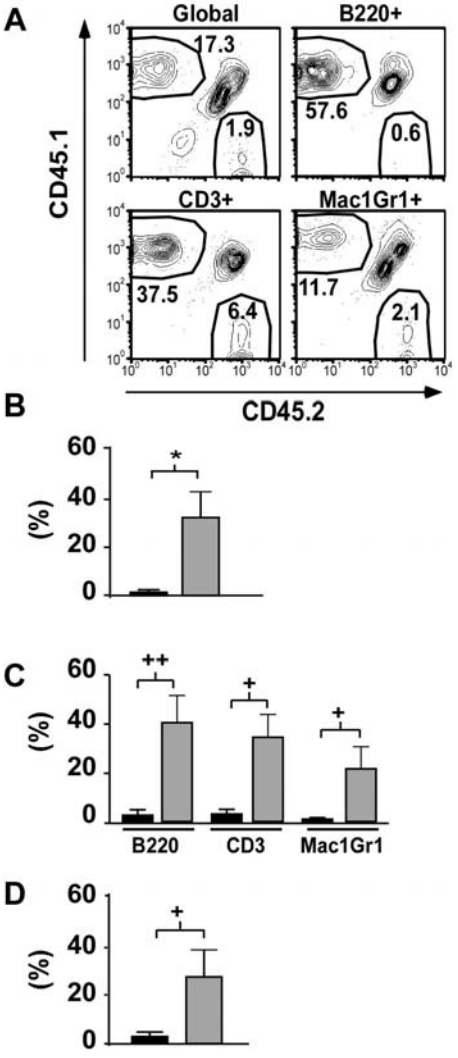

Figure 8. SHIP$^{-/-}$ purified HSC have compromised reconstituting activity. (A) FACS plots show the level of PB reconstitution 16-weeks after KTLS transplantation in a representative DC assay mouse using sorted SHIP$^{-/-}$ and WT KTLS. (B) Percentage of global reconstitution 16 weeks after transplantation of sorted KTLS (SHIP$^{-/-}$ (black) and WT (grey)) (n=11 over 2 different experiments). (C) Proportion of lymphoid and myeloid PB cells derived from SHIP$^{-/-}$ (black) or WT (grey) WBM 16-weeks after KTLS transplantation. (D) Percentage of global reconstitution 12 weeks after sorted KFLS transplantation (SHIP$^{-/-}$ (black); WT (grey)) (n=7). Data acquired using FACS Calibur, CellQuest software (BD Biosciences) and analysis done with FlowJo. Significance was established using the unpaired student t test (Prism 4): *p<0.01, ++p<0.005 and +p<0.05. (mean ± SEM).

Reconstitution of different lineage by SHIP$^{-/-}$ KTLS was also significantly reduced (Figure 8C). Thus, SHIP$^{-/-}$ KTLS are capable of multi-lineage reconstitution, but are unable to sustain this activity for extended periods when in direct competition with WT KTLS (Figure 8C). Furthermore, SHIP$^{-/-}$ cells did not dominate the myeloid compartment as might have been expected from previous studies,[95,156] with only 1% of Mac1^{+}/Gr1^{+} cells being derived from SHIP$^{-/-}$ KTLS vs. 21% from WT KTLS (Figure 8C). This indicates that although SHIP$^{-/-}$ myeloid lineage progenitors have enhanced survival and can prevail over serially-transplanted competitors,[95,156] they are, nonetheless, unable to out-compete normal WT myeloid progenitors when derived from purified HSC in a chimeric transplant setting. As with KTLS cells, long-term global repopulation by SHIP$^{-/-}$ KFLS is significantly reduced (Figure 8D). These results demonstrate that SHIP expression is required by HSC in order to sustain long-term multi-lineage repopulation.

SHIP$^{-/-}$ HSC do not Exhibit Characteristics of Premature Differentiation

As HSC go down the path of differentiation, they lose the ability to self-renew and exhibit a higher proliferative state. Since we observed that SHIP$^{-/-}$ HSC proliferation is increased and engraftment is perturbed, we assessed by flow cytometry if SHIP$^{-/-}$ KTLS exhibited immunophenotypic characteristic of early differentiation. It has been shown that KTLS cells with high levels of c-Kit (c-Kit^{hi}) are enriched for LT-HSC activity, as opposed to the c-Kit^{lo} population that is not

able to support long-term multi-lineage repopulation.[174] This assay revealed that a significantly greater proportion of SHIP$^{-/-}$ TLS were c-Kit^{hi} as compared to WT KTLS cells (Figure 9A, B). There was a greater than 3 fold increase in the percentage of c-Kit^{hi}TLS in the SHIP$^{-/-}$ BM as compared to WT BM (Figure B).

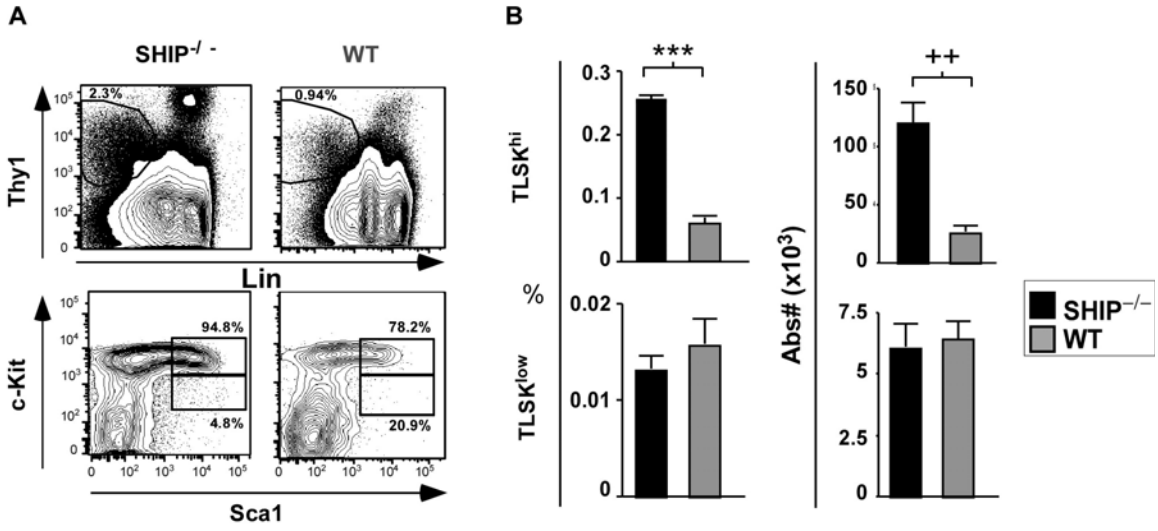

Figure 9. More SHIP$^{-/-}$ TLS cells express high levels of c-Kit as compared to WT. (A) Representative FACS plots showing detection of Lin^{-}Thy1^{+}Sca1^{+}c-Kit^{high} and Lin^{-} Thy1^{+}Sca1^{+}c-Kit^{low}. (B) Percentage (left column) and absolute number (right column) of Lin^{-}Thy1^{+}Sca1^{+}c-Kit^{high} (top row) and Lin^{-}Thy^{+}Sca1^{+}c-Kit^{low} cells). Absolute numbers calculated for 1 pair of femur and tibia. Data acquired on a FACS Aria with DiVa software, analyzed with FlowJo. Significance was established using the unpaired student t test (Prism 4). ***p<0.0001 and ++p<0.005. (mean ± SEM, n=4).

In fact, in SHIP$^{-/-}$ mice 95% of KTLS cells expressed high levels of c-Kit while only 78% of KTLS in WT mice (Figure 9A). This analysis revealed that the percentage and the mean absolute number of c-Kit^{hi}TLS cells in SHIP$^{-/-}$ WBM cells were 4 and 4.6 fold higher, respectively, as compared to WT littermates (Figure 9B). As LT-HSC differentiate towards short term (ST)-HSC phenotype, they begin expressing increasing amount of Mac-1 on their surface, they proliferate at a faster rate and have a reduced ability to self-renew.[159] Therefore, we assessed the level Mac1 expression on SHIP$^{-/-}$ KTLS cells in order to better characterize the HSC compartment in these mice. After gating on live KTLS cells, we looked at the level of Mac1 expression on SHIP$^{-/-}$ and WT HSC by flow cytometry. Since the histogram for Mac1 on KTLS was unimodal, we assessed the level of Mac1 expression using the mean fluorescence intensity (MFI) instead of percentages (Figure 10A, B). Our results revealed that SHIP$^{-/-}$ KTLS cells express comparable levels of Mac1 molecules on their surface as WT KTLS (Figure 10A, B), suggesting that the proportion of ST-HSC contained in SHIP$^{-/-}$ KTLS fraction is not increased as compared to WT control. Thus, according to this phenotypic assay, SHIP$^{-/-}$ KTLS do not exhibit characteristic of premature differentiation.

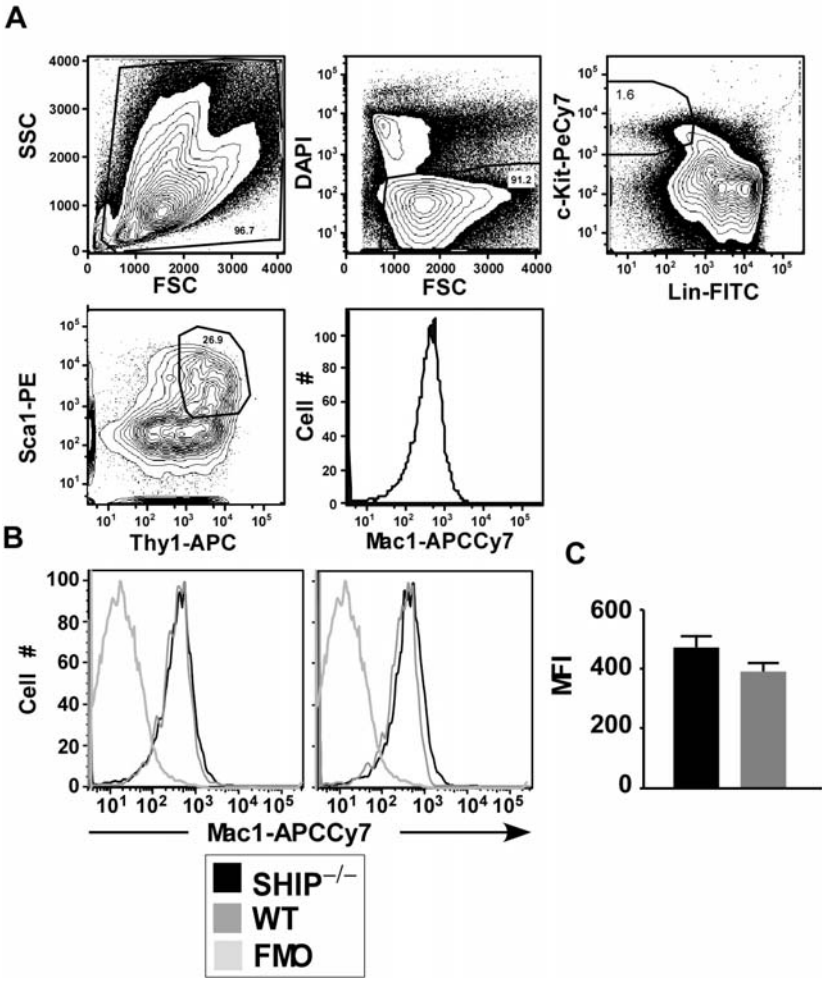

Figure 10. SHIP$^{-/-}$ KTLS express similar levels of Mac1 as compared to WT KTLS. (A) Representative FACS plots showing detection of Mac1 expression (histogram) on KTLS. (B) Two representative overlay histogram of Mac1 expression for SHIP$^{-/-}$ (black) and WT (grey) KTLS. (C) Graph comparing the MFI of Mac1 expression for SHIP$^{-/-}$ and WT KTLS. Data acquired on a FACS Aria with DiVa software, analyzed with FlowJo. Statistical analysis was done using the unpaired student t test (Prism 4). (mean ± SEM, n=4).

SHIP$^{-/-}$ HSC Self-Renew to a Lesser Extent than WT HSC in Transplanted Mice

Our data suggest that SHIP-deficient mice have increase in HSC number and proliferation. However, once transplanted these cells did not reconstitute the host was well as WT HSC. One of the hypothesis proposed to explain these observation was that SHIP$^{-/-}$ HSC might be unable to differentiate. In that case, SHIP$^{-/-}$ HSC would be present in the BM and self-renew without having the ability to differentiate and reconstitute the host PB. Therefore, we assessed the level of reconstitution of the different hematopoietic organs of transplanted mice at least 6 months after transplantation. Three of the CRU transplanted mice were sacrificed and their spleen, BM and PB were assessed for granulocyte/macrophage and lymphoid reconstitution. This assay revealed that every lineage in every organ except for Mac1Gr1 in PB was significantly less reconstituted by SHIP$^{-/-}$ WBM cells as compared to WT WBM cells (Figure 11A). The majority of the lineages were reconstituted to less than 25% by SHIP$^{-/-}$ WBM cells.

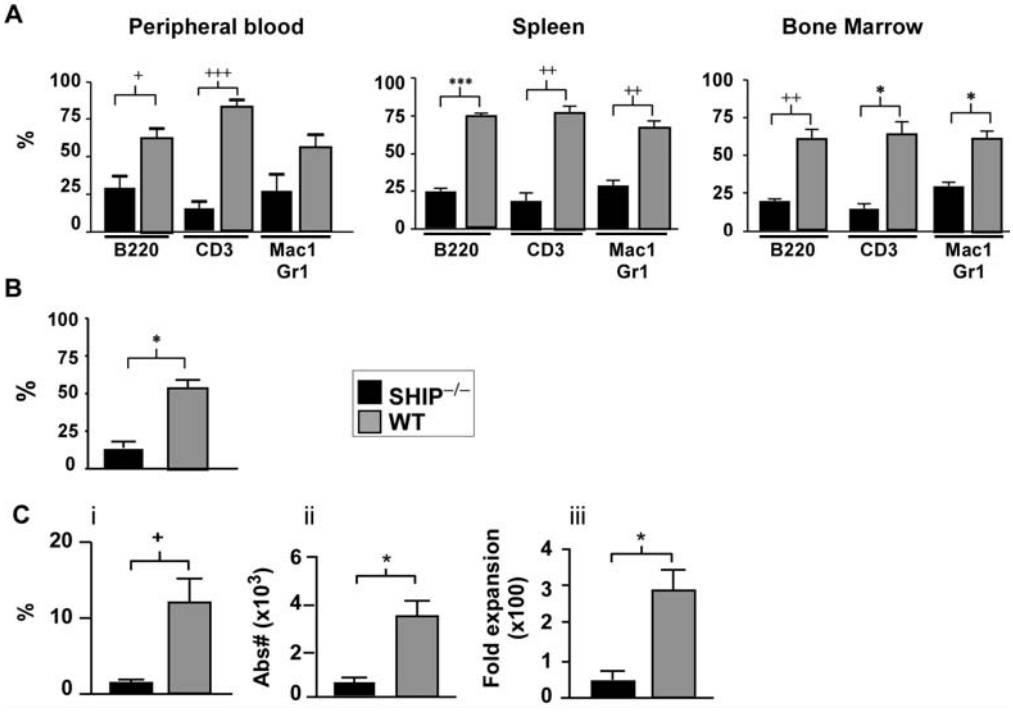

Figure 11. SHIP$^{-/-}$ HSC do not engraft and self-renew as well as WT HSC, although transplanted in equal numbers. (A) CD45.1 mice were irradiated (1000 rads) and transplanted with 1 million CD45.2 SHIP$^{-/-}$ and 1 million CD45.1 WT WBM. Percentage of lymphoid and myeloid PB, spleen and BM cells derived from SHIP$^{-/-}$ (black) or WT (grey) WBM >16 weeks after transplantation. (B) Percentage of KTLS cells in the BM that are derived from SHIP$^{-/-}$ (black) or WT (grey) WBM. (C) CD45.1xCD45.2 mice were irradiated (600 and 400 rads at 3-hour interval) and transplanted with 2x10^5 CD45.2 SHIP$^{-/-}$ and 2x10^5 CD45.1 WT KTLS cells with 4x10^5 CD45.1xCD45.2 Sca1$^-$ cells. First bar graph shows the percentage of KTLS cells derived from SHIP$^{-/-}$ (black) or WT (grey) KTLS cells. Second bar graph Absolute numbers of SHIP$^{-/-}$ and WT KTLS found in 1 pair of femur and tibia SHIP$^{-/-}$ (black) or WT (grey) KTLS cells. Third bar graph compares fold expansion for SHIP$^{-/-}$ and WT KTLS cells SHIP$^{-/-}$ (black) or WT (grey) KTLS cells. Data acquired using FACS Vantage, DiVa software and analysis done with FlowJo. Significance was established using the unpaired student t test (Prism 4): *p<0.01, +++p<0.0005, ++p<0.005 and +p<0.05. (mean ± SEM, n=3)

We then had to consider that the SHIP$^{-/-}$ HSC could self-renew but not differentiate as efficiently as WT. Thus, we observed the level of reconstitution of the KTLS compartment. Briefly, BM cells were enriched for HSC by lineage depletion using the AutoMACS (Miltenyi Biotec, Auburn, CA, USA), and then stained for KTLS, CD45.1 and CD45.2 in the presence of DAPI. This assay revealed that the percentage of KTLSCD45.2^{+} (SHIP$^{-/-}$) over the total amount of KTLS cells was 13.8 ± 4.8%, while 57.3 ± 7.2% of KTLS were CD45.1^{+} (WT) (Figure 11B). Therefore, the capacity of SHIP$^{-/-}$ WBM cells to reconstitute the HSC compartment of a transplanted mouse is significantly lower than he one of WT WBM cells, p=0.007 (Figure 11B). This result correlates with the lower reconstitution of the different hematopoietic organs by SHIP$^{-/-}$ CD45.2 cells (Figure 11A). In the CRU assay the recipient is CD45.1, therefore, we could not totally exclude that a portion of CD45.1+ KTLS came from the host. To address this issue, we assessed the level of KTLS reconstitution in DCA transplanted mice more than 12 months after transplantation. In this case the recipients are CD45.1xCD45.2, thus WT (CD45.1) and SHIP$^{-/-}$ (CD45.2) cells can be differentiated from the host. In these transplanted mice, it was also obvious that CD45.2 SHIP$^{-/-}$ KTLS cells composed a significantly reduced portion of the KTLS compartment as compared to WT (Figure 11Ci). The absolute numbers of SHIP$^{-/-}$ KTLS cells contained in one hind limb were reduced 6.4-fold as compared to the number of WT KTLS (Figure 11Cii). Furthermore, the fold expansion of KTLS cells calculated based on the amount of transplanted KTLS cells and the total amount of KTLS recovered in the recipients revealed that SHIP$^{-/-}$ KTLS only

expanded 44 ± 25-fold compared to 287 ± 56 fold for WT KTLS. Thus, SHIP$^{-/-}$ KTLS did no self-renew with the same efficiency than WT KTLS p=0.008 (Figure 11Ciii). These results confirm that SHIP$^{-/-}$ WBM and KTLS cells cannot reconstitute the hematopoietic system of a lethally irradiated mouse as efficiently as WT cells. The higher proliferative profile of SHIP$^{-/-}$ HSC should have given them an advantage in the reconstitution assay. Therefore, we had to further investigate why SHIP$^{-/-}$ HSC are not able to accomplish long-term reconstitution.

SHIP$^{-/-}$ HSC Have a Lower Rate of Spontaneous Apoptosis

It was reported that SHIP$^{-/-}$ mice have increased osteoporosis caused by an increase in osteoclast activity.[101] The HSC niche is dependent on the presence of osteoblasts, the counter part of osteoclasts, to properly sustain the hematopoietic compartment.[132] Thus, any disruption of the balance between osteoblasts and osteoclasts could destroy the niche necessary for HSC survival, resulting in anoikis-associated apoptosis of the HSC compartment. If SHIP$^{-/-}$ HSC exhibited increased apoptosis, this could contribute to the decreased ability of SHIP$^{-/-}$ HSC to accomplish long-term repopulation. Therefore, we assessed the level of apoptosis in SHIP-deficient HSC and we found that a significantly lower proportion of SHIP$^{-/-}$ HSC were apoptotic relative to WT HSC as measured by Annexin V staining (Figure 12A). In fact, 11.1% of WT HSC (KTLSFlk2-) stained with Annexin V while only 1.1% of SHIP$^{-/-}$ HSC did. TUNEL analysis

done on SHIP$^{\Delta IP/\Delta IP}$ HSC also revealed that SHIP-deficient HSC were undergoing apoptosis at half the rate of WT HSC in the BM (Figure 12B). Thus, the lack of long-term repopulating activity of SHIP$^{-/-}$ HSC activity appears not to be associated with anoikis-induced apoptosis of the compartment.

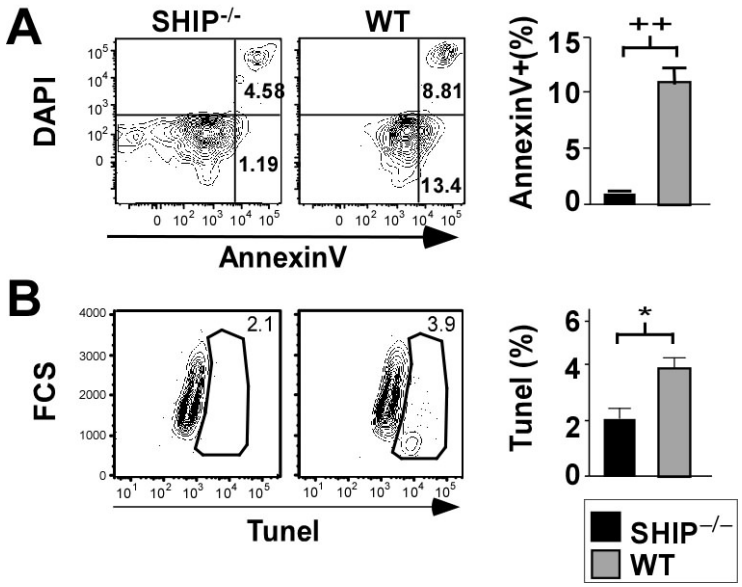

Figure 12. SHIP$^{-/-}$ HSC exhibit decreased apoptotic rate. (A) Representative FACS plots of DAPI vs. Annexin V after gating on KTLSFlk2^{-} cells. Bar graph shows the percentage of KTLSFlk2^{-} that are apoptotic based on the Annexin V^{+} and DAPI^{-} staining, SHIP$^{-/-}$ (black); WT (grey). (B) Representative FACS plots for TUNEL staining after gating on KTLS cells. Bar graph represents the percentage of KTLS cells positive for TUNEL staining, SHIP$^{-/-}$ (black); WT (grey). Data acquired using FACS Aria, DiVaII software and analysis done with FlowJo. Significance was established using the unpaired student t test (Prism 4): *$p<0.01$ and ++$p<0.005$. (mean ± SEM, n≥3).

In vivo Homing of SHIP$^{-/-}$ Stem/Progenitors to the BM is Significantly Reduced as Compared to WT

We considered that the diminished repopulation observed for SHIP$^{-/-}$ HSC could result from an inefficiency of SHIP$^{-/-}$ HSC to home and be retained in the BM niche. Thus, we assessed the homing capacity of SHIP$^{-/-}$ stem/progenitor cells compared to WT cells in an in vivo homing assay.[147,175] Sca1^{+}Lin^{-} cells from the BM of SHIP$^{-/-}$ and WT mice were isolated, stained with fluorescent dyes, and injected into irradiated recipient mice. The frequency of SHIP$^{-/-}$ and WT Sca1^{+}Lin^{-} cells present in the recipient BM and spleen was later assessed by flow cytometry (Figure 13A). Using a total of 12 recipients for each genotype, we found that SHIP$^{-/-}$ stem/progenitor cells reached the BM with a significantly reduced efficiency relative to WT stem/progenitor cells (Figure 13B). Furthermore, we observed that SHIP$^{-/-}$ Sca1^{+}Lin^{-} cells did not home to the spleen as well as WT Sca1^{+}Lin^{-} cells (Figure 13C). These results suggest that SHIP$^{-/-}$ HSC are impaired in their ability to home and be retained in hematopoietic organs. This deficiency likely contributes to their inability to engraft and sustain multi-lineage hematopoiesis.

Figure 13. SHIP$^{-/-}$ Sca1^{+}Lin^{-} cells do not home to the BM as efficiently as WT Sca1^{+}Lin^{-}.

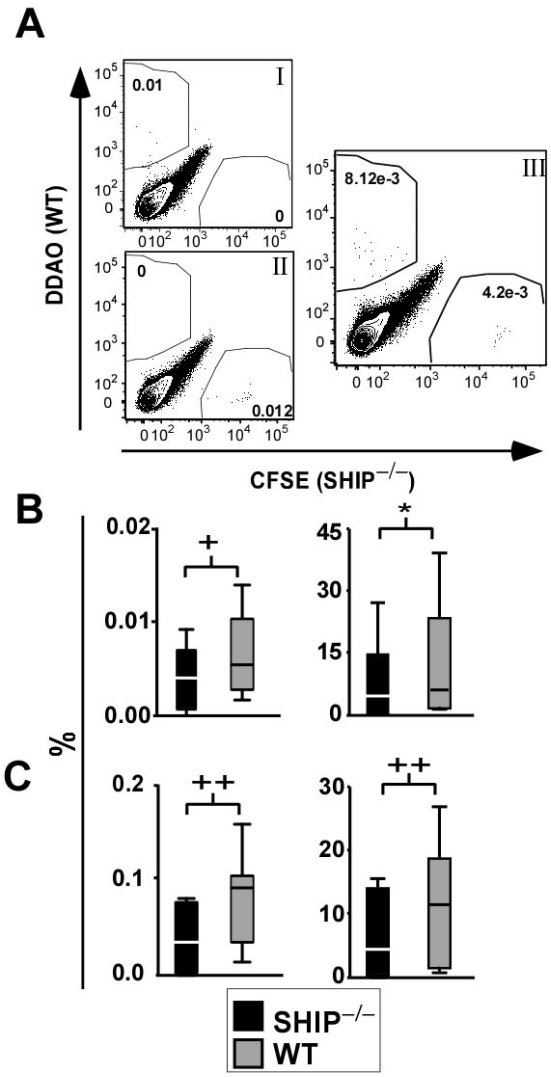

(A) Representative FACS plot of BM from transplant recipients after gating on live cells. (I) Shows BM from control recipient 12-14 hours after transplantation with 0.5x10^{6} WBM stained with 1 μM DDAO . (II) Shows BM from control recipient 12-14 hours after transplantation with 0.5x10^{6} WBM stained with 0.5 μM CFSE. (III) Representative FACS plot of BM from a mouse 12-14 hours after transplantation with 2x10^{5} SHIP$^{-/-}$ Lin^{-}Sca1^{+} cells stained with 0.5 μM CFSE and 2x10^{5} WT Lin^{-}Sca1^{+} cells stained with 1 μM DDAO. (B) Left: Percentage of dye^{+} SHIP$^{-/-}$ (black) or WT (grey) Sca1^{+}Lin^{-} cells found in the recipient BM 12-14 hours after transplantation. Right: Percentage of SHIP$^{-/-}$ (black) or WT (grey) Sca1^{+}Lin^{-} cells that trafficked to and was retained in BM of recipients over the total number of cells injected, 12-14 hours after transplantation. (C) Left: Percentage of stained SHIP$^{-/-}$ (black) or WT (grey) Sca1^{+}Lin^{-} cells found in the spleen of recipients 12-14 hours after transplantation. Right: Percentage of SHIP$^{-/-}$ (black) or WT (grey) Sca1^{+}Lin^{-}cells that reached the spleen of recipients over the total number of cells injected, 12-14 hours after transplantation. Data acquired using FACS ARIA, DiVaII and analysis done with FlowJo. Significance was established using the stratified Wilcoxon-Mann Whitney test using StatXact (Cytel Software Corporation, Cambridge, MA, USA): +p<0.05, *p<0.01 and ++p<0.005. (mean ± SEM, n=12).

Reduced Surface Expression of CXCR4 and VCAM-1^{+} on KTLS Cells in SHIP$^{-/-}$ BM

CXCR4, VCAM-1 and VLA-4 are all known to play prominent roles in homing and trafficking of HSC and other hematopoietic cells to BM.[151,158,176] Thus, we decided to examine the level of expression of these markers on SHIP$^{-/-}$ HSC cells compared to WT HSC. By flow cytometry, we observed a 2.5-fold reduction in the surface expression of the CXCR4 receptor on SHIP$^{-/-}$ KTLS relative to WT KTLS (Figure 14A, B). Flow cytometry analysis showed a reduction in VCAM-1 surface expression on SHIP$^{-/-}$ HSC cells as compared to WT HSC (Figure 14A). We found that 22.1±2.5% of SHIP$^{-/-}$ KTLS were positive for VCAM-1 while 50.8±6.9% of WT KTLS were (Figure 14A, B). The VCAM-1 MFI values for SHIP$^{-/-}$ KTLS were also reduced by 3-fold as compared to WT KTLS (Figure 14B). However, not all homing molecules showed a reduced level of expression. For example, the percentage of KTLS cells expressing VLA-4 as well as their MFI values in SHIP$^{-/-}$ BM cells were unchanged compared to WT BM. Furthermore, contrary to SHIP$^{-/-}$ KTLS, SHIP$^{-/-}$ Lin^{+}c-Kit^{-} and Lin^{-}c-Kit^{+} cells did not exhibit a significant difference in the level of VCAM-1 and CXCR4 expression as compared to WT Lin^{+}c-Kit^{-} cells (Figure 15). We also observed the level of VCAM-1 and CXCR4 expression in the KLS and KLSThy1- populations to evaluate if SHIP deficiency impacted the expression of these markers in different progenitor population or only in the HSC enriched KTLS population. We observed that the reduction in CXCR-4 expression is specific to

the KTLS population (Figure 14). The KLS population, which contains HSC and mostly early and late progenitor cells did not exhibit a significant difference in their ability to express CXCR4 in the absence of SHIP as compared to WT controls (Figure 16Bi-Ci). Furthermore, we observed no significant difference in the level of CXCR4 expression by $SHIP^{-/-}$ $KLSThy1^{-}$ cells as compared to WT control (Figure 17Bi-Ci). However, percentage of $VCAM\text{-}1^{+}$ KTL (Figure 16Cii) and $KLSThy1^{-}$ (Figure 17Cii) were both reduced by 2-fold in $SHIP^{-/-}$ mice BM as compared to WT control. These results suggest that SHIP might impact VCAM-1 expression in different cell types, including KTLS (Figure 14), KLS (Figure 16), and $KLSThy1^{-}$ cells (Figure 17), while SHIP appears to affect CXCR4 expression mostly in KTLS cells (Figure 14 - 17). Interestingly, the late progenitor cells (lin^{-} $cKit^{+}$) and differentiated cells ($Lin^{+}cKit^{-}$) (Figure 15) in $SHIP^{-/-}$ mice had a comparable level of CXCR4 and VCAM-1 expression as compared to WT. Reduction of VCAM-1 and CXCR4 expression on the $SHIP^{-/-}$ HSC suggests these cells may be hampered in their ability to traffic and be retained in the BM, consistent with the decreased BM homing and retention we observe (Figure 13).

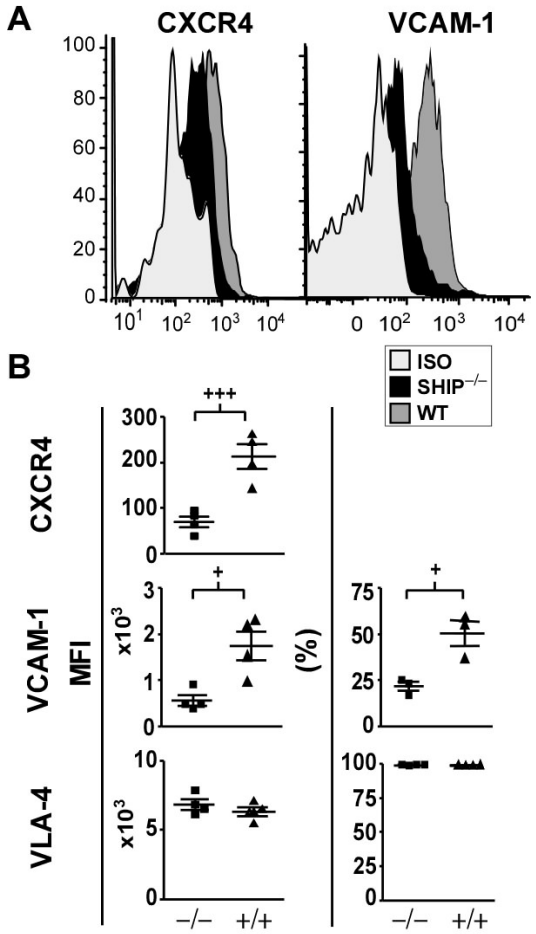

Figure 14. SHIP$^{-/-}$ HSC express lower levels of CXCR4 and VCAM-1 molecules as assessed by flow cytometry. (A) A representative histogram of CXCR4 (left) and VCAM-1 (right) expression on live (DAPI$^-$) KTLS cells (isotype control (light grey), SHIP$^{-/-}$ (black), and WT (grey)). (B) The plots on the left represent the mean fluorescence intensity (MFI) of KTLS cells for CXCR4, VCAM-1, and VLA-4, respectively and the plots on the right show the percentage of KTLS cells positive for VCAM-1 and VLA-4, respectively (SHIP$^{-/-}$ (square); WT (triangle)). Data acquired using FACS ARIA, DiVaII and analysis done with FlowJo. Significance was established using the unpaired student t test (Prism 4): +++$p<0.0005$ and +$p<0.05$. (mean ± SEM, n≥3).

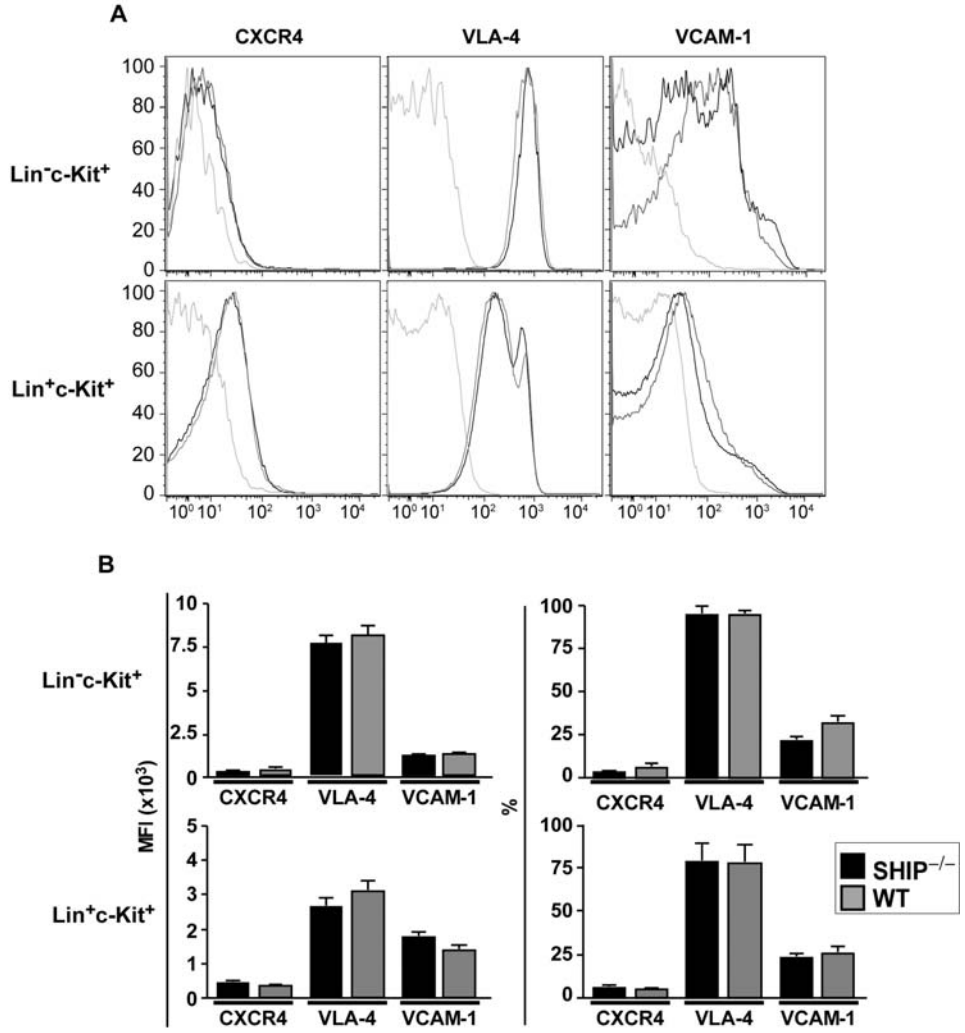

Figure 15. SHIP$^{-/-}$ late progenitor and differentiated cells express the same levels of homing molecules as assessed by flow cytometry. (A) A representative histogram of CXCR4 (left) and VCAM-1 (right) expression on live (DAPI^{-}) Lin^{+}c-Kit^{-} (isotype control (light grey), SHIP$^{-/-}$ (black), and WT (grey)). (B) The plots on the left represent the mean fluorescence intensity (MFI) of Lin^{-}c-Kit^{+} (top) and Lin^{+}c-Kit^{-} (bottom) cells for CXCR4, VCAM-1, and VLA-4, and the plots on the right show the percentage of Lin^{-}c-Kit^{+} (top) and Lin^{+}c-Kit^{-} (bottom) cells positive for CXCR4, VCAM-1 and VLA-4. (SHIP$^{-/-}$ (black); WT (grey)). Data acquired using FACS ARIA, DiVaII and analysis done with FlowJo. Statistical analysis was done using the unpaired student t test (Prism 4). (mean ± SEM, n≥3).

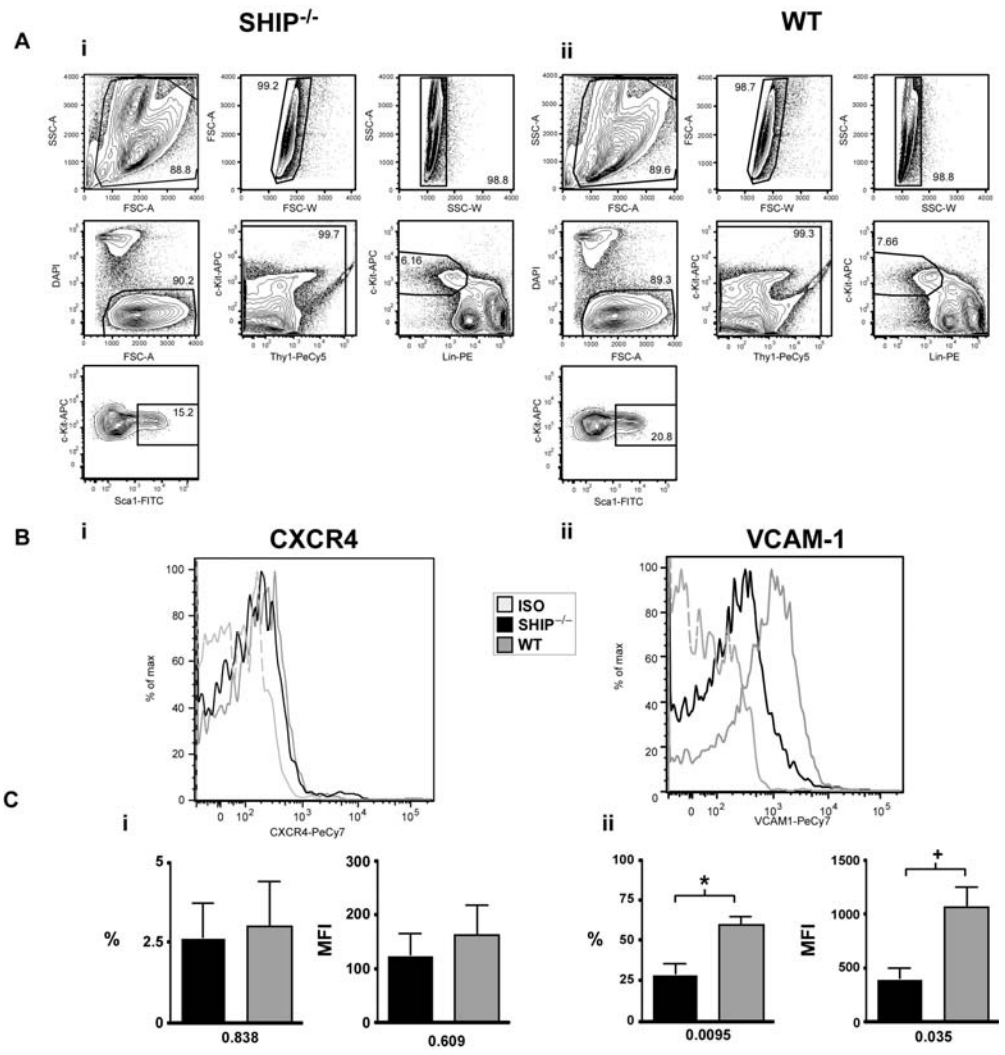

Figure 16. SHIP$^{-/-}$ early progenitors express the same levels of CXCR4 and have a reduced percentage of VCAM-1+ cells. (A) FACS plot representing gating strategy for the analysis of CXCR4 and VCAM-1 expression on KLS cells for (i) SHIP$^{-/-}$ and (ii) WT BM cells. (B) A representative histogram of CXCR4 (i) and VCAM-1 (ii) expression on live (DAPI^{-}) Lin^{-}c-Kit^{+}Sca1^{+} (isotype control (light grey), SHIP$^{-/-}$ (black), and WT (grey)). (C) (i) Bar graphs representing the percentage and MFI of Lin^{-}c-Kit^{+}Sca1^{+} cells for CXCR4 expression. (ii) Bar graphs representing the percentage and MFI of Lin^{-}c-Kit^{+}Sca1^{+} cells for VCAM-1 expression. Data acquired using FACS ARIA, DiVaII and analysis done with FlowJo. Statistical analysis was done using the unpaired student t test (Prism 4). (mean ± SEM, n≥3).

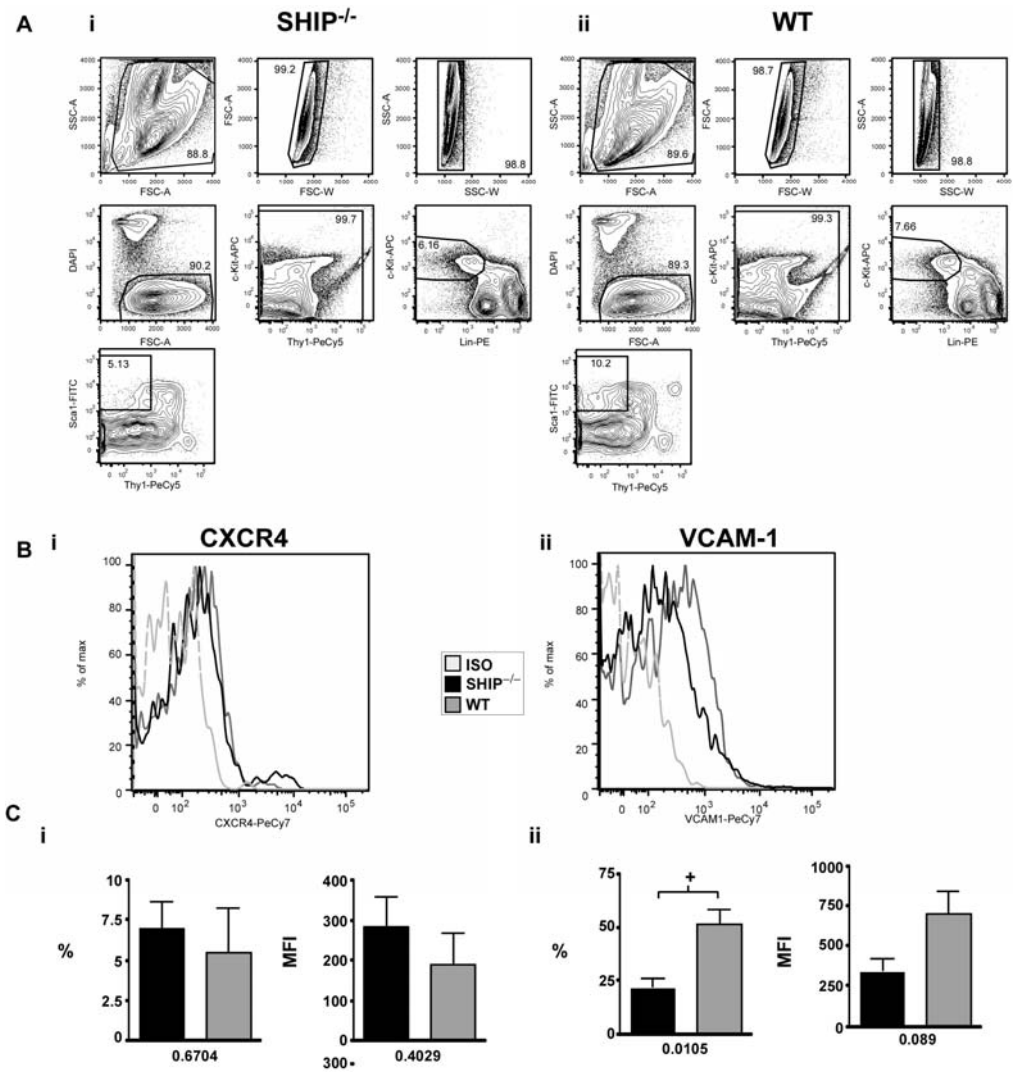

Figure 17. SHIP$^{-/-}$ early progenitors express the same levels of CXCR4 and have a reduced percentage of VCAM-1^{+} cells. (A) FACS plot representing gating strategy for the analysis of CXCR4 and VCAM-1 expression on KLSThy1^{-} cells for (i) SHIP$^{-/-}$ and (ii) WT BM cells. (B) A representative histogram of CXCR4 (i) and VCAM-1 (ii) expression on live (DAPI^{-}) Lin^{-}c-Kit^{+}Sca1^{+}Thy1^{-} (KLSThy1^{-}) (isotype control (light grey), SHIP$^{-/-}$ (black), and WT (grey)). (C) (i) Bar graphs representing the percentage and MFI of Lin-c-Kit+Sca1+ cells for CXCR4 expression. (ii) Bar graphs representing the percentage and MFI of KLSThy1^{-} cells for VCAM-1 expression. Data acquired using FACS ARIA, DiVaII and analysis done with FlowJo. Statistical analysis was done using the unpaired student t test (Prism 4). (mean ± SEM, n≥3).

Elevated Levels of Soluble VCAM-1 Levels in SHIP$^{-/-}$ Mice Sera

Interestingly, we observed that SHIP$^{-/-}$ mice sera contained an increased level of soluble VCAM-1 (sVCAM-1) (Figure 18). This molecule once released in the circulation through proteolytic cleavage remains active and can still bind VLA-4 receptor.[177,178] Thus, sVCAM-1 has the potential to hinder the interaction of leukocyte and HSC with endothelium.[179,180] Therefore, elevated sVCAM-1 could potentially bind VLA-4 receptor on HSC and prevent its interaction with endothelium-bound VCAM-1 and prevent its homing to the BM. This particular scenario could in part explain why we see an increase in HSC number in the periphery and maybe why we see a decrease in the homing properties of these cells. One theory for the latter hypothesis would be that sVCAM1 bind the VLA-4 receptor, preventing their interaction with membrane-bound VCAM-1.

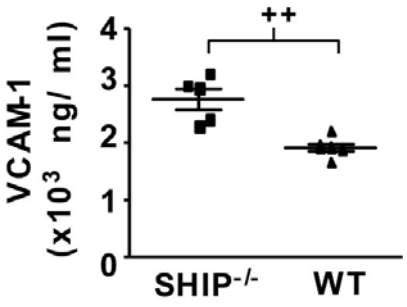

Figure 18. sVCAM-1 levels are significantly increased in SHIP$^{-/-}$ sera as compared to WT littermates. Blood was obtained by sub-mandibular bleed and collected in regular Eppendorf tube to allow coagulation. The sera was then collected and sent for analysis by ELISA (Charles River Laboratories Inc.). ELISA was then performed to assess the level of different cytokines. Significance was established using the unpaired student t test (Prism 4): ++$p<0.005$ (mean ± SEM, n≥3). Collaboration with D. Woods and WG Kerr Ph.D.

Discussion

In this study, we show that SHIP$^{-/-}$ mice had increased HSC in their BM, spleen and PB than WT littermates based on analysis using multiple HSC phenotypes. An expansion of the HSC compartment was also observed in a second SHIP-deficient model, in which the inositol phosphatase region was targeted, the SHIP$^{\Delta IP/\Delta IP}$.[97] This latter model is deficient for SHIP expression and, presumably s-SHIP expression, contrary to the SHIP$^{-/-}$ model. s-SHIP is an isoform expressed in ES cells and HSC but not in differentiated cells.[49] Our studies show that SHIP$^{\Delta IP/\Delta IP}$ HSC have a similar phenotype to the SHIP$^{-/-}$ HSC as compared to WT showing an expansion of the HSC compartment, decreased apoptosis rate and decreased level of CXCR4 expression. According to our data, the ablation of both isoforms did not result in a more severe HSC phenotype. However, additional studies should be done to further assess the role of s-SHIP in this cell type.

The increase in HSC numbers observed in SHIP-deficient mice may partly result from the increased proliferation and decreased apoptotic frequency observed in the SHIP$^{-/-}$ HSC compartment. These results are consistent with SHIP being a negative regulator of several signaling pathways downstream of receptors that impact HSC proliferation and survival, such as *c-mpl*, IL-3R, CXCR4, Flt3 and c-Kit, which induce cell proliferation and/or survival through

activation of the MAPK and PI3K/Akt pathways.[15,25,47,181-187] Moreover, SHIP$^{-/-}$ myeloid and hematopoietic progenitor cells are hyper-responsive to several of these factors.[18] The enhanced survival and proliferation of SHIP$^{-/-}$ HSC could partially explain the decreased repopulating ability of these cells as it was shown that cycling HSC engraft less efficiently than resting HSC.[146,165,167]

Homing and eventual engraftment of HSC following transplantation has been shown to rely on the expression and activity of several surface molecules, including VLA-4, VLA-5 and CXCR4.[151,188,189] The CXCR4 receptor induces cell migration towards an increasing gradient of SDF-1/CXCL12.[149] Treatment of NOD/SCID mice with SDF-1 leads to the mobilization of HSC to PB[150] and treatment of human HSC with anti-CXCR4 antibody prior to transplantation in NOD/SCID mice results in HSC engraftment failure.[151] Furthermore, CXCR4 and SDF-1-deficient mice are embryonic lethal since HSC fail to migrate from the FL to the BM, where definitive hematopoiesis would take place. In addition, one of the ligands for VLA-4, VCAM-1, which is usually found on stromal/endothelial cells, has been shown to be expressed in hematopoietic cells such as Mac-1^{+}, B220^{+} and, more interestingly, c-Kit^{+} cells.[158] Even though the role of VCAM-1 on hematopoietic stem/progenitor cells remains to be fully elucidated, there is evidence that it is involved in their retention in the BM, as shown for B cell progenitors.[158] With that information in mind, the reduction in the percentage of HSC expressing CXCR4 and VCAM-1 receptors in SHIP$^{-/-}$ BM can provide a basis for the decrease in SHIP$^{-/-}$ HSC ability to home to the BM, as shown by our

in vivo homing assays (Figure 13). This inefficiency of SHIP$^{-/-}$ HSC to reach and be retained in the HSC niche could contribute to their impaired self-renewal and long-term repopulating capacity. In previous studies, *in vitro* stimulation of murine BM stem/progenitor cells with different cytokines was shown to induce cell cycle, decrease VLA-4 expression and compromise engraftment.[146] In our study, the increase in HSC cell cycle observed *in vivo* did not necessarily correlate with a decrease in VLA-4 expression, but caused a decline in long-term engraftment capacity. We observed that decreased CXCR4 and VCAM-1 expression on KTLS cells correlated with a reduction in the homing process. Moreover, CXCR4 has been shown to participate in the activation of VLA-4 and VLA-5 to promote human HSC attachment and extravasation, resulting in homing of HSC to the BM niche.[189] The reduction in the CXCR4 receptor seen on SHIP$^{-/-}$ HSC might also dampen this process and, thus, HSC homing. Furthermore, it has been shown that CXCR4 and VCAM-1 are important for the retention of HSC or hematopoietic progenitors in the BM.[157,158] Interestingly, we find that SHIP$^{-/-}$ mice have an increased number of HSC cells in their spleen (Table 1 and Figure 5A, B) and peripheral blood (data not shown), consistent with the down modulation of CXCR4 and VCAM-1 on SHIP$^{-/-}$ HSC. On the other hand, the increased level of sVCAM-1 in the plasma of SHIP$^{-/-}$ mice could hinder the interaction between HSC and endothelium and dampen the homing and retention process of these cells.

Even though we observed a reduction in engraftment by both the DC and CRU assay, the defect seems greater in the DC assay, where equal numbers of purified SHIP$^{-/-}$ and WT HSC are co-transplanted. This suggests that in the CRU assay, where WBM cells are used, the increased number of HSC in SHIP$^{-/-}$ BM might partially compensate for the reduced levels of CXCR4 and VCAM-1 on SHIP$^{-/-}$ HSC, resulting in better engraftment by SHIP$^{-/-}$ HSC in the CRU assay as compared to the DC assay.

The CRU assay included in this study showed a decrease in the repopulating ability of SHIP$^{-/-}$ WBM, while previous studies revealed that SHIP$^{-/-}$ WBM had comparable repopulating activity in a limiting-dilution CRU assay.[156] The different results observed between the two CRUs might stem from the variation in the assays themselves. In the Harrison CRU assay, healthy competitor cells are utilized, while the limiting-dilution CRU assay requires the use of competitor WBM weakened by two serial transplantations.[190] Thus, the compromised WBM competitors in the latter CRU assay may be unable to compete for the niche as efficiently as normal WT WBM against SHIP$^{-/-}$ WBM. Furthermore, the calculation method for the Harrison CRU assay differs from the one used for the limiting-dilution assay, which might result in a different assessment of repopulating activity by the two assays.

In summary, our findings demonstrate a role for SHIP in the maintenance of the HSC compartment. SHIP appears to be critical for the negative control of

HSC proliferation and survival as well as impacting the ability of HSC to home and be retained in the BM niche.

Materials and Methods

Mice

SHIP$^{-/-}$ mice were generated by deletion of the promoter and first exon of SHIP via a Cre-*lox*P strategy and then backcrossed to the C57BL6/J background.[43] SHIP$^{\Delta IP/\Delta IP}$ mice were created using a Cre-*lox*P strategy targeting the inositol phosphatase encoding region. SHIP$^{\Delta IP/\Delta IP}$ mice are on a 129SvJ background and were kindly provided by Dr. Jeffrey Ravetch (Rockefeller University, NY, USA).[97] For all experiments, germline SHIP-deficient and WT mice were 6-8 weeks of age. For the inducible model, SHIP fl/fl mice were backcrossed to MxCre germline. The resulting SHIP fl/fl MxCre+ and MxCre- mice were treated 3 times with 625 μg polyIC in the course of 7 days. At least 20 days after the last treatment, the mice were sacrificed and experiment was performed. As recipients for transplantation experiments we used 8-12 weeks old B6.SJL-*Ptprca Pep3b*/BoyJ (CD45.1) (Jackson Laboratory Bar Harbor, Maine, USA) and a CD45.1xCD45.2 strain generated by intercrossing C57BL6/J (CD45.2) and B6.SJL-*Ptprca Pep3b*/BoyJ (CD45.1) mice. Animal experiments

were conducted in compliance with institutional guidelines at the University of South Florida.

Cell Isolation

BM cells were flushed from intact femurs and tibia. Splenocytes were isolated by crushing the spleen with a syringe plunger. All cells were collected in tissue media (TM) composed of RPMI, 3% fetal bovine serum (FBS), and 10mM HEPES (Gibco BRL/Invitrogen, Carlsbad, CA, USA). Cells were then filtered through a 70μm strainer (BD Biosciences, San Jose, CA) and red blood cells (RBC) were lysed at room temperature (RT) for 2-5 minutes in 1xRBC lysis buffer (eBioscience, San Diego, Ca, USA). The remaining cells were then centrifuged and resuspended in staining media (SM) composed of 1xDulbecco-Phosphate buffered saline (D-PBS), 3% FBS, and 10mM HEPES (Gibco BRL/Invitrogen). PB was obtained by retro-orbital (RO) or sub-mandibular bleeding, collected in microtainers with K_2EDTA (BD, Franklin Lakes, NJ, USA), and RBC lysed twice to obtain PB mononuclear cells (PBMC), which were resuspended in SM.

HSC Phenotype

All antibodies were from BD Biosciences except where noted. All flow cytometry data were analyzed with FlowJo Software (Tree Star, Inc. Ashland,

OR, USA). BM cells, splenocytes or PBMC were treated with Fc block (2.4G2) and then stained on ice for Lineage$^{-/low}$c-Kit^{+}Sca1^{+}Thy1^{+} (KTLS) phenotype.[159] The stain included, Sca1-PE (E13-161.7), c-Kit-APC (2B8), Thy1.2-Cychrome (53-1.2) and a lineage (Lin) panel-FITC: CD2(RM2-5), CD3ε (145-2C11), CD4(GK1.5), CD5(53-7.3), CD8α(53-6.7), B220(RA3-6B2), Gr-1(RB6-8C5), Mac-1(M1/70), NK1.1(PK136), and Ter119(TER-119) (eBioscience). For Lin^{-}c-kit^{+}Sca1^{+}CD48^{-}CD150^{+} (KLSCD48^{-}CD150^{+}),[162] the same Lin panel was used with the addition of CD34–FITC (RAM34) along with Sca1-biotin (E13-161.7), c-Kit-APCCy7 (2B8) (eBioscience), CD48-PE (HM48-1), CD150-Alexa647 (9D1) (Serotec Inc., Raleigh, NC, USA), followed with streptavidin-PeCy7. The cells were then resuspended in SM containing 75ng/ml of 4',6-diamidino-2-phenylindole dihydrochloride (DAPI) for dead cell exclusion (Sigma-Aldrich, St.Louis, MO, USA). Analysis was done on a FACS Vantage or FACS Aria using DiVaII software (BD Biosciences). For the c-Kit^{+}Flk2^{-}Lin$^{-/low}$Sca1^{+} (KFLS) phenotype,[160] we used Sca1-FITC, c-Kit-APC and the above mentioned Lin panel-PE with the addition of the Flk2 antibody (A2F.10-1). After staining, the cells were washed and resuspended in SM containing 7-amino-actinomycin D (7-AAD) (BD Biosciences) for dead cell exclusion. Acquisition was done on a FACS Calibur with CellQuest software (BD Biosciences). For the side population (SP) analysis, BM cells were stained following standard procedure.[163] Analysis was done on a FACS Vantage using DiVaII. For the analysis of Mac 1 expression on KTLS, the same Lin panel (FITC) as the one defined above was used with the

exception of Mac1. The same antibody clones as the one mentioned above were used, but they were conjugated to different fluorochromes: Sca1-PE, c-Kit-PeCy7, Thy-APC, Ma1-ApcCy7. DAPI was used for dead cell exclusion and the data acquired on FACS Aria with DiVaII software.

For homing marker analysis, Lin-depletion of BM cells was done on the AutoMACS (Miltenyi Biotec) using the Lin-PE panel described above, with the exclusion of CD2, anti-PE magnetic beads (Miltenyi Biotec). The Lin-depleted fraction was stained for KTLS and CXCR4 (2B11/CXCR4), VCAM-1 (429), or VLA-4 (9C10) on biotin, followed by staining with streptavidin-PeCy7. DAPI was used for dead cell exclusion. Data was acquired on a FACS Aria using DiVaII.

Cell Cycle Analysis

BM cells were enriched either for $Sca1^+$ or $c\text{-}Kit^+$ cells using AutoMACS (Miltenyi Biotec). $Sca1^+$ or $c\text{-}Kit^+$ cells were then stained for the KTLS or KFLS, then fixed in Cytofix/Cytoperm solution (BD Biosciences) for 30-min on ice, washed in Perm/Wash buffer and incubated with 4-10ng/ml Hoechst dye 33342 (Sigma-Aldrich) in Perm/Wash buffer overnight at 4^oC. The DNA content was measured 24-hrs later on the FACS Vantage and analyzed using FlowJo software.

CRU Assay

CD45.1 recipient mice were given antibiotic water -- sulfamethaxazole and trimethorprim oral suspension 40mg/ml (Hi-Tech Pharmacal CO., INC. Amityville, NY, USA) prior to receiving a single dose of 9.5-Gy 3-hours before transplantation. One million WBM cells from CD45.2 $SHIP^{-/-}$ or WT mice along with $1x10^6$ CD45.1 WBM cells were injected retro-orbitally into recipients, as per Harrison.[169] Transplanted mice were later assessed for PB multi-lineage reconstitution. Repopulating units (RU) were calculated as per Harrison *et al.*:[169]

RU = (10 * CD45.2 repopulation(%))/(100 – CD45.2 repopulation(%)).[169]

DC Assay

The DC assay was modified from Domen *et al*.[173] Donor BM cells were magnetically enriched for $Sca1^+$ cells on AutoMACS (Miltenyi Biotec). The $Sca1^+$ fraction was stained for $Lin^{-/low}c\text{-}Kit^+Sca1^+Thy1^{low}$ or $Lin^{-/low}Flk2^-c\text{-}Kit^+Sca1^+$ and sorted twice in the presence of DAPI using the FACS Vantage DiVAII. For the KTLS transplantation, 200 CD45.1 WT and 200 CD45.2 $SHIP^{-/-}$ KTLS cells were injected with $4x10^4$ $Sca1^-$ CD45.1/45.2 WBM cells. For the KFLS transplantation, 100 CD45.1 WT and 100 CD45.2 $SHIP^{-/-}$ KFLS cells were injected with $4x10^5$ CD45.1/45.2 $Sca1^-$ cells. CD45.1/45.2 recipients had been previously irradiated

with a split dose of 10Gy at 3-hour interval and given antibiotic water, as mentioned above.

Assessment of Multi-Lineage Reconstitution

For the first 4 months after transplantation the level of PB reconstitution was assessed, every 4 weeks, as a measure of engraftment of $SHIP^{-/-}$ and WT HSC. PBMC were treated with Fc block, then stained with CD45.1-PE(A20), CD45.2-FITC (104), and APC-conjugated Lin markers; B220, CD3, or Mac1/Gr1 (clones as previously mentioned). The cells were then washed and resuspended in SM containing 7-AAD to exclude dead cells. Data acquired on FACSCalibur with CellQuest and analyzed with FlowJo. To assess the level of reconstitution of differentiated cells in the BM, spleen and PB 6 to 8 months after transplantation, we used the same antibody clones mentioned above except that Mac1 was conjugated to APCCy7 and Gr1 to APC. Furthermore, DAPI was used for dead cell exclusion and data was acquired on a FACSAria using DiVaII software. To assess the level of KTLS reconstitution, BM cells were enriched for Sca1 on the AutoMACS (Miltenyi Biotec) using the Sca1-Biotin and anti-biotin magnetic beads (Miltenyi Biotec). $Sca1^{+}$ cells were then stained for Lin-FITC, Sca1-biotin, c-Kit-APCCy7, Thy1-APC, CD45.1-PE and CD45.2-PerCPCy5.5. The Sca1-biotin was revealed using Streptavidin-PeCy7. DAPI was used for dead cell exclusion. Data was acquired on FACS Vantage with DiVaII software.

Annexin V Assay and TUNEL Assay

BM cells were isolated stained with c-Kit-APCCy7, Thy1.2-APC, Lin-FITC, Sca1-Biotin and Flk2-PE on ice, biotin was revealed by streptavidin-PeCy7. The cells were then incubated with Annexin V (BD Biosciences) according to the manufacturer's protocol. Analysis was done on a FACSAria using DAPI for dead cell exclusion. TUNEL assay was performed using the *In situ* cell death detection Kit following manufacturer's instruction (Roche Applied Science, Indianapolis, IN, USA). First, BM cells were depleted of Lin^+ cells using Lin-PE, anti-PE beads, and the autoMACS (Miltenyi Biotec), Lin^- cells were then stained for KTLS and TUNEL.

In Vivo Homing Assay

Homing assays were optimized from previous protocols.[147,175] BM cells from 6-8 week old $SHIP^{-/-}$ and WT mice were isolated from hind/fore limbs and from vertebral column. BM cells were then RBC lysed, Fc blocked for 15 minutes, then depleted of Lin^+ cells using Lin-PE, followed by anti-PE beads, using autoMACS (Miltenyi Biotec). Lin^- cells were then stained for Lin-PE, Sca1-FITC and DAPI and $Sca1^+Lin^-$ cells were sorted on the FACS Aria. After sorting, the cells were stained with 1μM of 9-H-(1,3-dichloro-9,9-dimethylacridin-2-one-7-

yl) phosphate (DDAO-SE) (Molecular Probe/Invitrogen, Carlsbad, CA, USA) and/or 0.5 μM carboxyfluoroscein succinimidyl ester (CFSE) (Molecular Probe/Invitrogen) for 15 minutes at 37°C, washed and centrifuged at 300xg for 7 minutes at 4°C. Cells were then resuspended in PBS with 1mM HEPES and an equal number of live $Sca1^{+}Lin^{-}$ $SHIP^{-/-}$ and WT cells ($2x10^{5}$ cells of each genotype) were then injected into irradiated recipient mice (1000 rads 3 hours prior to transplantation). For some experiments, both CFSE stained $SHIP^{-/-}$ and WT $Sca1^{+}Lin^{-}$ cells were injected in different recipients. In others, CFSE stained $SHIP^{-/-}$ and DDAO stained WT $Sca1^{+}Lin^{-}$ were injected in the same recipients. Twelve to 14 hours after injection, BM cells and splenocytes were isolated from recipients and directly analyzed on a FACS Aria in the presence of DAPI. Five million events were collected for each recipient.

Measurement Cytokines and Growth Factors Levels in Mice Sera

Blood was obtained by sub-mandibular bleed, collected in a regular Eppendorf tube and left at RT for 4 hours to allow coagulation. The blood was then stored at 4°C overnight. The following day, blood clots were removed using a wooden stick and the remaining blood was centrifuged at 4000 RPM for 10 minutes at 4°C. The sera was then isolated by taking the supernatant and sent for analysis at a custom based service at Charles Rivers Laboratories Inc., where ELISA for multiple cytokines and growth factors was performed.

Section II: Influence of SHIP on Megakaryocytes and Megakaryocyte Progenitors

Introduction

Megakaryocytes

Platelets are responsible for repair of vascular damages, wound repair, innate immune response, and metastatic tumor cell biology.[191] In human, 1 x 10^{11} platelets are produced each day in order to maintain proper balance, and during time of crisis, this number can increase up to 10 fold.[192] Mature megakaryocytes (MK) that are responsible for the production of platelets arise from the differentiation and maturation of megakaryocyte progenitors (MKP). In turn, MKP are derived from early myeloid progenitors, which also give rise to granulocytes/monocytes and erythrocytes (Figure 4). The different stages of MKP differentiation, from MKP proliferation to platelet shedding, and the diverse cytokines influencing that process, are depicted in Figure 19. From early progenitor proliferation, MKP maturation to platelet shedding by MK, the megakaryocyte lineage has a unique way to control its homeostasis, mainly through chemokines, growth factors, and cytokines.[193-196]; [197-210] As it is shown on Figure 19, some cytokines are more important for the early development or

proliferation of MKP, such as IL-3 and c-KitL, while others, including IL-6 and mostly TPO impact MK maturation and platelet release. One major component of MK maturation is the process of endomitosis, which generates MK that have an average DNA content of 32N, and exhibit an increase in cell size, mRNA content, and protein production.[211,212] After fragmentation of polyploid MK, approximately 3000 platelets are generated,[213] all of which are small cells that lack a nucleus, but have a highly organized cytoskeleton, the major necessary components to control thrombosis; unique receptors and specialized secretory granules.[214,215] The level of platelet in an organism must be tightly regulated to prevent blood clot due to unwarranted production of platelet or excessive bleeding caused by a decrease in platelets levels.

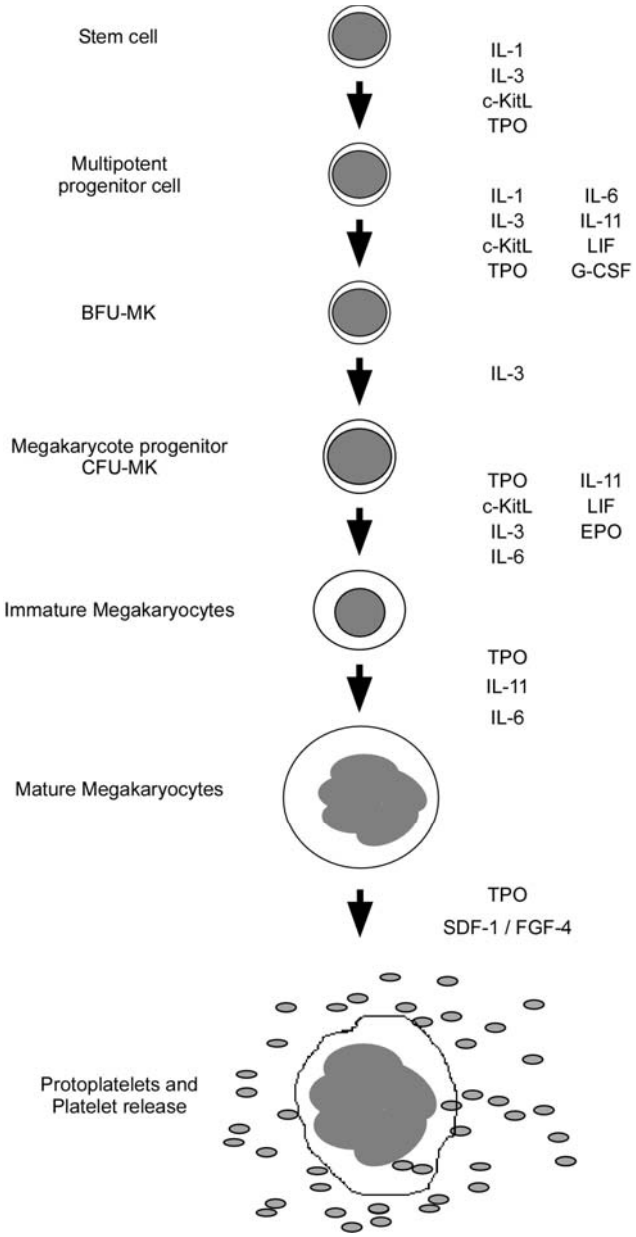

Figure 19. Megakaryocytopoiesis and cytokines that influence the process. The different steps of megakaryocytopoiesis are influenced by many cytokines *in vitro* and *in vivo.*[216,217] While the *in vivo* deletion of IL-3, IL-6, IL-11 and LIF does not affect megakaryocyte development, knockout mouse model for SF, TPO, and its receptor *Mpl* exhibit a megakaryocyte development defect. Interestingly, treatment of $Tpo^{-/-}$ and $Mpl^{-/-}$ mice with FGF-4 and SDF-1 induced platelet production to levels comparable to WT.[200]

The Involvement of SHIP in MK Signaling Pathway

Early on many cytokines, including IL-3, IL-6, IL-11, LIF, c-KitL, Epo and G-CSF have been shown to impact megakaryocytopoiesis and thrombopoiesis.[193-197] It was shown that they can influence megakaryocyte progenitor (MKP) proliferation and differentiation, *in vitro,* in a synergistic manner, none of them being sufficient to promote megakaryocytopoiesis alone. However, it was always believed that megakaryocytopoiesis was controlled by a major growth factor that still had to be discovered. Even though the cytokine TPO was not physically isolated before 1994, the word thrombopoietin was first used in 1958 to describe a factor that would stimulate platelet production in mice and human.[201-203]

In 1994, several groups identified and cloned the humoral factor primarily responsible for MKP and MK proliferation and maturation.[204,205,209] These groups identified TPO, as a molecule that can bind to *c-mpl*,[204,205,209] a cellular proto-oncogene from a human erythroid leukemia cell line with strong homology to *v-mpl,* murine myeloproliferative leukemia virus oncogene.[218,219] Administration of TPO leads to a strong enhancement of MKP/MK proliferation, maturation and polyploidization,[205,207,210] as well as a dramatic increase in platelet numbers.[208] TPO is constitutively produced by kidney and liver, and the control of its production appears not to be at the mRNA levels but to depend on platelet numbers.[220] One of the major mechanism by which TPO regulates

megakaryocytopoiesis appears to be based on the level of free (unbound) TPO available in the blood,[221] such that free TPO levels in the blood are inversely proportional to the amount of platelets.[222] If platelets levels are high, most of the TPO is bound to platelets, leading to a decrease in the megakaryocytopoiesis process. As levels of free TPO increase in the blood after injury or platelet insult, the megakaryocytopoiesis process is induced in order to replace the lost platelets.

TPO was initially thought to be a lineage specific cytokine that induces megakaryocytopoiesis *in vivo* and *in vitro.* However, TPO is now known to have an important role in the biology of several other hematopoietic cell types such as erythrocytes,[223-225] granulocytes/macrophage,[223-225] neutrophils-colony forming cells (CFC),[225] and hematopoietic stem/progenitor cells.[184,225-227] Although TPO is the primary regulator for megakaryocytopoiesis, it has been shown that *c-mpl* and TPO deficient mice still have a reduced level of functional platelets, their numbers being 85% that of WT mice.[206,228] This suggests that other factors can impact megakaryocytopoiesis independently of TPO. It was demonstrated by several groups that SDF-1 can impact thrombopoiesis and in combination with other chemokines can compensate for TPO deficiency.[198,199,205,229,230] In fact, SDF-1 and FGF-4 have recently been shown to have the capacity to palliate TPO deficiency.[200] Simultaneous administration of SDF-1 and FGF-4 to $Tpo^{-/-}$ and *c-mpl*$^{-/-}$ mice, through an adenoviral system, led to a recovery of platelet numbers similar to the one observed in WT mice.[200] It appears that these chemokines are

important for the interaction of MK with sinusoidal BM endothelial cells, promoting their maturation and platelet shedding.[198,200] It was also shown that SDF-1 induces transendothelial MK migration and platelet production *in vitro*[199] and *in vivo*.[230] Moreover, SDF-1 appears to enhance human thrombopoiesis in xenotransplanted NOD/SCID mice.[231] Interestingly, it was shown that SHIP might impact signaling pathways downstream of SDF-1.[27,152] In that study, the authors observed that CXCR4 engagement by its ligand SDF-1, led to phosphorylation and recruitment of Shp-2. In this cell context, Shp-2 was found in a protein complex including the proteins SHIP, cbl, and fyn.[27] Furthermore, SHIP-deficient myeloid progenitors exhibit enhanced chemotaxis towards SDF-1.[152]

When TPO binds to *c-mpl*, it induces phosphorylation and/or activation of an array of signaling molecules including proteins in the JAK/STAT pathway, STAT3, STAT5, Shc, Lyn, SHIP and PI3K.[191,232-236] In that cell context, PI3K converts $PI_{(,4,5)}P2$ to $PI_{(3,4,5)}P3$, the latter can then recruit PH domain containing proteins, leading to Akt activation, increased cell survival and proliferation of MK.[235] Interestingly, TPO activation of PI3K in mature platelets result in enhanced α-granule secretion and thrombin induced aggregation activation.[237]

SHIP has been shown to oppose PI3K signaling by removing the 5' phosphate of $PI_{(3,4,5)}P3$,[2,3,5] and to be phosphorylated following *c-mpl*

engagement by TPO in mature MK and *c-mpl* transfected BA/F3 cells.[235] Therefore, SHIP could block this key signaling pathway downstream of the *c-mpl* receptor [152,238] On the other hand, engagement of *c-mpl* by TPO leads to Shc phosphorylation and association with Grb2/SOS, resulting in the promotion of Ras activation of the MAPK pathways.[24,239,240] Knowing that SHIP can compete with Grb2 for binding to Shc, SHIP could negatively control the MAPK pathway activation.[1] Furthermore, other cytokines that have been shown to play a role in megakaryocytopoiesis are known to stimulate or to depend on SHIP for the dampening of their signaling pathways, including IL-3, c-KitL, and G-CSF.[3,13,22,216,241,242] Interestingly, $Lyn^{-/-}$ mice exhibit an increase in megakaryocytopoiesis.[243,244] Lyn kinase is a negative regulator of cell signaling pathways downstream of receptors for different cytokines including M-CSF and TPO.[45,236] Lyn is known to phosphorylate and recruit SHIP to the membrane after cytokine stimulation of the cells. Since SHIP is important for the negative control of several signaling pathways downstream of cytokines implicated in megakaryocytopoiesis, we hypothesize that SHIP-deficient mice might show an increase in megakaryocytopoiesis and thrombopoiesis.

Aims:

1) Assess the level of MK and MKP in SHIP$^{-/-}$ mice hematopoietic organs by flow cytometry as compare to WT mice.
2) Attempt to identify the factors responsible for the perturbation of the MK compartment.

Results

MKP are Increased in the BM and Spleen of SHIP-Deficient Mice

We analyzed BM, spleen and PB from SHIP$^{-/-}$, SHIP$^{\Delta IP/\Delta IP}$, and their respective WT littermates to determine the size of the MKP compartment *in vivo* by flow cytometry (Figure 20A), using an immunophenotype defined by Hodohara and colleagues,[245] Lin^{-}c-Kit^{+}CD41^{+}, which contains the majority of CFU-Mk activity. We observed an expansion of the MKP compartment in the BM of SHIP$^{-/-}$ and SHIP$^{\Delta IP/\Delta IP}$ mice as compared to their WT littermates (Figure 20Bi). In fact, SHIP$^{-/-}$ and SHIP$^{\Delta IP/\Delta IP}$ BM showed a mean 18.1-fold and 50-fold increase, respectively, in the absolute number of MKP relative to WT controls (Figure 20Bi). However, the numbers of MK, as defined by the immunophenotype Lin^{-}c-Kit^{-}CD41^{+}, were decreased by a mean 2-fold in SHIP$^{-/-}$ and SHIP$^{\Delta IP/\Delta IP}$ BM as compared to WT control (Figure 20Ci).

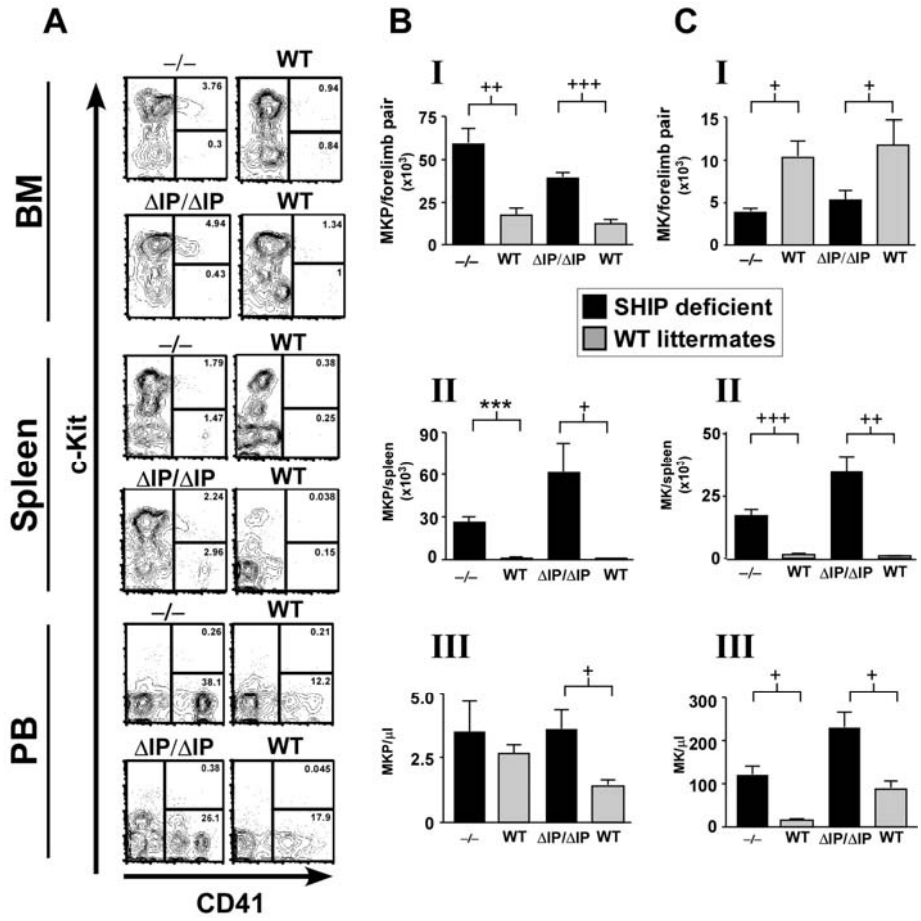

Figure 20. Increased number of MKP in SHIP-deficient BM. (A) Flow cytometry analysis of BM, spleen, and PB from SHIP$^{-/-}$ (-/-) and SHIP$^{\Delta IP/\Delta IP}$ (ΔIP/ΔIP) and WT littermates. Representative flow cytometry plot of c-Kit *vs.* CD41 after gating on live cells and Lin$^-$ cells. MKP are in the upper right quadrant and MK in the lower right quadrant. Percentages for each population are indicated on the plot. (B) Bar graph showing the absolute numbers of MKP (Lin$^-$c-Kit$^+$CD41$^+$) cells in (I) BM (sum of 2 femurs + 2 tibias), (II) whole spleen and (III) per μl of PB. (C) Bar graph showing the absolute numbers of MK (Lin$^-$c-Kit$^+$) cells in (I) BM (sum of 2 femurs + 2 tibias), (II) whole spleen and (III) per μl of PB. Bar graphs showing the different SHIP-deficient models (black) and their respective WT littermates (gray). Data acquired using FACS Calibur, CellQuest software and analysis done with FlowJo. Significance was established using the unpaired student t test (Prism 4): ***p<0.0001, +++p<0.0005, ++p<0.005, and +p<0.05. (mean ± SEM, n≥3). Collaboration with N. Parquet and LE Perez MD.

The observation of splenocytes for the presence of MKP and MK by flow cytometry (Figure 20A, Bii, Cii) revealed that SHIP$^{-/-}$ and SHIP$^{\Delta IP/\Delta IP}$ spleens exhibited higher percentages of MKP and MK as compared to WT littermates (data not shown). The absolute number of splenic MKP was increased by at least 30-fold in both, SHIP$^{-/-}$ and SHIP$^{\Delta IP/\Delta IP}$ mice, as compared to their respective WT littermates (Figure 20B$_{II}$). Furthermore, the absolute number of splenic MK was increased by a mean 10.9-fold in SHIP$^{-/-}$ spleen as compared to WT littermates (Figure 20C$_{II}$). SHIP$^{\Delta IP/\Delta IP}$ mice exhibited an even more dramatic increase in the absolute number of splenic MK as compared to WT control (Figure 20Cii). Analysis of PB for the presence of MK and MKP by flow cytometry revealed that it contains very few MKP, with an average of 3 to 5 MKP/μl. Using this method, we observed that the number of MKP was not significantly increased in SHIP$^{-/-}$ mice when compared to WT (Figure 20B$_{III}$). However, MKP numbers were slightly, but significantly higher, in SHIP$^{\Delta IP/\Delta IP}$ PB as compared to WT littermates (Figure 20B$_{III}$). Furthermore, in the PB of SHIP$^{-/-}$ mice there was a mean 7.7-fold increase in the absolute number of MK and the same trend was observed for SHIP$^{\Delta IP/\Delta IP}$ mice (Figure 20C$_{III}$).

We then combined the number of MKP and MK present in the BM and spleen in SHIP-deficient mice as compared to WT controls (Figure 21). In both, the SHIP$^{-/-}$ and SHIP$^{\Delta IP/\Delta IP}$ mice, the total MKP numbers were increased by a

mean 3.5-fold as compared to their respective WT littermates (Figure 21A). Despite an increase in total MKP numbers in SHIP-deficient mice, we observed that these mice have a comparable total number of MK as compared to WT littermates (Figure 21B). Thus, the decrease in MK numbers observed in SHIP-deficient BM (Figure 20Bi) is compensated for by the increase in splenic MK numbers (Figure 20Ci). This results in SHIP-deficient mice containing a comparable number of total MK as compared to WT littermates.

Figure 21. Total MKP but not total MK numbers are increased in SHIP-deficient mice are compared to WT. The total number of MKP and MK was calculated by adding the absolute number MKP or MK in the spleen and whole BM of one mouse. To calculate the number of MKP and MK in the whole BM of a mouse, multiply the number of MKP or MK in one femur by a 16.6.[156] (A) Total absolute number of MKP in the spleen and whole BM of SHIP-deficient mice and their WT littermates. (B) Total absolute number of MK in the spleen and whole BM of SHIP-deficient mice and their WT littermates. Data acquired using FACS Calibur, CellQuest software and analysis done with FlowJo. Significance was established using the unpaired student t test (Prism 4): +++p<0.0005 and ++p<0.005. (mean ± SEM, n≥3).

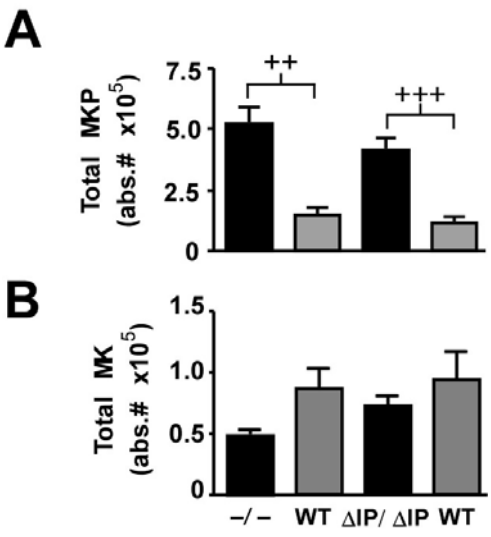

MKP and MK are Increased in BM and Spleen of SHIP-Ablated Mice

To observe if inhibition of SHIP during adulthood could also result in an increase in MKP production, we used the MxCre model. This model is described in the previous section on SHIP and HSC. Briefly, the treatment of MxCRE+$^{fl/fl}$ mice with polyIC will lead to Cre recombinase expression through Type interferon-inducible Mx1 promoter, and deletion of the gene section between two *lox*P sites. In this case, the promoter and the first exon of the SHIP gene will be deleted resulting in the ablation of SHIP expression. As control, MxCre^{-}/SHIP$^{fl/fl}$ are treated with polyIC in the same manner than the MxCRE+$^{fl/fl}$ mice. Twenty-one days after the last polyIC treatment, mice were euthanatized and the level of MKP was evaluated by flow cytometry (Figure 22Ai). As observed in Figure 19Bi we see an increase in the percentage of MKP in the BM and spleen of SHIP-ablated mice as compared to MxCre^{-} mice. Furthermore, we observe that SHIP-ablated BM contains approximately 4 times more MKP than their MxCre^{-} counterpart (Figure 22Bii). As for the germline SHIP$^{-/-}$, we also observe an increase in the percentage of MK present in the spleen (Figure 22Biii). This result suggests that mice that undergo normal development can also exhibit increased MKP numbers once SHIP is deleted during adulthood. This has some therapeutic implication, where SHIP inhibition could be used to increase in megakaryocytopoiesis in adult patients.

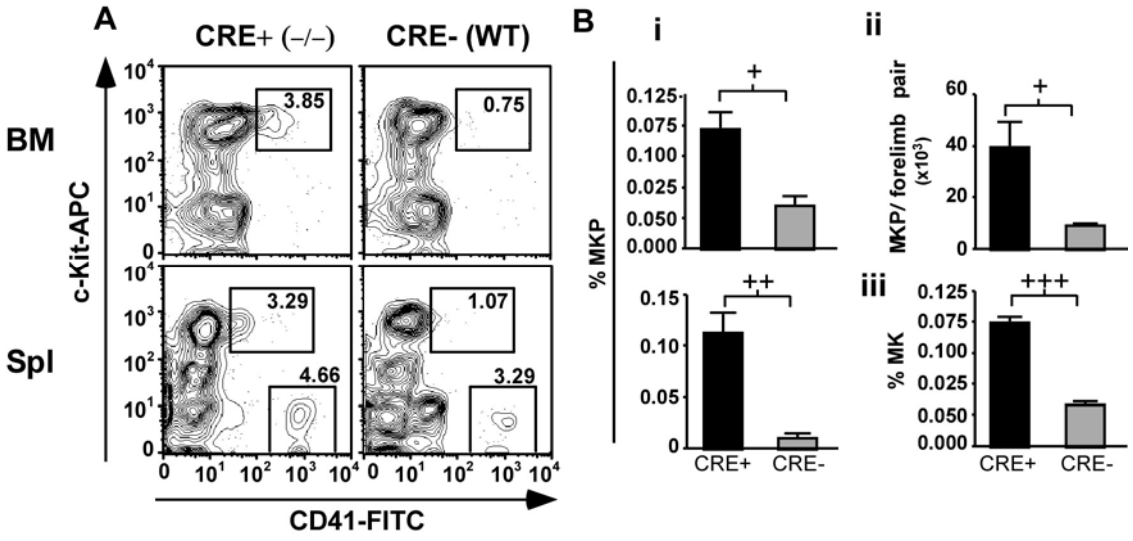

Figure 22. Significant increase in the percentage of MKP cells in SHIP-ablated BM and spleen. MxCre^{+} and MxCre^{-} mice with floxed SHIP alleles were treated with polyIC 3 times prior to being analyzed. (A) Representative FACS plots showing detection of and MK and MKP in the BM and spleen of MxCre^{+} and MxCre^{-} mice after treatment. (B) (i) Percentage of MKP in BM (top), spleen (Spl) (bottom) and of SHIP-ablated (black) and WT (grey) mice. (ii) Absolute number of MKP cells in BM (per femur and tibia pair). (iii) Percentage of MK found in the spleen. Data acquired on a FACS Calibur with CellQuest software (BD Biosciences, San Jose, CA), analyzed with FlowJo. Significance was established using the unpaired student t test (Prism 4). +++$p<0.0005$, ++ $p<0.005$, and +$p<0.05$. (mean ± SEM, n≥3).

Platelet Levels are Lower in SHIP-Deficient Mice as Compared to WT Mice

One striking observation is that despite the profound expansion of the MKP in $SHIP^{-/-}$ and $SHIP^{\Delta IP/\Delta IP}$ mice, these mice do not exhibit increased platelet levels relative to WT controls, when measured by hematolyzer (Table 2). The analysis of $SHIP^{-/-}$ and $SHIP^{\Delta IP/\Delta IP}$ PB revealed that these mice have a significant reduction in their platelet as compared to WT littermates (Table 2). Furthermore, $SHIP^{-/-}$ as well as $SHIP^{\Delta IP/\Delta IP}$ mice PB have a significantly lower percentage of hematocrit. SHIP heterozygous mice platelet and hematocrit levels were not significantly different than the WT levels. The hematocrit percentages and platelet counts observed in PB isolated from SHIP heterozygous mice were not significantly different than the one observed for the WT PB (Table 2) all p values being above 0.5. Except for $SHIP^{+/-}$ PB hematocrit percentage (p=0.072), all heterozygous values shown in Table 2 were significantly difference than the values observed for their respective SHIP-deficient PB.

Table 2. Platelet and Hematocrit counts in SHIP-deficient mice.

Mice genotype	Platelet levels (#x10^3/μl)	Hematocrit (%)
$SHIP^{-/-}$	672.8 ± 43.4^{++}	42.5 ± 1.4^{+}
$SHIP^{+/-}$	848.9 ± 35.7	45.2 ± 0.5
$SHIP^{+/+}$ (C57Bl6)	803.7 ± 31.5	46.6 ± 0.5
$SHIP^{\Delta IP/\Delta IP}$	455.4 ± 81.1^{++}	43.1 ± 1.4^{++}
$SHIP^{+/\Delta IP}$	652.3 ± 28.0	46.8 ± 0.5
$SHIP^{+/+}$(129SvJ)	647.9 ± 28.0	47.0 ± 0.6

$^{+}$ $p < 0.05$ compared to their respective WT littermates
$^{++}$ $p < 0.05$ compared to their respective WT and SHIP heterozygous littermates

SHIP-Deficient MK are Morphologically Different than WT MK

BM histopathology revealed that MK in SHIP$^{-/-}$ BM have a hypolobulated micromegakaryocytic morphology when compared to WT BM, which contains mature hyperlobulated MK (Figure 23A). The increase in MK numbers found by flow cytometry in the SHIP-deficient spleens was corroborated by morphology, where the spleens of SHIP-deficient mice have a qualitative increase in the number of MK (Figure 23B). These observations suggest a shift in the site of megakaryocytopoiesis from the BM to the spleen. This is in agreement with other findings suggesting that the spleen of SHIP-deficient mice becomes the site of intense extramedullar hematopoiesis.[95,156,246]

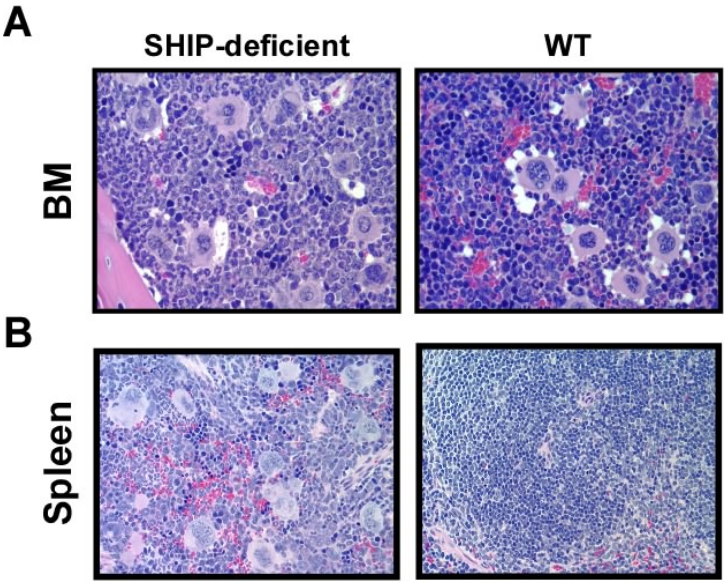

Figure 23. Hematoxylin-eosin staining of SHIP-deficient WT BM and spleen. (A) Hematoxylin-eosin staining of SHIP$^{-/-}$ and WT BM section, photographed at 63x. (B) Hematoxylin-eosin staining of SHIP$^{\Delta IP/\Delta IP}$ and WT spleen section, the images were photographed at 40x (spleen). Cells were visualized on a Leica DM LB microscope. Pictures were taken using a RTcolor Spot camera (Diagnostic Instrument Inc) with Spot Advance v3.0 software. Collaboration with N. Parquet and L.E. Perez MD.

Comparable Ploidy Distribution in SHIP$^{-/-}$ MK as Compared to WT

The hypolobulated micromegakaryocytic morphology of SHIP$^{-/-}$ BM MK cells observed by histology suggested that these cells did not mature properly. Therefore, we evaluated the ploidy distribution in BM and splenic SHIP$^{-/-}$ MK, as endomitosis is an obligatory step towards MK maturation. However, these results revealed that SHIP$^{-/-}$ BM and splenic MK cells have a similar ploidy distribution than WT MK (Figure 24). Thus, SHIP$^{-/-}$ Lin^{-}CD41^{+} cells do exhibit a similar ploidy distribution, thus have a comparable ability to undergo endoreplication as compared to WT Lin^{-}CD41^{+} cells (Figure 24A, B).

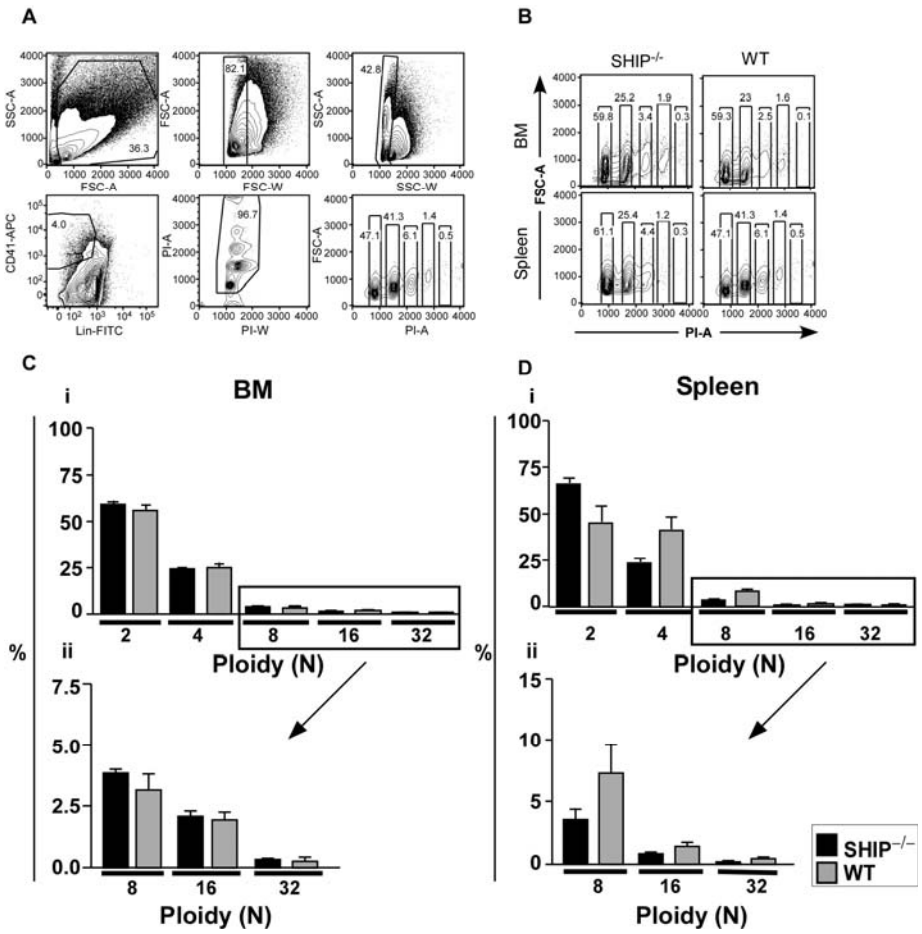

Figure 24. SHIP$^{-/-}$ MK undergo endocytosis with the same efficiency as WT MK. BM cells and splenocytes from SHIP$^{-/-}$ and WT mice were enriched for CD41+ on AutoMACS, stained with Lin-panel and CD41-biotin/SA-APC, fixed/permeated and stained with PI in the presence of RNase. (A) Representative gating strategy to obtain the final FACS plot used to calculate the DNA content of Lin$^-$CD41$^+$ cells. (B) Representative FACS plot used to calculate the DNA content of BM and spleen Lin$^-$ CD41$^+$ cells for SHIP$^{-/-}$ and WT. (Ci) Bar graph representing the percentage of BM Lin$^-$ CD41$^+$ cells in the different ploidy stage visible on the plot. (Cii) Bar graph with emphasis on the higher ploidy distribution for BM Lin$^-$CD41$^+$ cells. (Di) Bar graph representing the percentage of spleen Lin$^-$CD41$^+$ cells in the different ploidy stage visible on the plot. (Dii) Bar graph focusing on the higher ploidy distribution for spleen Lin$^-$ CD41$^+$ cells Data acquired using FACS LSR, DiVaII (BD Biosciences). Statistical analysis was done using the unpaired student t test (Prism 4). (mean ± SEM, n≥3).

TPO Levels are Increased in SHIP$^{-/-}$ Plasma as Compared to WT

It has been proposed that SHIP might contribute in the control of pathways downstream of *c-mpl*, and the lack of SHIP could result in a higher response to TPO stimulation as compared to WT littermates. However, an increase in sera TPO levels could also result in increased megakaryocytopoiesis. Therefore, we assessed the level of TPO in SHIP$^{-/-}$ mice sera. Consistent with the decreased platelet levels (Table 2) and the increased megakaryocytopoiesis (Figure 20) observed in SHIP$^{-/-}$ mice, we saw that SHIP$^{-/-}$ sera contained a significantly higher concentration of TPO as compared to WT mice. ELISA performed on SHIP$^{-/-}$ and WT sera revealed that SHIP$^{-/-}$ sera had a concentration of 12.8 ± 0.2 ng/ml of TPO while WT had 11.67 ± 0.2 ng/ml (Figure 25A). Although this is only a difference of 1.2 ng/ml, it is statistically significant according to an unpaired student t test ($p<0.005$) (Figure 25A). Furthermore, IL-6, a cytokine that has been shown to impact early megakaryocytopoiesis[216] and TPO production during inflammation,[247] was increased in SHIP$^{-/-}$ mice sera as compared to WT (Figure 25B), this was also observed in another SHIP knock-out model at the mRNA level. However, not all factors shown to impact megakaryocytopoiesis were increased in SHIP$^{-/-}$ mice as shown in Figure 25C, LIF levels in SHIP$^{-/-}$ mice were not significantly different from WT mice. The increase in IL-6 and TPO observed in SHIP$^{-/-}$ sera could contribute to the increase in megakaryocytopoiesis observed in these mice.

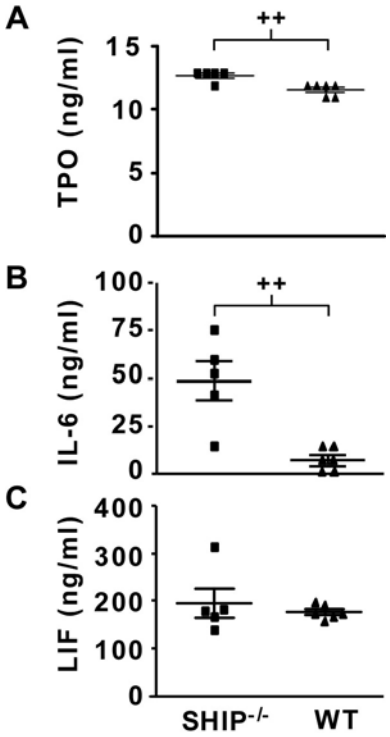

Figure 25. TPO levels are significantly increased in SHIP$^{-/-}$ sera as compared to WT littermates. Mice were bled by sub-mandibular bleeding and the blood was collected in regular Eppendorf tube to allow coagulation. The sera was then collected and sent for analysis by ELISA (Charles River Laboratories Inc.). (A) Levels of TPO in SHIP$^{-/-}$ (square) and WT (triangle) sera. (B) Levels of IL-6 in SHIP$^{-/-}$ (square) and WT (triangle) sera. (C) Levels of LIF in SHIP$^{-/-}$ (square) and WT (triangle) sera. Significance was established using the unpaired student t test (Prism 4). ++ $p<0.005$ (mean ± SEM, $n\geq3$). Collaboration with D. Woods and WG Kerr Ph.D.

Discussion

The ablation of SHIP results in an augmentation of MKP production. However, we observe that the total number of MK in SHIP-deficient mice is comparable to the one observed in WT. The decrease number of MK in the BM of SHIP-deficient mice appears to be compensated for by a dramatic increase in splenic MK. Therefore, there are some indications that in SHIP-deficient mice the mature MK leave the BM prematurely to be found in the periphery, in the spleen and PB. The shift in MK localization from the BM to the periphery might result from an increased responsiveness to SDF-1, which can cause trans-endothelial migration of MK from the BM to the circulation.[198-200] Thus, SHIP may participate in the control of pathways downstream of CXCR4 mediating MK migration, as it does in myeloid progenitors.[152] Alternatively, the increase in peripheral MK might result from extramedullar hematopoiesis as it was shown that SHIP-deficient spleen contain elevated levels of HSC[156,246] and hematopoietic progenitors (Figure 21B).[95]

We observe that MK cells in the BM of SHIP-deficient mice are hypolobulated and less mature than the one found in WT BM by looking at morphology (Figure 23). This would suggest that SHIP-deficient BM MK cells do

not mature properly. However, we observed that BM, like splenic, SHIP$^{-/-}$ MK exhibited a comparable ploidy distribution as the one seen for WT MK cells. This result suggests that the SHIP-deficient BM MK mature as well as WT BM MK. Alternatively, SHIP$^{-/-}$ MK might exit the BM prematurely, before the shedding of platelets, as they might be more responsive to SDF-1 induced migration signaling.

Platelet levels limit megakaryocytopoiesis by sequestering TPO.[216] These platelets have *c-mpl* receptors on their surface that can bind TPO molecules.[248] Therefore, it has been suggested that the level of free-TPO in circulation is inversely proportional to platelet levels.[249] Thus, a decrease in platelet levels would cause an increase in free-TPO and stimulate megakaryocytopoiesis in order to replenish the platelet stock. In SHIP-deficient mice, we observed a significant decrease in platelet levels and, consequently, a significant increase in TPO levels as compared to WT controls. The increase in free-TPO might stimulate the proliferation and/or survival of MKP in SHIP-deficient mice, leading to an expansion of the megakaryocytic compartment. Furthermore, SHIP-deficient MKP could be hyper-responsive to the free-TPO available since it was shown previously that SHIP is phosphorylated after *c-mpl* engagement with TPO in primary MK and *c-mpl* transfected Ba/F3 cells.[235]. Administration of TPO to patients or test animals causes the increase in platelet levels only a few days, 3 to 5, after treatment.[250] This suggests that TPO does not regulate directly release of platelet but mainly the proliferation and maturation of MKP and MK

respectively. Thus, the increase in MKP numbers but not in platelet levels in SHIP$^{-/-}$ mice might further suggest that megakaryocytopoiesis and platelet shedding are regulated by different mechanisms.

Furthermore, it is worth noting that SHIP has been shown to be present in human platelets and to be responsible for the production of $PI_{(3,4)}P2$ during aggregation dependent activation of platelets. $PI_{(3,4)}P2$ in human platelets was shown to mediate actin assembly for filopodial growth,[251] and sustained exposure of integrin GpIIB-IIa leading to irreversible aggregation.[251-253] This process is probably hindered in SHIP-deficient platelet since it is responsible for removing the 5' phosphate of $PI_{(3,4,5)}P3$, to create $PI_{(3,4)}P2$. Thus, SHIP-deficient platelet might have compromised function, affecting their activation status and causing premature elimination from the circulation.

As mentioned earlier, we observe a significant decrease in the mean platelet numbers in SHIP$^{-/-}$ mice as compared to WT mice. This could in part explain the increase in TPO levels observed in these mice. However, researches have shown that inflammation can contribute to increasing TPO production.[247] Actually, cytokines produced by monocytes, including macrophages, can induce a chain reaction, involving an increase in IL-6 levels, promoting increased production of TPO by the liver.[191,247] SHIP$^{-/-}$ mice have increased number of macrophages in their BM, spleen and periphery,[95] and we observe that these mice exhibit significantly higher IL-6 levels (Figure 25B). In fact, we observed

that SHIP$^{-/-}$ mice have 49 pg/ml of IL-6 in their sera as compared to 1 pg/ml for WT (Figure 25B). This increase IL-6 sera concentration could induce TPO production by the liver

Furthermore, we observe that both SHIP-deficient models exhibit a decrease in hematocrits as compared to their respective WT (Table 2). Helgason *et al* reported that F2 SHIP$^{-/-}$ mice (129 mice backcrossed twice to C57Bl6 mice) have no difference in hematocrit levels compared to WT. However, a more recent publication reveals that F6-7 SHIP$^{-/-}$ mice exhibit a significant decrease in hematocrit levels as compared to WT.[254] In this later paper, it was mentioned that the increased severity of the erythroid defect might result from backcrossing onto C57Bl6 strain. However, since the SHIP $^{\Delta IP/\Delta IP}$ mice are on a mixed background, this explanation seems unlikely. Looking back at the data published in 1998, there was already a great difference in the percentage of hematocrits between WT and SHIP-deficient mice with 50.7±1.0% for WT versus 42.4±5.7 for SHIP-deficient mice. However the standard error mean was large for SHIP-deficient mice, probably caused by a small sample population.[95] In the second study, they seem to have used a larger sample group,[254] which could have helped reduce the standard error mean, and show a significant difference between the two sample groups.

Our results suggest that SHIP negatively controls pathways promoting early megakaryocytopoiesis. However, the fact that we observe a similar level of MK in SHIP$^{-/-}$ and WT mice suggests that different pathways control MKP proliferation, MK maturation and platelet shedding. On the other hand, SHIP-deficient MK could leave the BM prematurely due to increased responsiveness to SDF-1, which could hamper MK maturation and the platelet shedding process.

These findings suggest that SHIP could be targeted *in vivo* to increase the pool of MKP, and subsequently enable this compartment to replenish platelets more rapidly following myeloablative chemotherapy and radiation treatment. However, this assumes that SHIP deficiency does not adversely impact MK maturation, platelet shedding from MK or platelet function.

Materials and Methods

Mice Strains

SHIP$^{-/-}$ mice (F9 or F10 X C57BL6/J) produced in our laboratory have a deletion of the SHIP promoter and first exon.[43] A second SHIP-deficient mouse model was also analyzed, SHIP$^{\Delta IP/\Delta IP}$ (129SvJ),[97] in which the inositol phosphatase domain is deleted was kindly provided by Dr. Jeffrey Ravetch, Rockefeller University, NY, USA. All studies described herein were conducted on six to eight week-old adult mice. For the inducible model, SHIP fl/fl mice were

backcrossed to MxCre germline. The resulting MxCre+$^{fl/fl}$ and MxCre-$^{fl/fl}$ mice were treated 3 times with 625 μg polyIC in the course of 7 days. Mice were analyzed at least 21 days after the last injection. Experiments were performed in compliance with institutional guidelines of the University of South Florida.

Cell Isolation

Isolation of BM cells and splenocytes was as described previously.[246] Following red blood cell (RBC) lysis, the cells were resuspended in staining media..[246] PB was obtained from the retro-orbital sinus, sub-mandibular bleed or heart puncture. For MKP analysis of PB, RBC were lysed twice in 1x RBC lysis buffer (eBioscience). Cells were then resuspended for antibody staining.

Flow Cytometry Analysis and Antibodies

Staining of MKP and MK was performed as per Hodohara *et al*[245] All antibodies were from BD Biosciences except when mentioned otherwise. The cells were treated with anti-CD16/CD32 (2.4G2) to block Fc receptors and then stained with a Lin panel-PE, CD41-FITC(MWReg30), and c-Kit-APC(2B8). The Lin- panel was CD3ε(17A2), CD4(GK1.5), CD8α(53-6.7), B220(RA3-6B2), Gr-1(RB6-8C5), Mac-1 (M1/70) (Caltag, Burlingame, CA) and Ter119(TER-119). Dead cells were excluded using 7-AAD (BD Biociences). Data was acquired on

a FACS Calibur using the FACS Quest software and analysis was done using FlowJo 4.5.

Platelet Analysis

Blood was collected by heart puncture or sub-mandibular bleed and platelets were quantified using the CellDyn 3700 hematology analyzer (Abbott Diagnostic, Dallas, Texas USA).

Histopathology

Bone and spleen were fixed in 10% buffered paraformaldehyde. Bone were first decalcified using Routine Acid Decalcification (RDO; Apex engineering Products, Plainfield, IL, USA), followed by sectioning. The spleen and bone sections were then stained with hematoxylin-eosin after being deparaffinized with xylene. Briefly, slides were stained using the modified Meyer's hematoxylin and eosin phloxine B solution (Fisher Scientific, Suwanee, GA, USA) according to a modified Armed Forces Institute of Pathology (AFIP) protocol. Cells were visualized on a Leica DM LB microscope. Pictures were taken using a RTcolor Spot camera (Diagnostic Instrument Inc) with Spot Advance v3.0 software.

Ploidy assay

BM cells were isolated from hind/fore limb and vertebral column. Briefly, cells were incubated with CD41-biotin antibody (Serotec, Raleigh, NC, USA) on ice and then with anti-biotin beads (Miltenyi Biotec) at 4°C. $CD41^+$ cells were then selected using the autoMACS (Miltenyi Biotec). Collected $CD41^+$ cells were stained with Lin panel-FITC as mentioned above and with streptavidin-APC (BD Biosciences). The cells were fixed in 1% formaldehyde (Sigma-Aldrich) for 15 minutes on ice and then incubated overnight in a 70% ethanol solution at -20°C. The day after, the cells were washed carefully of any residual ethanol with PBS and incubated for at least 3 hours in a propidium iodine (PI) solution composed of 50 μg/ml PI, 0.1% Triton X-100, 2.5U/ml RNase in PBS without Ca or MG (all from Sigma-Aldrich except for the PBS which was from Gibco BRL/Invitrogen).

Measurement of Cytokines and Growth Factors Levels in the Sera of Experimental Mice

Blood was obtained by sub-mandibular bleed, collected in a regular Eppendorf tube and left at RT for 4 hours to allow coagulation. The blood was then stored at 4°C overnight. The following day, blood clots were removed using a wooden stick and the remaining blood was centrifuged at 4000 RPM for 10 minutes at 4°C. The sera was then isolated by taking the supernatant and sent for analysis at a custom based service at Charles Rivers Laboratories Inc., where ELISA for multiple cytokines and growth factors was performed.

Section III: Natural Killer Cells and SHIP

Introduction to Natural Killer Cells

NK cells were first defined as a cell fraction residing in the spleen, with the ability to spontaneously kill tumor cells without prior immunization.[255-257] However, it is now known that NK cells are found in the BM, liver and PB. NK cells are derived from the same progenitor cell as T-lymphocytes, either the common lymphocyte progenitor in BM or the NK-T cell precursor in fetal liver.[258] Although common in origin key difference do exist between the two cell types. One primordial distinction is that NK cells do not undergo the maturation process that T-cells go through in the thymus and are unable to accomplish gene rearrangement for the production of antigen specific receptors.[259] Furthermore, NK cells are part of innate immunity, and the first line of defense of an organism against viral infection and tumorigenic transformation of host cells.[255-257] These cells can kill target cells either by direct cell-mediated cytotoxicity or by secretion of soluble factors. To this effect they can produce diverse cytokines, such as IL-5, IL-10, IL-13 and GM-CSF.[260] However, NK cells secrete predominantly interferon-γ (IFN-γ), which helps control tumor cell proliferation and kill virally infected cells.[261,262] In fact, it was shown that NK cells store IFN-γ transcripts,[263]

which can be rapidly released upon stimulation. They also express molecules member of the Tumor necrosis factor (TNF) family such as, TNFα, Fas ligand (FasL) and TNF related apoptosis inducing ligand (TRAIL), which bind to death domain-containing receptors on target cells causing their apoptosis.[264,265] Most importantly, NK cells contain granules storing perforin and granzyme,[266-268] all of which can be secreted shortly after stimulation. For example, perforin dependent cytotoxicity can be mediated within 20 minutes after activation of NK cells.[269] Thus, as soon as these cells encounter a potential target, they are ready for action. It is therefore suited that NK cells be tightly regulated by an array of receptors that trigger activation and inhibitory response depending on the target cell and cytokines present.[270] This fine balance between inhibition and activation prevents inadvertent killing of normal healthy host cells.

Activation of NK cells by engagement of activating receptors leads to the stimulation of kinases that triggers cytolysis of target cell. The whole process remains to be further elucidated, but to date we know that several molecule become phosphorylated or recruited during NK cells activation, including Syk,[271] SLP-76,[272] ZAP-70,[273] Linker for activation of T cell (LAT),[274] Shc,[275] PI3K,[276,277] PLCγ1 and 2.[278-280] Interestingly, it was observed that NK cells ablated for Syk and ZAP-70 can develop normally and lyse tumor cells *in vitro* and *in vivo.*[281] Thus, these molecules are used for activation of NK cells but are not essential. On the other hand, simultaneous inhibition of PI3K and Src kinases prevented

the cytolytic activity of these mutant NK cells and strongly reduced that of WT NK cells, suggesting that distinct and redundant signaling pathways act in a synergistic manner to trigger cytotoxicity.[281] To this end, PI3K is known to mediate the production of $PI_{(3,4,5)}P3$, which lead to calcium increase and activation of PLCγ molecules. PLCγ-2 ablated NK cells were shown to be greatly reduced in their ability to lyse target cells and secrete IFN-γ in response to stimulation of signaling pathways mediated by DNAX adapter protein-10 (DAP-10), which contains an ITAM motif.[279] Furthermore, PLCγ-2 ablated NK cells have a disrupted receptor repertoire, particularly for Ly49 receptors.[279]

NK Cell Receptors

As mentioned above NK cell cytotoxic activity is regulated by a fine balance between activating and inhibitory receptors. The inhibitory receptors expressed by NK cells are many and differ in structure and ligand specificity. These receptors are encoded in a defined region on chromosome 6 that was named “the NK cell gene complex”.[282] This chromosomal region encodes for series of receptor molecules that can form disulfide–bound homodimers, characterized by being type II integral membrane proteins with C-type lectin domains. The NK cell gene complex encode for the activation receptor such as CD69[283] and for members of the Nkrp1 (NKR-P1A, B, C) multigene family.[282,284] Nkrp1-C, also called NK1.1, and part the of the Nkrp1 family[285] is expressed on

NK cell and a subset of T cells, and even though its ligand is unknown it is believed that NK1.1 is an activation molecule since antibody cross-linking leads to activation of NK cells and lysis of target cells.[286] Most importantly for this work, the NK cell gene complex encodes for members of the Ly49 receptor family, which is composed of at least 23 members (Ly49A through W) (Table 3).[287] The ligands for 14 of these receptors are known so far (Table 3).[287]

Table 3. Functions and ligands of Ly49 NK cell receptors

Receptor name	*Function*	*Cellular Ligands*	*Viral ligand*
Ly49A	Inhibitory	D^b, D^d, D^p, D^k	
Ly49B	Inhibitory	?	
Ly49C	Inhibitory	K^b, K^d, K^k, D^d, D^b	
Ly49D	*Activating*	D^d	
Ly49E	Inhibitory	?	
Ly49F	Inhibitory	D^d	
Ly49G	Inhibitory	D^d, L^d	
Ly49H	*Activating*	D^b	MCMV-m157
Ly49I	Inhibitory	K^d	MCMV-m158
Ly49J	Inhibitory	K^b	
*Ly49K**	*Activating*	?	
Ly49L	*Activating*	K^k	
Ly49M	*Activating*	?	
*Ly49N**	*Activating*	?	
Ly49O	Inhibitory	D^b, D^d, D^k, L^d	
Ly49P	*Activating*	D^d	
Ly49Q	Inhibitory	?	
Ly49R	*Activating*	D^d, D^k, L^d	
Ly49S	Inhibitory	?	
Ly49T	Inhibitory	?	
Ly49U	*Activating*	?	
Ly49V	Inhibitory	D^b, D^d, K^k	
Ly49W	*Activating*	D^d, K^k	

* To date no full length transcript have been found

These receptors are disulfide–bound homodimers, type II trans-membrane proteins with C-type lectin-like domains. Ten of these appear to be activating receptors, of which some bind MCH class I molecules while others recognize MHC–like molecules produced by viruses. For example Ly49H recognizes m157 molecules produced by murine cytomegalovirus infected cells.[288,289] Ly49 activating receptors contain no ITIM motif and do not seem to become phosphorylated upon engagement with ligand. Instead they necessitate the interaction with ITAM-containing adapter molecule to exert their effect, such as death adapter protein 12 (DAP12),[290] CD3ζ,[291] DAP10,[292,293] and FcεRIγ,[294] the latter being responsible for binding to CD16 and stimulate antibody-dependent cellular cytotoxicity (ADCC).[295] DAP12 is a 16kDa protein with an aspartic acid residue in its transmembrane region, which can interact with the asparagine on Ly49D transmembrane region upon its engagement.[296] After this interaction, tyrosine in the ITAM of DAP12 becomes phosphorylated,[297] which leads to a activation of signaling events involving the phosphorylation of Syk, PLCy-1 and calcium mobilization.[290,296] It was also shown that the SH2 domain of Syk can interact with DAP12 phosphorylated tyrosine.[296,297] The activation and/or phosphorylation of these effector molecules will lead to the release of perforin, granzyme and cytokines to kill the target cell and stimulate a complete immune response.

The activation of NK cells has to be counterbalanced by inhibitory signaling in order to prevent inadvertent attack of host cells. To this effect, NK cells rely on the presence of inhibitory receptors that recognize MHC class I molecules on host's cells such as receptors of the Ly49 receptors family. The inhibitory receptor Ly49A was the first one to be cloned from the NK cell gene complex.[298] The human counter part of the Ly49 inhibitory receptors are the killer cell inhibitory receptors (KIRs), which belong to the Ig superfamily.[299] KIRs and Ly49 receptors evolved separately into totally different molecules that both have the ability to negatively control NK cell activation through recognition of MHC Class I molecules. Furthermore, they both exhibit a cytoplasmic ITIM sequence, and both were observed to associate with Shp-1 and/or Shp-2 after engagement, leading to inhibitory signaling.[300,301]

Like human KIRs, murine Ly49 receptors such as Ly49 A, C, G2 and I, have a cytoplasmic ITIM motif that becomes tyrosine-phosphorylated upon engagement by self MHC class I molecules.[302-304] The murine ITIM sequence was first identified as a 13 amino acid sequence on FcγRIIB receptor necessary for inhibitory function.[305,306] ITIMs are now know to be present in several receptors involved in immunological processes and are usually composed of 6 amino acids (I/V/L/S)-X-Y-X-X-(L/V).[307] Upon engagement of inhibitory receptors, such as Ly49A and G2, the tyrosine residue in the ITIM becomes phosphorylated and can then recruit molecules that contain a SH2 domain such

as Shp-1[308] and possibly Shp-2.[309] Once activated, these molecules can then dephosphorylate and therefore deactivate Syk, PLCγ-1/2, ZAP70, and Shc, which would participate in the stimulation of cytotoxic response.[310] These inhibitory receptors are responsible for preventing unwanted attack against host cells, however, once an infected or cancerous cells down-regulate expression of their MHC class I molecule, Ly49 inhibitory receptors can not be engaged and NK cells are then free to kill. This process was first described by Karre and his colleagues, who observed that an H-2B deficient lymphoma was rejected by the host, while a lymphoma that expressed MHC molecules would engraft in the host. They named this concept the "missing-self hypothesis" (Figure 26).[311] It was later confirmed by other groups who noticed that β2-microglobulin deficient cells would get rejected by irradiated MHC-matched mice while β2-microglobulin expressing cells could engraft successfully.[312,313] These studies relate that NK cells will be inhibited from killing a possible target cell when this one expresses the right MHC molecules. The MHC molecules bind inhibitory receptors on NK cells, which then block activation pathway.

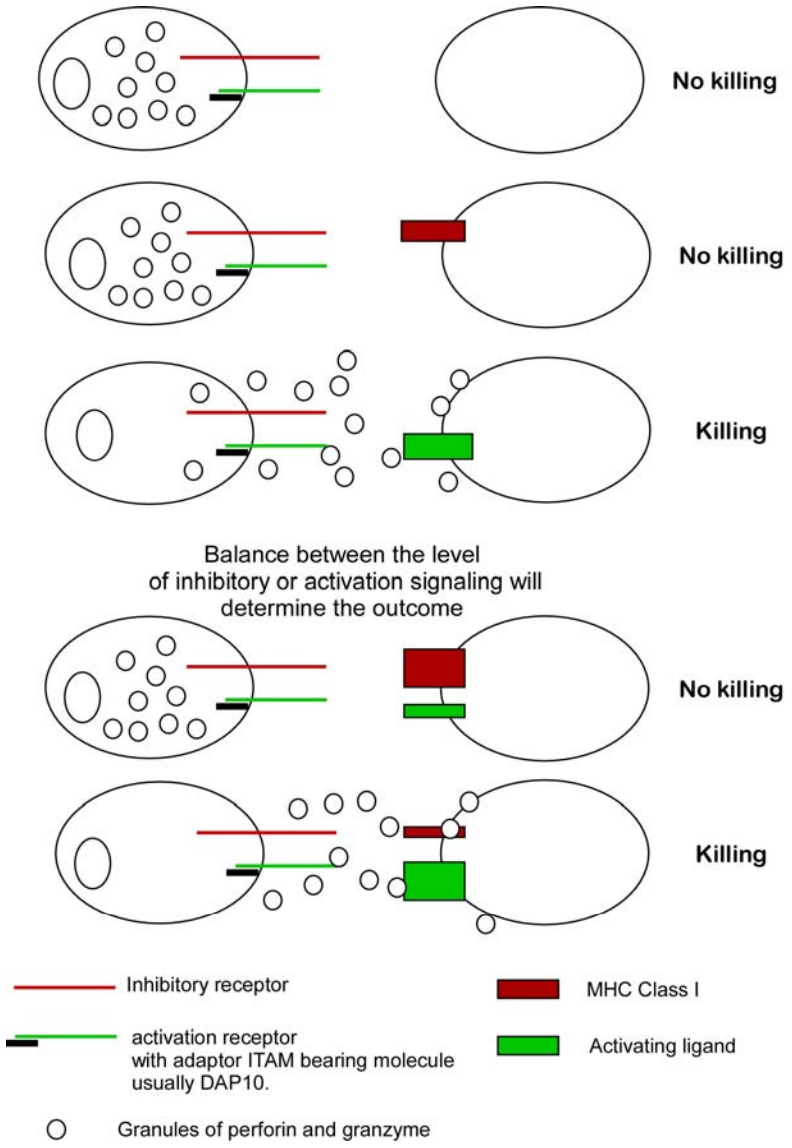

Figure 26. Missing-self hypothesis. Graphic representation of the possible outcomes when a NK cell encounters a possible target cell. MHC class 1 or non-MHC class I molecules expressed by the host can be recognized by inhibitory receptors on NK cells, dampening the possible response of NK cells. The level of activation and inhibitory signal received by the NK cell, and the qualitative difference in the signal transduced will determine the NK cell response. Loosely adapted from Lanier review on NK cells published in 2005.[314]

SHIP and NK Cell Development

The transcriptional regulation of Ly49 receptors remains to be fully elucidated. Why is their expression variegated? Why do certain subset of NK cells in the same individual express different but overlapping Ly49 receptors on their surface? Right before the proliferation phase, immature NK cells, which already express NK1.1 and the CD122 (IL-2 and IL-15 receptor β) receptor, acquire CD94-NKG2 and Ly49 receptors.[315] Thus, it is possible that upon acquisition of the Ly49 receptors, the cell subset that bear Ly49 engaged by the host MHC Class I molecules would be prompt to survive or proliferate. To this end, the Ly49 receptors specific for the host MHC molecule would guide the proliferation and survival of the NK cell subset that expresses it. Consistent with this hypothesis, the p85 subunit of PI3K can be recruited to the membrane by inhibitory Ly49 receptors to promote formation of $PI_{(3,4,5)}P3$. Even though that molecule has been implicated in the simulation of NK cells through activation of PLCy, it is possible that $PI_{(3,4,5)}P3$ recruit the PH containing protein AKT, which will promote survival and proliferation of the cell. Since SHIP contains an SH2 domain, it could be recruited to the membrane by Ly49 receptor phosphorylated ITIM motifs, where it would negatively control the survival and/or proliferation signal received by NK cells through dephosphorylation of $PI_{(3,4,5)}P3$. This event would prevent over-representation of a certain subset of receptors, thus, maintaining a proper repertoire of Ly49 receptor on NK cells.

Aims::

1) Define the NK cell compartment in SHIP$^{-/-}$ mice.

2) Identify factors contributing to the disruption of NK cell receptor repertoire.

Results

Spleen of SHIP$^{-/-}$ Have Increased Number of NK Cells

Analysis of the NK compartment in the spleen at different stages of ontogeny indicated that NK cells develop normally in juvenile SHIP$^{-/-}$ mice (Figure 27Ai, B). However, in SHIP$^{-/-}$ adult mice an abnormal population of NK cells appears that exhibit a 10-fold increase in the surface expression level of the NK receptor, NK1.1 (NK1.1^{hi}), as compared to WT controls (Figure 27Aii, Aiii). The NK1.1^{hi} population lacks CD3 and thus is not an NK-T cell population. The appearance of the NK1.1^{hi} population coupled with an increase in NK cells with a normal 2B4^{+}NK1.1^{+} staining profile (NK1.1^{+} cells) leads to a 2 to 3-fold increase in peripheral NK cells in SHIP$^{-/-}$ adult mice ($\geq$8 weeks), relative to wild-type littermates (Figure 27B).

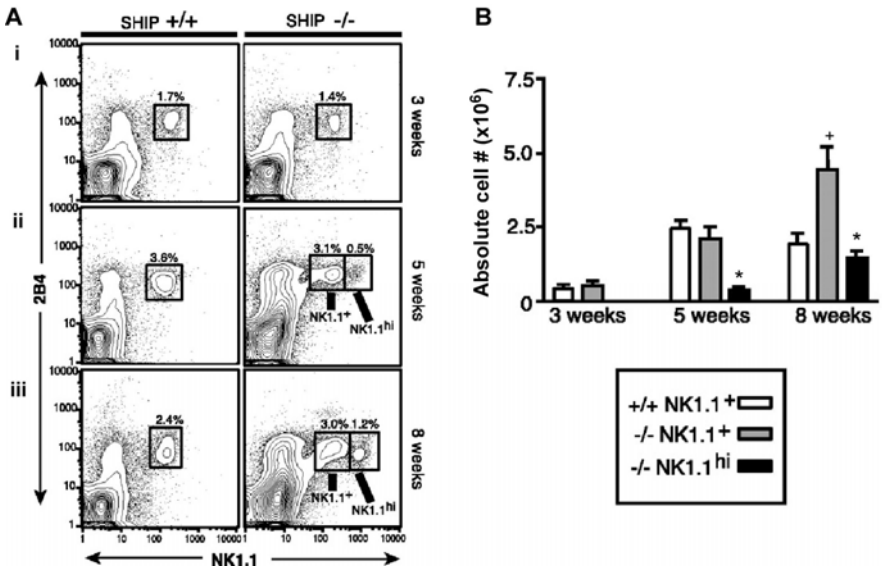

Figure 27. Increased NK cell numbers in SHIP$^{-/-}$. (A) FACS analysis of splenic NK cells in SHIP$^{+/+}$ and SHIP$^{-/-}$ littermates at different stage of ontogeny, at (i) 3, (ii) 5, and (iii) 8 weeks. Genotype and age of the mice at the time of sacrifice and analysis are indicated.. (B) Absolute splenic NK cell numbers in SHIP+/+ and SHIP-/- mice at different ages. Significance was established using the unpaired student t test (Prism 4). (mean ± SEM, n≥3). The values determined for SHIP$^{-/-}$ mice that are significantly different from that of their age-matched SHIP$^{+/+}$ counterparts are indicated by the following symbols: +p<0.05 and,* p<0.01. Collaboration with J. Howsen, T. Ghansah Ph.D., S. May and K.HT Paraiso MS.

Murine NK cells detect MHC class I molecules using receptors encoded by the Ly49 or CD94/NKG2 genes.[316] Expression of these MHC receptors is distributed among different NK subsets during the transition from neonate to adult. Because the number of peripheral NK cells increases in $SHIP^{-/-}$ mice during this period, we asked whether the relative representation of NK subsets expressing certain Ly49 and CD94 receptors might account for this increase. Indeed, the relative representation of several Ly49 receptors and CD94 was significantly altered in the $SHIP^{-/-}$ NK compartment of older mice when compared to $SHIP^{+/+}$ littermates (Figure 28). However, $SHIP^{-/-}$ weanlings, at 3 weeks of age, showed no skewing of their NK repertoire relative to wild-type littermates (Figure 28).

The NK cell receptor repertoire distortion was most pronounced in mice $\geq$8 weeks of age and was found in both the $NK1.1^{+}$ and the $NK1.1^{hi}$ populations. We found that $Ly49A^{+}$ and C/I^{+} NK cells were overrepresented in adult $SHIP^{-/-}$ mice, while $Ly49D^{+}$, $G2^{+}$ and $CD94^{+}$ were underrepresented (Figure 28). Because the overwhelming majority of the $NK1.1^{+}$ and $NK1.1^{hi}$ cell populations lacked Ly49I in adult $SHIP^{-/-}$ mice, the majority of the $Ly49C/I^{+}$ NK cells express only Ly49C. Thus, the repertoire distortion in adult $SHIP^{-/-}$ mice leads to an NK compartment dominated by a subset of cells expressing Ly49A and/or Ly49C, where Ly49D, G2, I can CD94 are underrepresented (Figure 28). *In vitro* and *in vivo* studies indicated that Ly49A and Ly49C can bind ligands in the H2b haplotype of $SHIP^{-/-}$

mice; however, these two receptors also bind and transmit inhibitory signals from ligands in most or all H2 haplotypes.[317-320] Therefore, SHIP deficiency leads to an NK inhibitory repertoire that is both, self-specific and promiscuous for other ligands.

A potential explanation for the repertoire disruption seen in SHIP$^{-/-}$ NK cells is that SHIP is recruited to certain inhibitory receptors expressed by NK cells to oppose intracellular signals that mediate survival of specific NK subsets expressing these receptors. Indeed, SHIP binds the phosphorylated ITIM motif of Ly49A *in vitro.*[42] These findings prompted us to examine whether SHIP associates *in vivo* with Ly49 receptors expressed by NK cells.

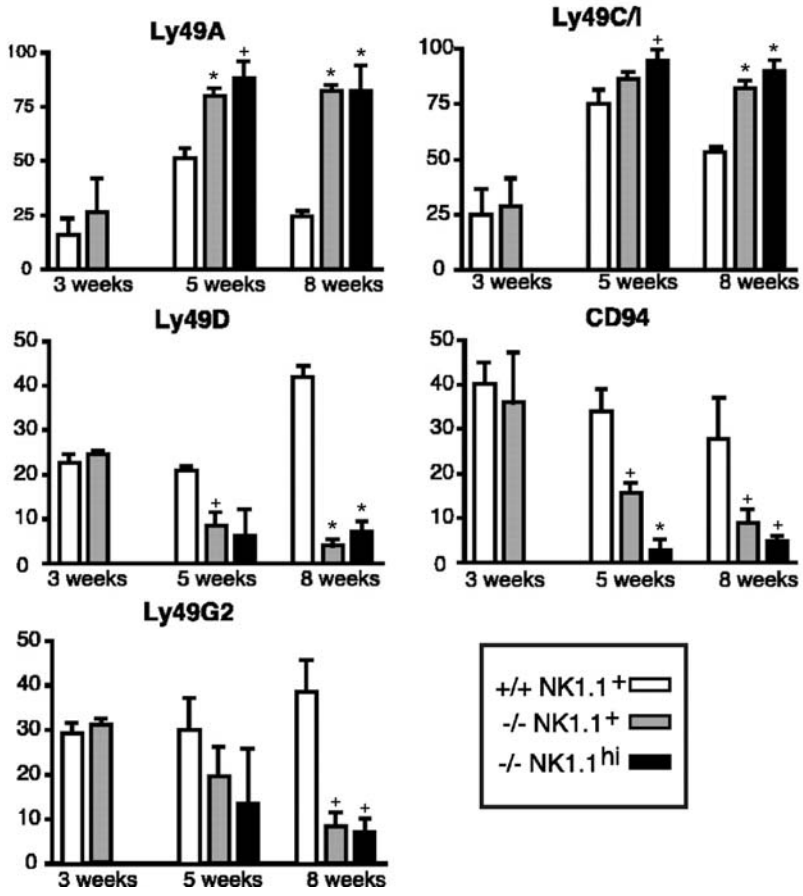

Figure 28. MHC class I receptors on peripheral NK cells in SHIP$^{-/-}$ mice. The mean percentage of peripheral NK cells expressing the indicated Ly49 or CD94 molecule after gating on 2B4^{+}NK1.1^{+} cells. The age and genotype of the mice are indicated. Significance was established using the unpaired student t test (Prism 4). (mean ± SEM, n≥3). Values determined for SHIP$^{-/-}$ mice that are significantly different from their age-matched SHIP$^{+/+}$ littermates are indicated: +p<0.05; * p<0.01. Collaboration with J. Howsen, T. Ghansah Ph.D., S. May and K.HT Paraiso MS.

SHIP is found associated with Ly49 receptors where it may control the level of $PI_{(3,4,5)}P3$ generated by PI3K and negatively regulate Akt phosphorylation

Analysis of potential SHIP interaction with different Ly49 receptors, revealed that SHIP is associated with Ly49A and Ly49C under physiological conditions (Figure 29A), but not with Ly49G2, Ly49F, or Ly49I (Figure 29B). As further confirmation that the protein co-precipitating with Ly49A and Ly49C is SHIP, we analyzed NK lysates from $SHIP^{+/+}$ and $SHIP^{-/-}$ mice (Figure 29C).

This analysis detected co-precipitation of SHIP with Ly49A and Ly49C only in the $SHIP^{+/+}$ NK lysates, confirming the specificity of the Western Blot. Because SHIP limits the *in vivo* survival of myeloid cells by opposing the PI3K/Akt pathway,[2,3] we examined whether Akt is activated in $SHIP^{-/-}$ NK cells *in vivo* based on its phosphorylation at Thr308.[321,322] We found that both Akt phosphorylation and total Akt protein levels were significantly increased in $SHIP^{-/-}$ NK cells relative to those in $SHIP^{+/+}$ NK cells (Figure 29D). The increase in total Akt levels is surprising; however, primary B cell activation leads to increased Btk levels in a PI3K-dependent manner.[323] This additional level of regulation may further amplify signals from PH domain-containing kinases, such as Akt or Btk, which are recruited to $PI_{(3,4,5)}P_3$. Taken together, these findings suggest the interplay of SHIP and PI3K may influence the relative survival of NK subsets expressing Ly49 receptors capable of recruiting these enzymes. Interestingly,

PI3K is recruited to human KIR and can activate Akt in human NK cells.[324] Thus, despite their evolutionary divergence in how they bind MHC class I molecules, murine Ly49 receptors and human KIR may recruit SHIP to limit the *in vivo* survival of NK subsets, just as both receptors recruit Shp-1 to limit NK effector functions.[310,325]

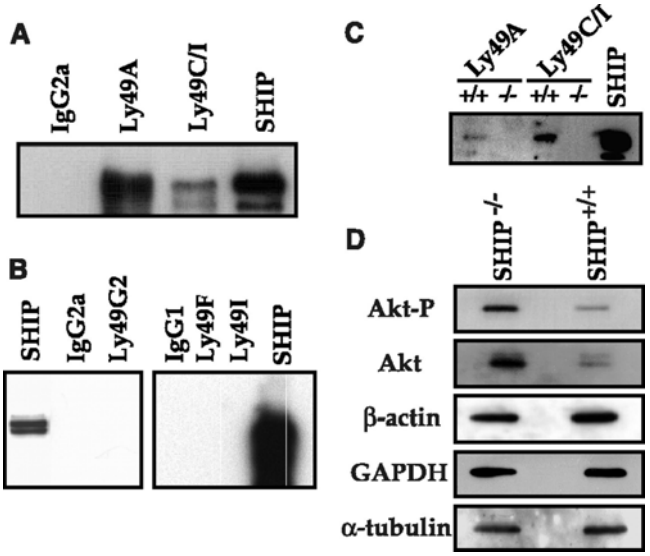

Figure 29. SHIP is recruited to NK inhibitory receptors in vivo to oppose activation of Akt. (A) Western blot detection of SHIP in Ly49A and Ly49C immunoprecipitates. Immunoprecipitation with a murine IgG2a antibody (IgG2a) was analyzed as a negative control and SHIP was immunoprecipitated as a positive control (SHIP). (B) Western blotting for SHIP in other Ly49 immunoprecipitates (Ly49G2, Ly49F, and Ly49I). (C) Western blot analysis of SHIP in Ly49A and Ly49C immunoprecipitates prepared from lysates of $SHIP^{+/+}$ (+/+) and $SHIP^{-/-}$ (–/–) NK cells. (D) Western blot analysis of Akt phosphorylation at Thr^{308} and total Akt protein in $SHIP^{+/+}$ and $SHIP^{-/-}$ NK cell lysates. To control for equal loading the blot was re-probed with antibodies specific for β-actin, GAPDH, and α-tubulin. Collaboration with T. Ghansah Ph.D., and K.H.T Paraiso MS.

DAP12 is Expressed by SHIP$^{-/-}$ BM Cells and NK Cells

According to our data, the disruption in NK cell receptor repertoire in SHIP$^{-/-}$ mice appears to result from a bias towards selection for Ly49A and C receptors, due to their increased survival. Consequently, the level of Ly49D^{+} NK cells in SHIP$^{-/-}$ mice is decreased was compared to WT mice. However, we wanted to determine if the decrease in Ly49D^{+} NK cells representation did not arise from a lack of DAP12 expression. It has been shown that Ly49D and other activation receptors require the presence of DAP12 to migrate to the cell surface.[326] Thus, we considered the possibility that Ly49D was not found on the surface of SHIP$^{-/-}$ NK cells due to the absence of its adaptor molecule DAP12. However, using reverse-transcription PCR (RT-PCR), we observed that DAP12 is expressed in SHIP$^{-/-}$ BM (Figure 30A) and SHIP$^{-/-}$ NK cells as well as WT (Figure 30B). Another molecule known to be involved in transduction of extra-cellular signaling by NK cell receptors is DAP10. Like for DAP12, we also observe that SHIP$^{-/-}$ and WT BM cells express the DAP10 adaptor molecule (Figure 31). Since we can detect DAP12 by RT-PCR it suggests that Ly49D receptors should reach the SHIP$^{-/-}$ NK cell if they were to be expressed.

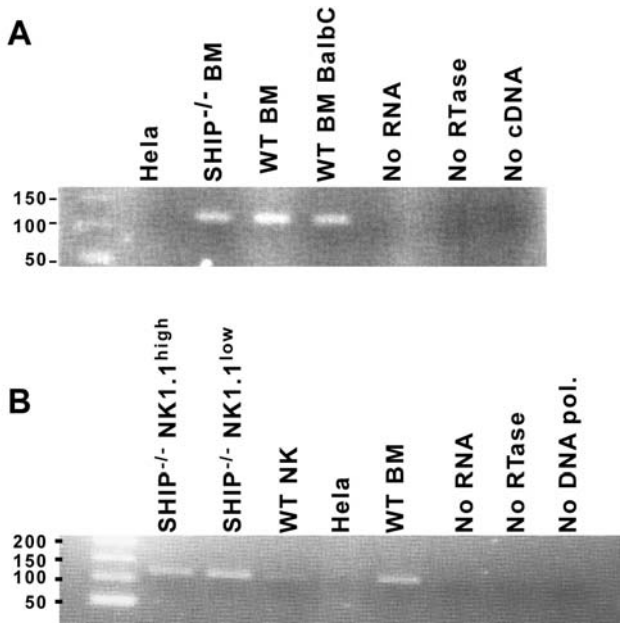

Figure 30. DAP12 is expressed in SHIP$^{-/-}$ and WT BM cells and NK cells. RNA from (A) BM and (B) NK cells was isolated and RT-PCR was performed to assess the presence of DAP12.

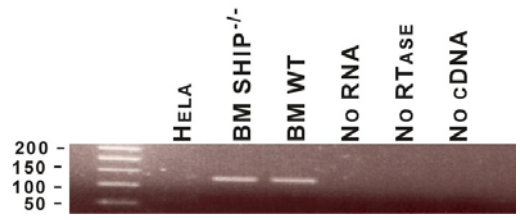

Figure 31. DAP10 is expressed in SHIP$^{-/-}$ and WT BM cells. RNA from BM cells was isolated and RT-PCR was performed to assess the presence of DAP10.

SHIP but not Shp-1 is Found Associated with Ly49A under Physiological Conditions

Signal transduction studies on NK cells have relied for a long time on the study of lymphokine-activated killer (LAK) cells. These cells are splenocytes that are grown for approximately 7 days in a media containing a combination of cytokines that promote NK cells proliferation. After this 7-day culture, the cells are collected and activation experiments are performed. Several group observed that when LAK cells were treated with pervanadate, Shp-1 was recruited to the tyrosine-phosphorylated ITIM sequence of Ly49A molecule.[308] Once to the membrane, Shp-1 can dephosphorylate molecules such as Syk, PLCγ-1/2, ZAP70, and Shc,[42,310] leading to their deactivation, preventing NK cell from killing target cells. Instead of culturing the cells for 7 days, we studied the biology of NK cells right after isolation, which would be closer to physiological condition. In this experiment we observe that SHIP does co-immunoprecipitate with Ly49A, while Shp-1 does not (Figure 32A, B). This confirms that the roles of SHIP and Shp-1 in NK cell biology are very different (Figure 33). While Shp-1 appears to be important for the control of activation signaling after Ly49 engagement, SHIP seems to play a role in NK cell homeostasis and maintenance of receptor repertoire.

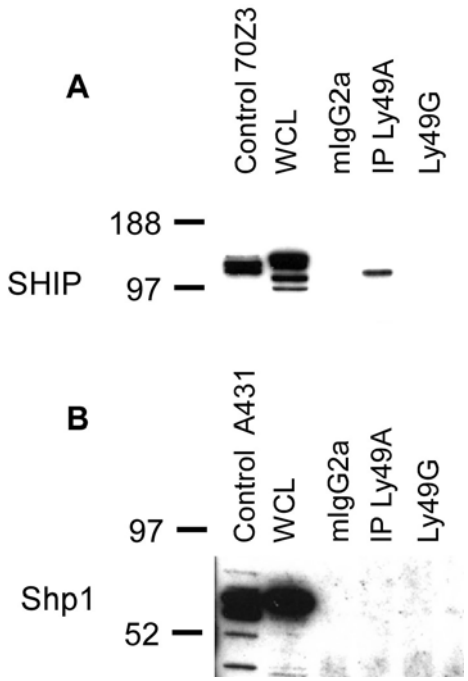

Figure 32. SHIP but not Shp-1 is recruited to NK inhibitory receptor Ly49A in vivo. (A) Western blot detection of SHIP in Ly49A IP, Ly49G, a murine IgG2a antibody (IgG2a) IP used as a negative control. WCL from 70Z/3 and NK cells (same lysate than the one used for IP) were used as positive control. (B) Western blot detection of Shp-1 in Ly49A IP, Ly49G, a murine IgG2a antibody (IgG2a) IP used as a negative control. WCL from A431 and NK cells (same lysate than the one used for IP) were used as positive control.

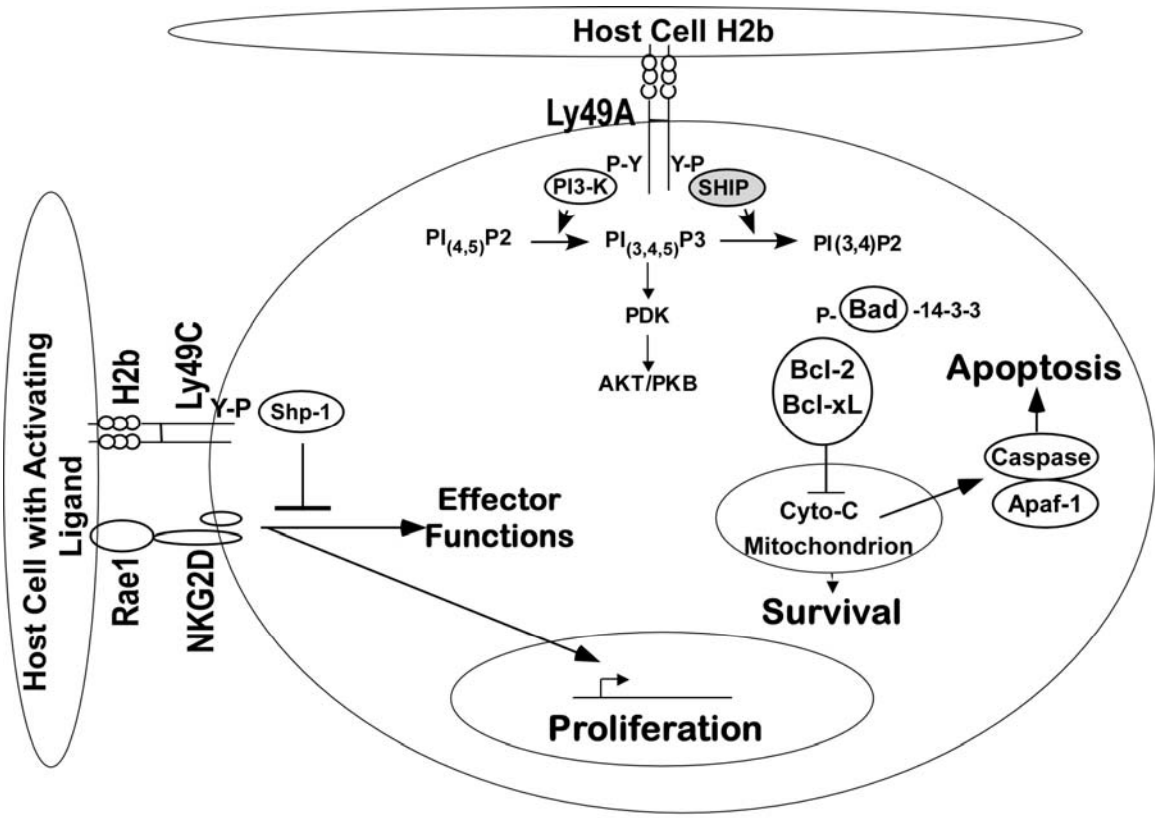

Figure 33. Signaling pathways downstream of Ly49A and C that can be influenced by SHIP in NK cells. As shown on this schematic representation of NK cells signaling pathways. SHIP, by being recruited to Ly49A and C can negatively control the survival and proliferation of NK cells in response to encounter with self H2b encounter. Once NK cell activation receptors are also engaged, Shp-1 will be recruited to the membrane to Ly49 receptors, where it will dephosphorylate kinases that, when activated, trigger an attack on target cells.

Discussion

Our study shows that F4 SHIP$^{-/-}$ mice have an increased number of peripheral NK cells, and that their receptor repertoire is disrupted. This suggests that NK cells might undergo some sort of selection process once they acquire their Ly49 receptors during development. The interaction of these NK cell inhibitory receptors with self MHC ligands may elicit signals that promote the survival or proliferation of these cells *in vivo.*[327] Thus, NK cells could be selected for their ability to be engaged by host MHC molecule (Table 3), which would ensure that the NK cells in an organism express the proper inhibitory receptors to prevent unwanted attack on self. SHIP, once recruited to the membrane by some of these Ly49 receptors could negatively regulate their survival and proliferation by controlling signaling pathways downstream of PI3K.

Alternatively, SHIP could be recruited to the membrane by Ly49 receptors to participate in the control of NK cell activation, as it has been shown to negatively control calcium influx in mast cells.[99,241] In addition, PI3K[276,277] and PLCy molecules[278-280] have been shown to play a role in NK cell activation. Since SHIP has the potential to dephosphorylate $PI_{(3,4,5)}P3$, it could downregulate these signaling pathways.[10,56-59,62,63] However, this scenario seems highly unlikely since SHIP$^{-/-}$ NK cells are unable to kill allogeneic transplant[43] and are not as efficient as WT NK cells in lysing target cell in an *in vitro* assay.[43]

On the other hand, SHIP is known to control signaling pathways downstream of cytokine receptors that can lead to activation of transcription factors, which could potentially impact Ly49 expression.[328,329] Up to this date the transcription regulation of NK cells receptors, including Ly49 receptors, appears to be highly stochastic with each receptor gene containing up to 3 separate promoters.[330] Thus, more studies are necessary to understand the mechanism for Ly49 variegated gene expression. Interestingly, NFκB has been implicated in the regulation of the probabilistic switch regulating Ly49 receptors expression.[331] Knowing that SHIP can impact NFκB activation,[332] SHIP-deficiency could perturb Ly49 transcription regulation. Interestingly, PLCγ2$^{-/-}$ mice also have a disrupted Ly49 receptor repertoire.[279] This suggests that pathways downstream of PI3K are important for the establishment of a proper Ly49 receptor repertoire.

Materials and Methods

FACS Analysis of the NK Cell Compartment and their Receptors

To analyze the peripheral NK cell compartment spleens were collected from mice at various ages. A single cell suspension was prepared by crushing of the spleen with a syringe plunger, and NH_4Cl lysis (Red blood cell lysis buffer, eBioscience) of erythrocytes. The cells were then stained with an antibody against the Fc receptor to prevent unspecific binding. All antibodies were from

BD Biosciences, except where mentioned. For the NK cell compartment assessment, splenocytes were stained with fluorescently conjugated antibody against the NK-associated markers 2B4-PE, NK1.1-FITC and CD3-APC. The cells were then incubated into a solution of 7AAD (5 μl per 1 million cells) for dead cell exclusion. Data acquired on FACS Calibur with CellQuest software, and analyzed with FlowJo. For the receptor repertoire analysis, isolated and Fc blocked splenocytes were stained with 2B4, NK1.1 and anti-Ly49A (A1), -Ly49C/I (5E6), -Ly49D (4E5), -Ly49G2 (4D11) or -CD94 (eBioscience). To distinguish Ly49C staining from Ly49I, cells were stained with NK1.1, Ly49C/I and Ly49I (YLI90). All biotin conjugates were revealed by Streptavidin-APC (eBioscience). Cells were then exposed to 7AAD for dead cell exclusion and data was acquired on FACS Calibur with CellQuest software, and analyzed with FlowJo.

Protein Lysis Buffers

Radioimmunoprecipitation (RIPA) buffer. The modified RIPA buffer protocol was obtained from the Upstate catalog. To prepare 100 ml of RIPA buffer, add 790 mg of Tris base (Fisher) to 75 ml of distilled water, add 900 mg of NaCl (Fisher), adjust the pH to 7.4 with HCl, then add 10 ml of 10% NP-40, 2.5 ml of 10% Na-Deoxycholate and 1 ml of 100 mM EDTA, adjust the final volume to 100 ml with distilled water and store at 4^{o}C until use. Right before using the buffer add protease and phosphates inhibitors to it. A cocktail of protease

inhibitors from Sigma-Aldrich was used at a concentration of 0.1%, or 10 μl of protease inhibitor cocktail in 1 ml of RIPA. For phosphates inhibitor, we use pervanadate ($NaVO_3$) to a final concentration of 1mM, thus add 10 μl of 100mM $NaVO_3$ to 1 ml of RIPA buffer.

Digitonin cell lysis buffer. First, weigh 0.5 g digitonin (CalBiochem, EMD Biosciences, Inc., San Diego, CA, USA) into a 50 ml tube add 25 ml ddH_2O and boil for about 2 h. Allow to cool on the bench and if a precipitate forms, boil again for longer period of time, until no more precipitates are found after cooling. Then, add the following reagents: 0.6 ml of 10 % Triton X-100, 1.5 ml of 5 M sodium chloride (NaCl), 10 ml of 100 mM Triethanolamine, pH 7.8, 125 μl of 1 M calcium chloride ($CaCl_2$), 50 μl of 1 M magnesium sulfate ($MgSO_4$), 25 μl of 20 % Sodium Azide and top with ddH_2O to 50 ml. As for the RIPA buffer, the protease and phosphatases inhibitors were added right before use. Immunoprecipitation was carried as mentioned in the next section. After immunoprecipitation, the precipitated beads were washed 4 times with a solution that prevents (or diminishes) the detection of unspecific interaction. This washing buffer surnamed FROPS buffer contains 30 ml of 5 M NaCl, 5 ml of 1M CHAPS, 50 ml of 1 M Tris pH8 brought up to 1 liter using deionized distilled water.

Biochemical Analysis of SHIP and Akt

NK-enriched C57BL6/J splenocytes were prepared by depletion of B cells and macrophages by adherence to nylon wool followed by T cell depletion using anti-CD3 plus complement. NK cells were then lysed in modified RIPA buffer or digitonin buffer. Prior to immunoprecipitation the NK cell lysates were pre-cleared twice by incubation with 0.25 μg of an murine or rat IgG2a antibody (BD Biosciences) and 50 μl of Protein A-Agarose or Protein G-Sepharose beads (Upstate, Charlottesville, VA, USA). The beads were pelleted at 15,000 RPM for 15 minutes at 4°C. The pre-cleared supernatants were immunoprecipitated with 2 μg of anti-Ly49A (A1), -Ly49C/I (5E6), -Ly49F (HBF-719), -Ly49G2 (4D11), -Ly49I (YLI-90) or IgG2a (BD Biosciences). To pre-clear the lysate and as a negative control for immunoprecipitation, mouse IgG2a was used for Ly49A and Ly49C/I immune precipitates, rat IgG2a was used for Ly49G2 immune precipitates, and mouse IgG1 was used to for Ly49F and Ly49I immune precipitates. Immune complexes were precipitated by addition of 50 μl of Protein A-Agarose (Ly49A, Ly49C/I) or Protein G-Sepharose (Ly49F, Ly49G2, Ly49I) beads. The immunoprecipitates were resolved on a 4-12% Tris-Bis polyacrylamide gel and transferred to a nitrocellulose membrane (Amersham Pharmacia, Piscataway, NJ). The filters were then probed with a 1:1000 dilution of anti-SHIP (P2C6, a kind gift of Larry Rohrschneider) and a horseradish peroxidase (HRP)-conjugated anti-mouse IgG secondary antibody (Amersham

Pharmacia) at a 1:80,000 dilution. The presence of SHIP was revealed using the SuperSignal West Femto reagent (Pierce Biotechnology Inc., Rockford, IL, USA). The results of the Ly49 immunoprecipitations in Figure 29 and 32 are representative of three independent analyses of NK-enriched splenocytes. For analysis of Akt activation lysates of purified NK cells from the spleens of $SHIP^{-/-}$ and $SHIP^{+/+}$ were prepared as above. Equal quantities of protein from cell lysates prepared from $SHIP^{+/+}$ and $SHIP^{-/-}$ NK cells were resolved on a 4-12% Tris-Bis polyacrylamide gel (Novex/Invitrogen, Carlsbad, CA, USA), transferred to a nitrocellulose membrane (Amersham Pharmacia) and the filters probed with an anti-Phospho-Akt(Thr308) antibody (Cell Signaling Technology, Danvers, MA, USA) at a 1:1000 dilution. The presence of Akt was detected by a HRP-conjugated donkey anti-rabbit IgG secondary antibody (Amersham Pharmacia) at a 1:2000 dilution and revealed using ECL substrate (Amersham Pharmacia). The blot was then stripped and reprobed in a similar manner using anti-β-actin (Cell Signaling Technology), anti-GAPDH (Research & Diagnostics Antibodies, Benicia, CA) and anti-α-tubulin (Oncogene Research, Cambridge, MA) as internal controls for protein loading. The detection of increased Akt levels and its activation is representative of three separate analyses of NK cell lysates from $SHIP^{-/-}$ and $SHIP^{+/+}$ mice.

RT-PCR for DAP10 and DAP12

Cells were isolated as mentioned above. For the NK cells RNA extraction, splenocytes were first treated with Fc block (CD16/CD32) for 15 minutes to prevent unspecific binding. The cells were then exposed to NK1.1-FITC (NK1.1) and CD3ε-PE (145-2C11). The FACS Vantage with the DiVa software was then used to sort $CD3^{-}NK1.1^{+}$ or $CD3^{-}NK1.1^{++}$ cells in the presence of 7AAD to exclude to dead cells. All antibodies were from BD Biosciences. RNA was isolated following the protocol for the RNAqueous-4PCR kit (Ambion, Austin, TX, USA). RT-PCR was performed using MultiScribe reverse transcriptase (Applied Biosystems, Foster City, CA, USA) protocol. Briefly, 5xRT-PCR buffer (4 μl), 25 mM $MgCl_2$ (2 μl) 10 mM dNTP (2 μl), RNase inhibitor (0.5 μl), 100 mM DTT (2 μl) and random hexamers (0.5 μl), were mixed with RNase free water (up to 20 μl) and RNA isolated from tested samples (equivalent of 10 000 cells). The enzyme, 0.3 μl of MultiScribe RTase was then added to the reaction right before starting the reverse transcription on a Px2 thermal cycler PCR machine (Thermo Electron Corporation, Waltham, MA) using the following program; 10 minutes at 25°C and 12 minutes at 42°C. The RT-PCR products were then placed at 4°C for 1-2 hours. 10 μl of the RT-PCR reaction was then used for a PCR reaction using the primers for specific genes. Briefly, cDNA (10 μl), RNase free water (25 μl), 5x AmpliTaq buffer, (8 μl) 25 mM $MgCl_2$ (2.5 μl), 10nM dNTP (3 μl), 20 μM DAP12 forward and reverse primers (.5 μl each) and 0.5 μl of AmpliTaq (Applied

Biosystems) were mixed then PCR reaction was performed. PCR reaction was done on Px2 thermal cycler PCR machine using the following program; 10 minute polymerase activation at 95^{o}C, 43 cycles of 25 second at 94^{o}C and 1 minute at 60^{o}C, and then a final incubation at 72^{o}C for 7 minutes. The expected PCR product for DAP12 was 120 nucleotides and the band on the 1.2% agarose gel appears to be 120. When the PCR was performed for DAP10, DAP 10 forward and reverse primers were used for the PCR reaction, otherwise every thing else was as mentioned earlier, a 126 base pairs sequence was expected, as seen on the 1.2% agarose gel. Primers used for DAP10: Forward: 5'-caa gtc aga cat cgg cag gtt c-3' and Reverse; 5'-gca tac ata caa aca cca ccc cta-3'. Primer used for DAP12 Forward: 5'- cct tcc tgt cct cct gac tgt g and Reverse 5'-tca ccc aga aca atc cca gc-3'.

Western Blot for Shp-1

Lysis and immunoprecipitation was carried as mentioned above. The same immunoprecipitate was then loaded on two different gels, one for Western blot with SHIP and the other one with Shp-1. The Western Blot and probing for SHIP was performed as mentioned above. The membrane to be probed for Shp-1 was then blocked in 5% non fat milk (NFM) in TBS (TBS-5%NFM) for 20 minutes at RT with constant agitation. The membrane was then incubated overnight at 4^{o}C in TBS-5%NFM containing 1 μg/ml of anti Shp-1 antibody

(Upstate). The morning after the membrane was washed twice in distilled water and incubated for 1.5 hour at RT in TBS-5%NFM containing HRP conjugated anti-rabbit antibody (Cell Signaling Technology) at a concentration of 1:80,000. The membrane was then washed twice in distilled water, and once in TBS-0.05% Tween 20 for 5 minutes. The membrane was washed another 5 x in distilled water and revealed using the SuperSignal West Femto for 5 minutes (Pierce Biotechnology Inc.).

Section IV: Murine ES Cells and s-SHIP

Introduction to ES Cells

Murine ES (mES) cells are pluripotent cell lines derived from the culture of preimplantation embryos or epiblasts.[333-335] These cells have the potential to differentiate into any cells of an organism. ES cells, contrarily to cells from 2-cells-stage embryo, can not form the trophoblast, and therefore, should be referred to as pluripotent and not totipotent.[336] ES cells can be derived and grown for several passages, without any intervention or immortalization agent. Throughout this process ES cells do not undergo senescence and retain their diploid karyotype. They can multiply in the absence of serum, if in the presence of feeder layer, and are not subject to contact inhibition or anchorage dependence.[337] Once ES cells are injected into a developing blastocyst, they have the potential to integrate that blastocyst and change parts of its genetic background. Successful integration of ES cells into blastocyst results in the colonization of germ cells.[337] These mice are then considered chimeras and can produce functional gametes containing the genetic background of the injected ES cells. Thus, ES cells have a tremendous potential to be used as a vehicle for introducing genetic modification in mice and many other organisms. It is

important to note that injection of ES cells in adult mice has been associated with the formation of teratocarcinoma.[334] The maintenance of ES cells *in vitro* is paramount for the development of genetic manipulation strategies, therefore understanding the process of self-renewal versus differentiation is very important.

The first mES cell lines were derived by growing these cells on fibroblast feeder layers. However, the presence of these feeder cells made the study of mES cell signaling very difficult. Then, Smith and Hoopers found that mES cells could be grown, undifferentiated, in the presence of FBS and LIF.[338-340] Furthermore, it was established recently that signaling by bone morphogenetic proteins (BMP) works together with LIF to maintain the pluripotency of mES cells.[341,342]

ES Cells Signaling Pathways

LIF and ES cells. In mES cells, LIF, coming from the feeder layer or given in the culture media as a recombinant protein, appears to be essential for the maintenance of ES cell pluripotency.[338-340] LIF is a factor that belongs to the IL-6 cytokine family, which also includes IL-11, ciliary neutropic factor, oncostatin M and cadiotrophin-1.[343] LIF engages the heterodimerization of receptor complex composed of LIFr and gp130, gp130 being a common receptor subunit of the IL-6 cytokine family receptor.[344,345] The heterodimerization of this complex leads to

activation of janus associated kinases (JAKs) that phosphorylate the receptor chain (Figure 34).

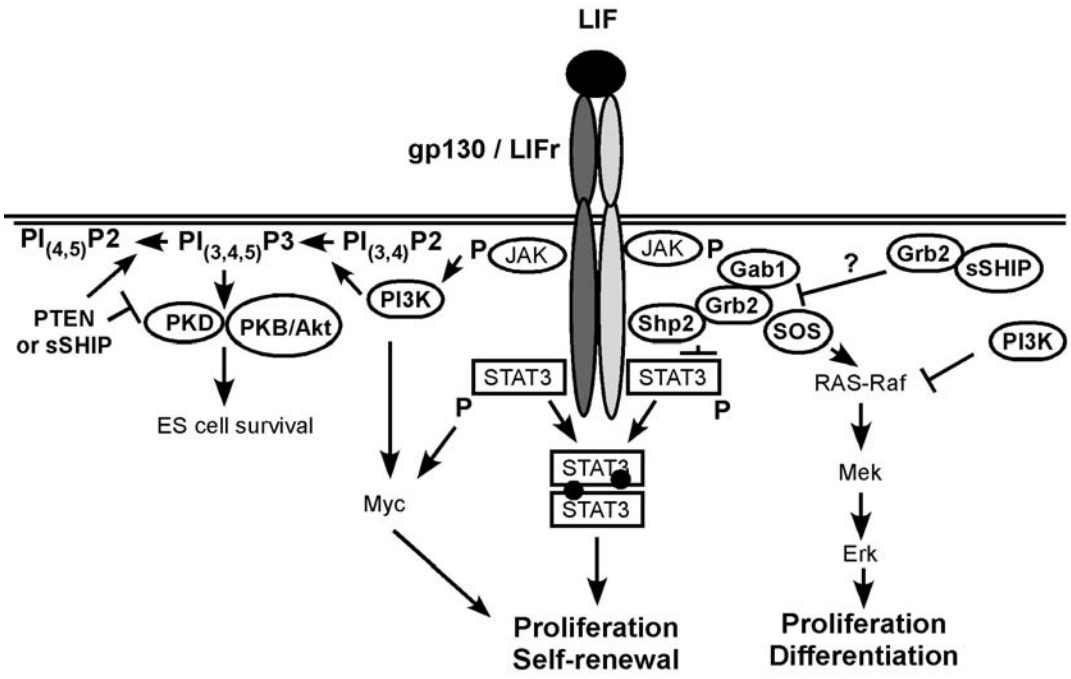

Figure 34. LIFR/gp130 receptor complex signal transduction pathways and how s-SHIP may impact them in pluripotent stem cells. Based on research from several groups, it was found that the LIFR/gp130 receptor complex can impact ES cell self-renewal and differentiation.[337,346-348] Although s-SHIP does not become phosphorylated after LIF stimulation, s-SHIP is constitutively present at the membrane and thus can impact the signaling pathways downstream of ES cell receptors. As illustrated above, LIFR/gp130 has the potential to trigger either differentiation or self-renewal depending on which downstream signaling components are activated.

The phosphorylated tyrosine on LIFr/gp130 complex can then serve as anchor site for SH2 containing domains. Some of the molecules recruited to the activated LIF/gp130 receptor complex consist of signal transducer and activator of transcription 3 (STAT3),[349] PI3K,[350] Erk,[337,351] and Shp-2.[352,353] These proteins can then be activated by surrounding kinases[354-356] and exert their effect. Interestingly, the activation and formation of protein complexes between these different proteins create a very fragile balance between self-renewal *vs*. differentiation during proliferation signaling.[337]

STAT3 stimulates ES cell self-renewal. In mES cells, LIF predominantly activates STAT3,[349] and it appears to be essential for self-renewal (Figure 34).[357] Consequently, down regulation of STAT3 through expression of a dominant negative protein causes ES cell to differentiate. Studies using a chimeric STAT3 molecule directly activated by estradiol showed that STAT3 is not only necessary but might even be sufficient to block differentiation of mES cells.[358]

ERKs antagonize ES cell self-renewal. While recruitment of STAT3 to the activated LIFr/gp130 leads to self-renewal of ES cell, recruitment of Shp-2 and Grb2 will lead to stimulation of the Erk1/2 (p42/44) and differentiation of ES cells (Figure 34).[346] Attenuation of ERK and Shp-2 signaling (by pharmacological inhibition of MAPK or by overexpression of Erk phosphatase) result in an

increase in self-renewal by reduction of differentiation.[347] However, inhibition of ERK does not replace the Stat3 requirement but enhances its action (direct or indirectly) in the promotion of ES cells self-renewal.[347] The balance between these two major signaling pathways is important for ES cells maintenance. Once phosphorylated, LIFr/gp130 receptor can recruit SH2 domain containing protein such as Shp-2.[352,353,356] Grb2 will then bind Shp-2, which will result in the recruitment of SOS to the membrane. Once SOS is at the membrane, it can then activate RAS/RAF/MAPK/Erk and downstream transcriptional factors such as, Myc, Ets, Elk, and SRF.[359]

Furthermore, Shp-2 also associates with Gab1, which can recruit PI3K.[360] The resulting phospholipids, $PI_{(3,4,5)}P3$, can then provide a binding site for the PH domain of Gab1, stabilizing the association of Shp-2/Gab1/Grb2/Sos complex at the membrane and facilitating coupling to RAS signaling pathway (Figure 34).[361] However, the production of $PI_{(3,4,5)}P3$ can also promote the recruitment of molecules that can increase survival or proliferation of the cells, such as Akt, which has been shown to stimulate ES cell self-renewal.[362]

Since SHIP, has been implicated in the control of several of these signaling pathways, s-SHIP might also impact some of these pathways. Even if s-SHIP lacks the SH2 domain and does not appear to bind Shc, it does bind Grb2 and might be involved in the control of protein complex formation of Grb2/Shp-2/Gab1/Sos, which leads to differentiation stimulation.[49] Furthermore,

s-SHIP has been shown to be constitutively located at the membrane[49] where it could hydrolyze the 5' phosphate of $PI_{(3,4,5)}P3$[363] and dampen signaling downstream of PI3K, such as Akt or Gab1 activation.

PI3K signaling in ES cells. Inhibition of PI3K using drug inhibitor or dominant negative delta85, led to a decrease in Akt, GSK3alpha/beta, and S6 proteins activity and an increase in Erk phosphorylation, resulting in a reduction of self-renewal.[350] One of the lipid phosphatases responsible for degradation of $PI_{(3,4)}P2$ and $PI_{(3,4,5)}P3$ levels, is PTEN. In fact, $PTEN^{-/-}$ ES cells have enhanced viability and rate of cell proliferation, correlated with increased level of $PI_{(3,4,5)}P3$ and phosphorylation of Akt, and inactivation of Bad (a pro-apoptotic protein).[364] The absence of PTEN results in an increased cell division rate, which is much more important in ES cells than in fibroblasts, suggesting that PI3K signaling is more important in ES cells than fibroblast.[337] Even though PTEN appears to be primarily responsible for $PI_{(3,4,5)}P3$ degradation and down modulation of PI3K effector signaling pathways in ES cells, s-SHIP could also have a role in this process.

s-SHIP

s-SHIP is a predicted 104/97kDa protein that is expressed by ES cells and HSC but not normal lineage differentiated cells.[43] s-SHIP can be amplified by RT-PCR using primers that span the carboxyl terminal end of SHIP but not by primers that bind the amino terminal region.[49] This is explained by the fact that s-SHIP sequence lacks the SH2 domain found in full-length SHIP.[49]

Studies revealed that s-SHIP is the murine homologue of human SIP-110. Similar to s-SHIP, SIP-110 is a 109kDa SHIP isoform protein that lacks the SH2 domain.[4] We observed that the first exon of SIP-110 and s-SHIP share 82% homology. Furthermore, s-SHIP has a 44 nucleotides sequence in its amino terminus that is not present in SHIP cDNA, this region was named stem-SHIP region (SSR).[49] In SIP-110, a similar 42 nucleotides SSR-like sequence is observed.[49] In our paper, it was proposed that s-SHIP, like SIP-110, resulted from the utilization of a different transcriptional start site than full-length SHIP, this start site would be embedded within the intron 5/6 of *SHIP*.[49] It was recently shown that the intron 5/6 contains a promoter region that can drive the expression of a green fluorescent protein (GFP) construct in knock-in mice stem/progenitor cells, including regions where breast mammary stem cells reside.[55] Interestingly, others observed that SHIP-deficient ES cells express s-SHIP at higher levels and for a longer period of time when primed to differentiate

than WT ES cells.[365] Since s-SHIP appears to be selectively expressed in ES cells and HSC, but not in lineage differentiated cells,[49] we were interested in studying the signaling pathways in which this protein might be involved.

s-SHIP and ES Cell

ES cells maintain pluripotency through stimulation of several signaling pathways.[366] *In vitro* culture of murine ES (mES) cells requires the presence of fibroblast feeder layer cells and/or LIF when grown on gelatin-coated paltes.[339,340,367] LIF engages the heterodimeric receptor complex composed of gp130 and LIF receptor (LIFR) and supports the culture of mES cells in the absence of a feeder layer.[368] Several signal transduction molecules have been shown to play a role in the survival, self-renewal, and/or proliferation of mES cells via the LIFR/gp130 axis, such as Stat3,[349] PI3K,[350] Erk,[337] and Shp-2.[347] Interestingly, the activation and formation of protein complexes among these different proteins establishes the delicate balance between self-renewal and differentiation pathways in pluripotent stem cells.[337]

In different cell models, several signaling pathways important for proliferation and survival downstream of PI3K can be downregulated by inositol phosphatases such as PTEN,[364,369] SHIP1, [3] and SHIP2.[77,370,371] In particular, SHIP1 can be recruited to the membrane, where it can hydrolyze the 5'-phosphate of $PI_{(3,4,5)}P3$ or $I_{(1,3,4,5)}P4$.[2] In this manner, these inositol

phosphatases oppose the activity of PI3K by preventing the recruitment of pleckstrin homology (PH) containing kinases such as Akt and Btk. Previously, we found that ES cells and, to a lesser extent, HSC, express an isoform of SHIP1, s-SHIP. This isoform is not expressed in normal mature hematopoietic cells, making this molecule an excellent candidate as a key factor in the regulation of stem cell signal transduction pathways.

In previous studies, we showed that s-SHIP interacts with Grb2 and does not with Shc.[49] In this present study, we show that s-SHIP is expressed by mES cells, but not by the mouse embryonic fibroblasts (MEF) that support their undifferentiated growth. MEF cells, however, do express the full-length SHIP isoform. In addition, we demonstrate that murine BM cells lacking the promoter and first exon of the full-length SHIP gene still express s-SHIP. This result confirms that expression of s-SHIP is not dependent on the upstream promoter active in differentiated cells. Knowing that the major growth factor for ES cell self-renewal and proliferation is LIF (Figure 34), we used this growth factor to stimulate ES cells to determine if it can stimulate s-SHIP phosphorylation. We observed that s-SHIP does not become tyrosine phosphorylated following stimulation of ES cells with LIF. Finally, we show that s-SHIP associates with gp130 *in vivo* in ES cells. These findings implicate s-SHIP in signaling pathways that control the self-renewal and differentiation of pluripotent stem cells.

Aims:

1) Define if s-SHIP is expressed in MEF and SHIP$^{-/-}$ BM cells.

2) Study what pathway s-SHIP might impact

Results

MEF Cells Express Full-Length SHIP, but Only ES Cells Express the s-SHIP Isoforms

In our previous study, we analyzed SHIP and s-SHIP protein expression in ES cells after transfer from MEF feeder layer to gelatin-coated dishes.[49] Occasionally, we would find by Western blot analysis that some ES cell cultures grown on gelatin would express some levels of the full length SHIP isoform.[49] We attributed this to residual contamination of the ES cell culture with MEF. To resolve this issue, we established a culture of MEF cells alone, ES cells on MEF cells, and ES cells on gelatin. Our suspicion that MEF cells express SHIP was confirmed as we found that MEF express the 145/135kDa full-length SHIP doublet, but not the s-SHIP 104/97kDa doublet (Figure 35). In a culture of ES cells growing on MEF cells, SHIP and s-SHIP are present (Figure 35). The protein lysate used in the third lane was produced using ES cells propagated on gelatin-coated dishes in the presence of LIF for several passages. This was done to reduce as much as possible the contribution of MEF cells to the analysis. The protein lysate of these ES cells, grown on gelatin, revealed that these cells express only the s-SHIP doublet (Figure 35).

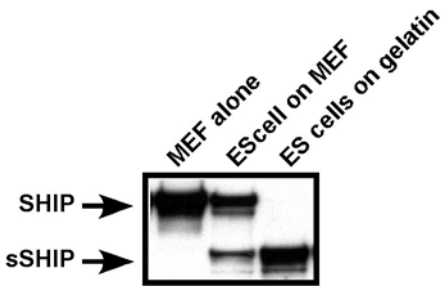

Figure 35. MEF cells express full-length SHIP, while ES cells express only s-SHIP. Protein lysates from MEF cells grown alone, ES cells grown on MEF cells, and ES cells grown on gelatin were analyzed for the expression of the different SHIP isoforms. Western blot was performed using the Novex/Invitrogen system. SHIP and s-SHIP were revealed using P2C6 anti-SHIP antibody and anti-mouse-HRP. Chemoluminescence was detected using SuperSignal Femto (Pierce Biotechnology Inc.).

SHIP$^{-/-}$ Murine BM Cells Express s-SHIP

In our laboratory, we established a SHIP$^{-/-}$ mouse model by deletion of the promoter and exon 1 of the *SHIP* gene using the Cre-*lox*P technology.[43] This deletion led to the ablation of SHIP production.[43] As previously published, bioinformatic analysis predicted that the s-SHIP and SIP-110 promoter is in the intron 5/6 of the *SHIP* gene.[49] Therefore, we theorized that SHIP$^{-/-}$ HSC might retain s-SHIP expression, since the internal promoter in intron 5/6 is intact in this SHIP$^{-/-}$ model. As we anticipated, s-SHIP mRNA is detected in SHIP$^{-/-}$ BM cells by nested RT-PCR (Figure 36). This result is consistent with a study by Rohrschneider *et al* (2005), in which the s-SHIP promoter region in *SHIP* intron 5/6 promotes transcription of a reporter gene in stem and or early progenitor cells of a transgenic mouse model.[55]

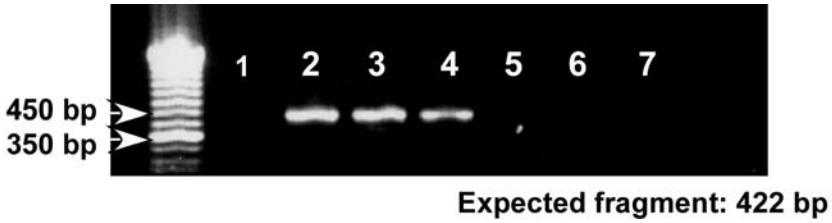

Figure 36. Nested RT-PCR detection of s-SHIP expression in SHIP$^{-/-}$ BM. Nested RT-PCR was performed, using sets of primers that span the SSR (1-44) region, unique to s-SHIP. Initial round of amplification (43 cycles) with primers F1-25 and R459-478, secondary round of amplification (43 cycles) with primers F21-41 and R439-463. Amplified DNA was then resolved on a 2% agarose gel. Legend: 1) Hela cells, 2) WT WBM C57BL6, 3) SHIP$^{-/-}$ WBM C57BL6, 4)WT WBM BalbC, 5) no RNA, 6) No RTase with RNA from WT C57BL6 BM cells, 7) No polymerase with RNA from WT C57BL6 BM cells).

s-SHIP Does Not Become Phosphorylated Following LIF Stimulation

The SHIP isoform expressed in mature hematopoietic cells is tyrosine phosphorylated upon stimulation by growth factor,[1,21,372] immune complexes,[5,34,372,373] or BCR engagement.[33,372,374] Phosphorylated SHIP is found associated with the adapter protein Shc, which facilitates its recruitment to the plasma membrane[33] where it can then act on phosphatidylinositol substrates. However, we found that s-SHIP is not tyrosine phosphorylated in either ES cells grown in LIF at steady state or ES cells deprived of LIF for 5 hours and subsequently stimulated with 2× LIF (Figure 37). It was also observed that s-SHIP does not associate with Shc either at steady-state or after LIF stimulation.[49] Instead, s-SHIP co-immunoprecipitates with Grb2.[49] Furthermore, it has been observed that SHIP or SIP110 do not need to be phosphorylated to exert their catalytic effect.[54] Thus, it is highly probable that s-SHIP, can control $PI_{(3,4,5)}P3$ accumulation in ES cells, despite not being phosphorylated.

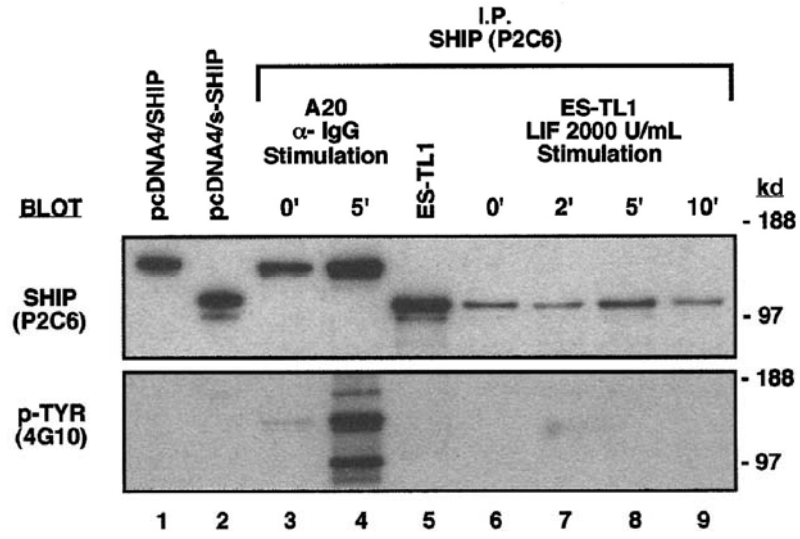

Figure 37. ES cells express the s-SHIP protein isoform that does not become phosphorylated following growth factor stimulation. Immunoprecipitation and immunoblot detection of s-SHIP in ES cell lysates. Lysate from ES-TL1 cells cultured in LIF was immunoprecipitated with the P2C6 anti-SHIP monoclonal antibody, separated on gels, transferred to membranes, and probed with P2C6, revealing 104-kd and 97-kd proteins (lane 5). No tyrosine phosphorylation of these proteins was detected when they were probed with the 4G10 anti-phosphotyrosine antibody. For comparison, lysates from 293T cells transfected with SHIP cDNA (lane 1) and s-SHIP cDNA (lane 2) were included in the blots. To further assess the tyrosine phosphorylation status of s-SHIP, timed LIF stimulation studies were performed. ES-TL1 cells incubated for 5 hours without LIF were stimulated with 2000 U/ml LIF for 0, 2, 5, or 10 minutes and were rapidly lysed. Equal amounts of total protein were immunoprecipitated with the P2C6 antibody and probed separately with the P2C6 and 4G10 antibodies (lanes 6-9). No tyrosine phosphorylation of s-SHIP was detected at any time point with the 4G10 antibody. For comparison, A20 B-lymphoid cells were stimulated with anti-IgG antibody for 0 or 5 minutes, lysed, immunoprecipitated with P2C6, and probed with P2C6 and 4G10 (lanes 3,4), showing prominent tyrosine phosphorylation of SHIP at 5 minutes. Molecular mass standards are indicated on the right. Collaboration with J. Ninos MD.

s-SHIP Associates with gp130 In Vivo

Grb2 has been shown to be present in protein complexes formed after gp130 engagement. Since Grb2 can associate with s-SHIP, we assessed the potential of s-SHIP to associate with gp130 in ES cells. As demonstrated in Figure 38A and B, s-SHIP is present in gp130 immunoprecipitates from protein lysates of ES cells at steady state. This result strongly suggests that s-SHIP is present in protein complexes that interact with gp130 in ES cells. Inhibition of the s-SHIP/gp130 association by preincubation of gp130 antibody with specific blocking peptides establishes the specificity of the interaction (Figure 38B). This result provides a direct link between s-SHIP and an important signaling component of the pathway influencing ES cell self-renewal.

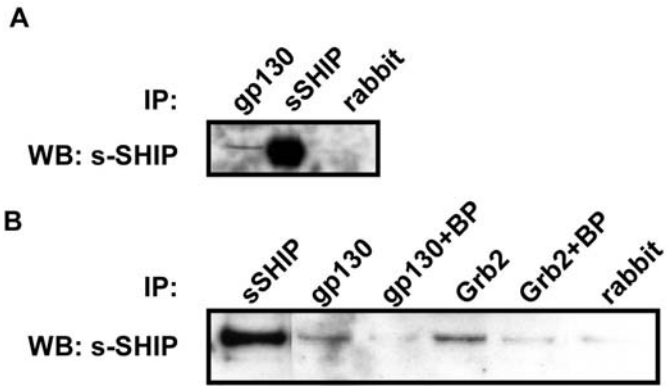

Figure 38. s-SHIP is associated with gp130 in ES cells. A) Lysates of ES cells grown on gelatin were immunoprecipitated with gp130 antibody, s-SHIP antibody (positive control) and rabbit antibody (negative control). (B) Lysates of ES cells grown on gelatin. Whole cell lysate (positive control), immunoprecipitate with gp130 antibody, immunoprecipitation with gp130 antibody previously blocked with specific peptides, immunoprecipitate with Grb2 antibody, immunoprecipitation with Grb2 antibody previously blocked with specific peptides, and immunoprecipitate with rabbit antibody (negative control).

Discussion

In this study, we show that s-SHIP co-immunoprecipitates with gp130. This further suggests that s-SHIP can be found intimately associated with protein complexes that impact self-renewal and proliferation pathways of mES cells. s-SHIP may interact with gp130 directly, or indirectly, through an intermediate such as Grb2. The exact role that s-SHIP plays in ES cell biology remains to be defined. As shown previously, s-SHIP is found constitutively at the plasma membrane in ES cells.[49] Furthermore, it has been shown previously that SIP110 phosphorylation is not required for enzymatic activity. Thus, s-SHIP could downregulate basal activation of Akt in these cells through degradation of $PI_{(3,4,5)}P3$.[363] In this context, the role of s-SHIP would be to limit cell survival (Figure 34). Interestingly, PI3K inhibition leads to a decrease in $PI_{(3,4,5)}P3$, resulting in Erk activation and a reduction in self-renewal. Therefore, s-SHIP may negatively control ES cell self-renewal. Since PTEN appears to be necessary for the control of pathway downstream of PI3K in ES cells,[364] s-SHIP and PTEN might have a redundant role in controlling this pathway.

Alternatively, s-SHIP would associate with Grb2 to prevent the formation of the protein complex composed of Shp-2, Grb2, and SOS, and thereby limit the activation of MAPK and the downstream differentiation of ES cells (Figure 34). In previous studies, it was shown that s-SHIP expression declines as the stem cell differentiates into specific lineages.[49,365] Furthermore, $SHIP^{-/-}$ ES cells express

higher levels of s-SHIP and for a longer period of than WT ES cells.[365] Thus, ES cells might express the s-SHIP isoform to inhibit differentiation stimuli, since it binds Grb2 constitutively, potentially preventing the association of Shp-2/Grb2/SOS protein complexes (Figure 34).

Interestingly, the $SHIP^{\Delta IP/\Delta IP}$ mice, produced by targeting the inositol phosphatase domain, are viable,[97] despite the likelihood that they do not express an enzymatically active form of s-SHIP. However, analysis of s-SHIP expression in primitive cell types or BM cells has not been demonstrated for this SHIP KO model. To date, there does not exist an $s\text{-}SHIP^{-/-}$ model, which maintains WT levels of full length SHIP, therefore it will be difficult to truly assess the role of s-SHIP in stem cell biology until such a mouse model is developed. In the meantime, studies in ES cells using RNA interference techniques to target s-SHIP expression will be useful in understanding the contribution of this protein in the control of self-renewal and differentiation in pluripotent stem cells. Most importantly, more studies are needed to completely define the relationship between s-SHIP, Grb2, and gp130 and their combined role in ES cell function.

Materials and methods

Propagation of mES Cells

For our studies, we used TL1 strain mES cells, which were a kind gift from Patricia A. Labosky, University of Pennsylvania, Philadelphia, Pennsylvania, USA. mES cells were first thawed on MEF cells and then transferred and passaged on gelatin-coated dishes. Petri dishes (100mm plates, Nunc, Fisher Scientific Inc. Suwanee, GA) were covered with 0.1% gelatin in ultrapure water (Chemicon International/Specialty Media, Phillipsburg, NJ, USA) for at least 30 minutes. The extra gelatin was then removed. Cells were cultured in KO DMEM media (Gibco BRL/Invitrogen), 15% ES cell qualified FBS (Invitrogen/Gibco BRL), 2 mM L-Alanyl-L-Glutamine (ATCC, Manassas, VA, USA), 0.1 mM Non-essential amino acids (Gibco BRL/Invitrogen), 0.1 mM β-mercaptoethanol (β-ME) (Sigma-Aldrich) with 1000 U/ml LIF (Chemicon International). ES cells were split every other day using a 0.05% trypsin-EDTA treatment for 3-5 minutes.

Preparation of mES Cell Lysates for Biochemical Analysis

ES cells were grown in the presence of 1000 U/ml LIF. In preparation for cell lysis, ES cells cell culture dish was placed on ice, the culture media was then removed and the cells were washed twice with PBS containing 1 mM sodium pervanadate ($NaVO_3$). ES cells were then lysed with modified RIPA buffer (Upstate) containing 1 mM $NaVO_3$ and protease inhibitor (Sigma-Aldrich). Lysis

was performed at 4°C for 45 to 60 minutes. Protein concentration was established using the BCA protein assay kit (Pierce Biotechnology Inc.).

Nested Reverse-Transcription Polymerase Chain Reaction Assay for Detection of s-SHIP Expression

Murine BM cells were isolated as mentioned previously. RNA was isolated from $1x10^6$ WT and $SHIP^{-/-}$ BM cells following the protocol for the RNAqueous-4PCR kit (Ambion). RT-PCR was performed using MultiScribe reverse transcriptase (Applied Biosystems) protocol. Briefly, 5xRT-PCR buffer (4 μl), 25 mM $MgCl_2$ (2 μl), 10 mM dNTP (2 μl), RNase inhibitor (0.5 μl), 100 mM DTT (2 μl) and random hexamers (0.5 μl) were mixed with RNase free water (up to 20 μl) and RNA isolated from tested samples (equivalent of $1x10^4$ cells). MultiScribe RTase enzyme, 0.3 μl, was then added to the reaction, for a total volume of 20 μl. The RT reaction was performed in a Px2 thermal cycler PCR machine (Thermo Electron Corporation, Waltham, MA) using the following program: 10 minutes at 25°C and then 12 minutes at 42°C. The RT products were placed at 4°C for 1-2 hours. Ten μl of the RT reaction product was then used for PCR amplification using a forward primer specific for the s-SHIP SSR region and a reverse primer specific for a region approximately 460 bp downstream of the s-SHIP SSR region.[49] Briefly, cDNA (10 μl), RNase free water (25 μl), 5x Amplitaq buffer (8 μl), 25 mM $MgCl_2$ (2.5 μl), 10nM dNTP (3 μl),

20 μM s-ship forward (1-25) and reverse (459-478) primers (0.5 μl each) and 0.5 μl of AmpliTaq (Applied Biosystems) were mixed prior to PCR amplification. Amplification was performed in a Px2 thermal cycler PCR machine using the following program: 10 minutes denaturation at 95^{o}C followed by 43 cycles of 25 seconds at 94^{o}C and 1 minute at 55^{o}C, with a final extension phase at 72^{o}C for 7 minutes. Twenty μl of the PCR reaction was then placed in a second PCR using the same conditions, except that the primers were internal to the first round amplification primers and targeted the s-SHIP nucleotides 21-41 (forward primer), within the SSR region, and 463-478 (reverse primer). All primers were obtained from Integrated DNA Technologies Inc. (Coralville, IA, USA). The expected PCR product for the s-ship nested PCR product is 442 base pairs, which coincides with the product seen on a 1.2% agarose gel. Primers used for s-SHIP nested PCR: Initial amplification: forward(1-25), 5'-gtt ccc act agt tgt tga act tta c-3' and reverse(478-459), 5'-tct cct tct ccg tct cca cc-3'; secondary amplification: forward(21-41), 5'-ttt acc ttg aac ctc tgc tcc-3' and reverse(463-439) 5'-cca cca aaa tca cca act tgt tta g-3'.

Western blot antibodies and techniques

The Western blots apparatus consisted of the Novex X-cell II system with Bis-Tris gel system (Novex/Invitrogen). Typically 4 to 12% gels were used (Novex/Invitrogen). Gels were run at RT for 2 hours at 150 Volts. Multi-Mark or

BenchMark (Novex/Invitrogen) protein ladders were used to correlate molecular weight of target proteins. Proteins were electrophoretically transferred to nitrocellulose membranes (Millipore, Billerica, MA, USA) for immunoblotting. The blots were initially washed twice for 2 minutes in a solution of PBS 0.05% Tween (PBS-T), then blocked for 1 hour at RT in 5% NFM in PBS with 0.05% Tween (5% NFM/PBS-T). The blots were washed 3 x 5 minutes in PBS-T and then incubated overnight at 4^{o}C in anti-SHIP monoclonal antibody solution of P2C6 antibody (a kind gift from Dr. Larry Rohrschneider) at a concentration of 1:1000, or the P1C1 monoclonal antibody (Santa Cruz Biotechnology Inc., Santa Cruz, CA) at a concentration of 1 μg/ml in 5%NFM/PBS-T. The following day, blots were washed at least three times for 10 minutes and incubated with anti-mouse-HRP conjugated antibody (Pierce Biotechnology Inc.) at concentration 1:80,000 for 2 hours at RT. The blot was then washed four times 5 minutes in PBS-T and exposed with SuperSignal West Femto for 5 minutes (Pierce Biotechnology Inc.).

Cell stimulation

ES-TL1 cells were split into 4 different 100-mm TC plates and grown overnight at 37^{o}C in ES media supplemented with 1000 U/ml LIF to approximate 80% confluence. LIF-supplemented media was removed, cells were washed twice with PBS, media without LIF was added, and cells were incubated for 5 hours. Cells were washed once with PBS and twice with Hanks balanced salt solution (HBSS, Mediatech). Then they were pre-incubated in HBSS at 37^{o}C for

10 minutes. Cells were stimulated by the addition of HBSS containing 2000 U/ml LIF and by incubation at 37°C for either 2, 5, or 10 minutes. A control ES plate (0 minute) containing HBSS without LIF was incubated at 37°C in parallel for 10 minutes. Stimulations were stopped by the removal of buffer and the addition of 10 ml ice-cold PBS/1 mM Na_3VO_4. PBS/Na_3VO_4 was removed, and 1mL ice-cold modified RIPA buffer was added immediately. Cells were scraped, and cell lysates were processed as described above. A20 cells were grown in RPMI and were washed once with PBS and twice with HBSS. Then 2×10^7 cells were placed in separate 15-mL conicals and were pre-incubated in HBSS at 37°C for 10 minutes. Cells were spun down, and HBSS was removed. After that, cells were stimulated with 1 ml HBSS containing 20 μg/ml goat anti-mouse IgG (Southern Biotechnology Associates, Birmingham, AL) and were incubated at 37°C for 5 minutes. Control A20 cells (0 minute) containing HBSS without anti-mouse IgG were incubated in parallel. Stimulations were stopped by placing the conicals on ice and adding 2 ml ice-cold PBS/Na_3VO_4. Cells were pelleted, supernatant was removed, and 1 ml ice-cold modified RIPA buffer was added. One mg in 1 ml of buffer was used for subsequent immunoprecipitation experiments.

Western blot analysis of gp130 immunoprecipitates

Equivalent amounts of protein lysate were first pre-cleared twice with 0.25 μg of appropriate nonspecific IgG isotype control followed by 50 μl of appropriate

50% agarose bead slurry (Protein A or G) (Upstate). The beads had previously been washed three times in cold PBS. They were then resuspended in PBS containing 1mM $NaVO_3$ to obtain a 50% slurry. The pre-cleared lysates were then exposed to specific polyclonal antibodies against gp130 (M-20) (Santa Cruz Biotechnology) and Grb2 (Santa Cruz Biotechnology) for 3 hours at 4^{o}C on a rotator. When peptide blocked antibodies were used for immunoprecipitation, gp130 and Grb2 antibodies were incubated with their respective blocking peptides (Santa Cruz Biotechnology) for at least 1 hour on a rotator at 4ºC prior to being used for immunoprecipitation. Once incubation with antibody was completed, 50 μl of Protein A or G agarose beads 50% slurry was then added to the immunoprecipitates and put on a rotator overnight at 4^{o}C. The following day, the supernatant was removed and beads were washed four times with FROP buffer (150 mM NaCl, 5 mM CHAPS, 50 mM Tris pH 8). LDS sample buffer with reducer (Novex/Invitrogen) was then added to the beads, and the bead/buffer mixture was heated at 100^{o}C for 5 minutes. Western blot analysis was then performed as described above.

FINAL DISCUSSION

One might be surprised to notice that through out this dissertation, SHIP is given multiple roles. For example, in HSC we attributed to SHIP the ability to impact proliferation, survival, homing and retention to the BM. In addition, a similar scenario was observed when we studied the role of SHIP in MKP. However, when we truly look at each of the signaling pathways that can be influenced by SHIP, each of them can be linked to a function attributed to SHIP. This protein can control proliferation through the regulation of the MAPK by sequestration of Shc.[1] Alternatively, it can contribute in the negative regulation of the Akt signaling pathway, which promotes cell survival and proliferation.[61] Furthermore, SHIP was shown to negatively control myeloid progenitor cell response to SDF-1, $SHIP^{-/-}$ myeloid progenitors being more responsive to SDF-1 stimulation than WT.[152] Additionally, SHIP by being a major regulator of the PI3K downstream effector pathway can impact hematopoietic cell response to diverse cytokines. Interestingly, PI3K is also known to bind to focal adhesion kinase (FAK),[375] and in this pathway, PI3K activation leads to the production of $PI_{(3,4,5)}P3$ which contributes to the control of cell motility by FAK. Thus, SHIP could contribute to the negative regulation of this pathway. Moreover, we observed that SHIP appears to contribute to the shaping of the NK cell receptor repertoire.

Our results suggest that SHIP regulates the NK cell receptor repertoire diversity through promotion of survival of certain NK cell subset. However, we can not exclude that SHIP could also participate in NK cell receptors transcription regulation. SHIP has been shown to influence I-κB activity, which regulates NFκB function. Most interestingly, NF-κB was shown to contribute to the regulation of Ly49 receptor expression.[331] More studies are needed to truly define the role of SHIP in all these different pathways. Furthermore, it is necessary to establish which isoform or isoforms are involved in each of these pathways in every cell type, since each isoform contains different combination of functional domains.

After studying SHIP for 5 years, it is clear to me that it plays different roles depending on the hematopoietic cells type, the cell context, and the cell environment. Another testament to its variegated role in the control of cellular function is the fact that SHIP has several isoforms and that each of them appear to be expressed differently in diverse cell types.[4,49,53] In theory, every SHIP isoform still contains a functional 5' inositol phosphatase enzymatic domain. Phosphatidylinositols are used to transmit signal from different external stimuli to activate cellular response that can lead to calcium mobilization, protein phosphorylation, cell proliferation, activation and survival. Therefore, SHIP has the potential to influence each of these pathways. However, the fact that these SHIP isoforms lack some of the protein interaction domain, will modify the

cellular context in which these isoforms will be recruited to the membrane or site of action. For example s-SHIP, which has no SH2 domain, will be restricted in its ability to interact with phosphorylated tyrosine. Another isoform, SHIPΔ183, lacks a region between the two NPXY leading to a disruption of a consensus sequence necessary for the binding of PI3K p85 subunit. Interestingly, the different isoform appear to be differentially expressed by diverse cell type. This can provide the cell with an isoform that will correspond to the need of that particular cell. For example, ES cells express only s-SHIP and not full length SHIP, while HSC express both isoforms.[49] It was also shown that untreated human BM cells express a 110kDa isoform, but when the same cells were treated *in vitro* with IL-3 and M-CSF to promote differentiation towards the myeloid lineage, full length SHIP was observed.[53]

Noteworthy are the observations linking SHIP-deficiency to premature aging. For example SHIP-deficient mice suffer from osteoporosis due to hyper-responsive osteoclasts.[101] Furthermore, $SHIP^{-/-}$ BM have an increased number of HSC, which are not as efficient as WT at reconstituting an irradiated host.[156,246] Moreover, the $SHIP^{-/-}$ hematopoietic system is skewed towards myeloid cell differentiation.[95] All of these are characteristics that have been associated with aging.[376-383] It would be interesting to address the hypothesis that SHIP deficiency causes accelerated aging in mice.

Although SHIP is known to influence many signaling pathways in different cell types, its deficiency is not associated with many diseases. SHIP appears to be absent in some forms of acute leukemias.[384] It was also associated with myeloproliferative disorder[95] and with osteoporosis.[101] Nevertheless, the study of the germline SHIP$^{-/-}$ mouse model did not allow confirming that SHIP mutation might be associated with any other disease, yet. It will be important to study the conditional knock-out system to establish more precisely if SHIP deletion or mutation during adulthood might participate in the development of cancers, allergic, auto-immune or inflammatory condition.

BIBLIOGRAPHY

1. Liu L, Damen JE, Cutler RL, Krystal G. Multiple cytokines stimulate the binding of a common 145-kilodalton protein to Shc at the Grb2 recognition site of Shc. Mol Cell Biol. 1994;14:6926-6935.

2. Damen JE, Liu L, Rosten P, et al. The 145-kDa protein induced to associate with Shc by multiple cytokines is an inositol tetraphosphate and phosphatidylinositol 3,4,5-triphosphate 5-phosphatase. Proc Natl Acad Sci U S A. 1996;93:1689-1693.

3. Lioubin MN, Algate PA, Tsai S, Carlberg K, Aebersold A, Rohrschneider LR. p150Ship, a signal transduction molecule with inositol polyphosphate-5-phosphatase activity. Genes Dev. 1996;10:1084-1095.

4. Kavanaugh WM, Pot DA, Chin SM, et al. Multiple forms of an inositol polyphosphate 5-phosphatase form signaling complexes with Shc and Grb2. Curr Biol. 1996;6:438-445.

5. Ono M, Bolland S, Tempst P, Ravetch JV. Role of the inositol phosphatase SHIP in negative regulation of the immune system by the receptor Fc(gamma)RIIB. Nature. 1996;383:263-266.

6. Kerr WG, Heller M, Herzenberg LA. Analysis of lipopolysaccharide-response genes in B-lineage cells demonstrates that they can have differentiation stage-restricted expression and contain SH2 domains. Proc Natl Acad Sci U S A. 1996;93:3947-3952.

7. Liscovitch M, Cantley LC. Lipid second messengers. Cell. 1994;77:329-334.

8. Loomis-Husselbee JW, Cullen PJ, Dreikausen UE, Irvine RF, Dawson AP. Synergistic effects of inositol 1,3,4,5-tetrakisphosphate on inositol 2,4,5-triphosphate-stimulated Ca2+ release do not involve direct interaction of inositol 1,3,4,5-tetrakisphosphate with inositol triphosphate-binding sites. Biochem J. 1996;314 (Pt 3):811-816.

9. Loomis-Husselbee JW, Walker CD, Bottomley JR, Cullen PJ, Irvine RF, Dawson AP. Modulation of Ins(2,4,5)P3-stimulated Ca2+ mobilization by ins(1,3,4,5)P4: enhancement by activated G-proteins, and evidence for the involvement of a GAP1 protein, a putative Ins(1,3,4,5)P4 receptor. Biochem J. 1998;331 (Pt 3):947-952.

10. Downward J. Lipid-regulated kinases: some common themes at last. Science. 1998;279:673-674.

11. Damen JE, Liu L, Cutler RL, Krystal G. Erythropoietin stimulates the tyrosine phosphorylation of Shc and its association with Grb2 and a 145-Kd tyrosine phosphorylated protein. Blood. 1993;82:2296-2303.

12. Pelicci G, Lanfrancone L, Grignani F, et al. A novel transforming protein (SHC) with an SH2 domain is implicated in mitogenic signal transduction. Cell. 1992;70:93-104.

13. Liu L, Damen JE, Ware MD, Krystal G. Interleukin-3 induces the association of the inositol 5-phosphatase SHIP with SHP2. J Biol Chem. 1997;272:10998-11001.

14. Carlberg K, Rohrschneider LR. Characterization of a novel tyrosine phosphorylated 100-kDa protein that binds to SHP-2 and phosphatidylinositol 3'-kinase in myeloid cells. J Biol Chem. 1997;272:15943-15950.

15. Zhang S, Mantel C, Broxmeyer HE. Flt3 signaling involves tyrosyl-phosphorylation of SHP-2 and SHIP and their association with Grb2 and Shc in Baf3/Flt3 cells. J Leukoc Biol. 1999;65:372-380.

16. Matsuguchi T, Salgia R, Hallek M, et al. Shc phosphorylation in myeloid cells is regulated by granulocyte macrophage colony-stimulating factor, interleukin-3, and steel factor and is constitutively increased by p210BCR/ABL. J Biol Chem. 1994;269:5016-5021.

17. Sattler M, Salgia R, Shrikhande G, et al. The phosphatidylinositol polyphosphate 5-phosphatase SHIP and the protein tyrosine phosphatase SHP-2 form a complex in hematopoietic cells which can be regulated by BCR/ABL and growth factors. Oncogene. 1997;15:2379-2384.

18. Liu Q, Sasaki T, Kozieradzki I, et al. SHIP is a negative regulator of growth factor receptor-mediated PKB/Akt activation and myeloid cell survival. Genes Dev. 1999;13:786-791.

19. Zamorano J, Keegan AD. Regulation of apoptosis by tyrosine-containing domains of IL-4R alpha: Y497 and Y713, but not the STAT6-docking tyrosines, signal protection from apoptosis. J Immunol. 1998;161:859-867.

20. Jiang H, Harris MB, Rothman P. IL-4/IL-13 signaling beyond JAK/STAT. J Allergy Clin Immunol. 2000;105:1063-1070.

21. Lioubin MN, Myles GM, Carlberg K, Bowtell D, Rohrschneider LR. Shc, Grb2, Sos1, and a 150-kilodalton tyrosine-phosphorylated protein form complexes with Fms in hematopoietic cells. Mol Cell Biol. 1994;14:5682-5691.

22. Hunter MG, Avalos BR. Phosphatidylinositol 3'-kinase and SH2-containing inositol phosphatase (SHIP) are recruited by distinct positive and negative growth-regulatory domains in the granulocyte colony-stimulating factor receptor. J Immunol. 1998;160:4979-4987.

23. Hunter MG, Jacob A, O'Donnell L C, et al. Loss of SHIP and CIS recruitment to the granulocyte colony-stimulating factor receptor contribute to hyperproliferative responses in severe congenital neutropenia/acute myelogenous leukemia. J Immunol. 2004;173:5036-5045.

24. Drachman JG, Griffin JD, Kaushansky K. The c-Mpl ligand (thrombopoietin) stimulates tyrosine phosphorylation of Jak2, Shc, and c-Mpl. J Biol Chem. 1995;270:4979-4982.

25. Drachman JG, Kaushansky K. Dissecting the thrombopoietin receptor: functional elements of the Mpl cytoplasmic domain. Proc Natl Acad Sci U S A. 1997;94:2350-2355.

26. Marchetto S, Fournier E, Beslu N, et al. SHC and SHIP phosphorylation and interaction in response to activation of the FLT3 receptor. Leukemia. 1999;13:1374-1382.

27. Chernock RD, Cherla RP, Ganju RK. SHP2 and cbl participate in alpha-chemokine receptor CXCR4-mediated signaling pathways. Blood. 2001;97:608-615.

28. Wain CM, Westwick J, Ward SG. Heterologous regulation of chemokine receptor signaling by the lipid phosphatase SHIP in lymphocytes. Cell Signal. 2005;17:1194-1202.

29. Fong DC, Malbec O, Arock M, Cambier JC, Fridman WH, Daeron M. Selective in vivo recruitment of the phosphatidylinositol phosphatase SHIP by phosphorylated Fc gammaRIIB during negative regulation of IgE-dependent mouse mast cell activation. Immunol Lett. 1996;54:83-91.

30. D'Ambrosio D, Fong DC, Cambier JC. The SHIP phosphatase becomes associated with Fc gammaRIIB1 and is tyrosine phosphorylated during 'negative' signaling. Immunol Lett. 1996;54:77-82.

31. Ravichandran KS, Lee KK, Songyang Z, Cantley LC, Burn P, Burakoff SJ. Interaction of Shc with the zeta chain of the T cell receptor upon T cell activation. Science. 1993;262:902-905.

32. Smit L, de Vries-Smits AM, Bos JL, Borst J. B cell antigen receptor stimulation induces formation of a Shc-Grb2 complex containing multiple tyrosine-phosphorylated proteins. J Biol Chem. 1994;269:20209-20212.

33. Saxton TM, van Oostveen I, Bowtell D, Aebersold R, Gold MR. B cell antigen receptor cross-linking induces phosphorylation of the p21ras oncoprotein activators SHC and mSOS1 as well as assembly of complexes containing SHC, GRB-2, mSOS1, and a 145-kDa tyrosine-phosphorylated protein. J Immunol. 1994;153:623-636.

34. Chacko GW, Tridandapani S, Damen JE, Liu L, Krystal G, Coggeshall KM. Negative signaling in B lymphocytes induces tyrosine phosphorylation of the 145-kDa inositol polyphosphate 5-phosphatase, SHIP. J Immunol. 1996;157:2234-2238.

35. Brunet A, Bonni A, Zigmond MJ, et al. Akt promotes cell survival by phosphorylating and inhibiting a Forkhead transcription factor. Cell. 1999;96:857-868.

36. Biggs WH, 3rd, Meisenhelder J, Hunter T, Cavenee WK, Arden KC. Protein kinase B/Akt-mediated phosphorylation promotes nuclear exclusion of the winged helix transcription factor FKHR1. Proc Natl Acad Sci U S A. 1999;96:7421-7426.

37. Damen JE, Liu L, Ware MD, Ermolaeva M, Majerus PW, Krystal G. Multiple forms of the SH2-containing inositol phosphatase, SHIP, are generated by C-terminal truncation. Blood. 1998;92:1199-1205.

38. Moran MF, Koch CA, Anderson D, et al. Src homology region 2 domains direct protein-protein interactions in signal transduction. Proc Natl Acad Sci U S A. 1990;87:8622-8626.

39. Ellis C, Moran M, McCormick F, Pawson T. Phosphorylation of GAP and GAP-associated proteins by transforming and mitogenic tyrosine kinases. Nature. 1990;343:377-381.

40. Osborne MA, Zenner G, Lubinus M, et al. The inositol 5'-phosphatase SHIP binds to immunoreceptor signaling motifs and responds to high affinity IgE receptor aggregation. J Biol Chem. 1996;271:29271-29278.

41. Tridandapani S, Kelley T, Pradhan M, Cooney D, Justement LB, Coggeshall KM. Recruitment and phosphorylation of SH2-containing inositol phosphatase and Shc to the B-cell Fc gamma immunoreceptor tyrosine-based inhibition motif peptide motif. Mol Cell Biol. 1997;17:4305-4311.

42. Daws MR, Eriksson M, Oberg L, Ullen A, Sentman CL. H-2Dd engagement of Ly49A leads directly to Ly49A phosphorylation and recruitment of SHP1. Immunology. 1999;97:656-664.

43. Wang JW, Howson JM, Ghansah T, et al. Influence of SHIP on the NK repertoire and allogeneic bone marrow transplantation. Science. 2002;295:2094-2097.

44. Kimura T, Sakamoto H, Appella E, Siraganian RP. The negative signaling molecule SH2 domain-containing inositol-polyphosphate 5-phosphatase (SHIP) binds to the tyrosine-phosphorylated beta subunit of the high affinity IgE receptor. J Biol Chem. 1997;272:13991-13996.

45. Baran CP, Tridandapani S, Helgason CD, Humphries RK, Krystal G, Marsh CB. The inositol 5'-phosphatase SHIP-1 and the Src kinase Lyn negatively regulate macrophage colony-stimulating factor-induced Akt activity. J Biol Chem. 2003;278:38628-38636.

46. Phee H, Jacob A, Coggeshall KM. Enzymatic activity of the Src homology 2 domain-containing inositol phosphatase is regulated by a plasma membrane location. J Biol Chem. 2000;275:19090-19097.

47. Liu L, Damen JE, Ware M, Hughes M, Krystal G. SHIP, a new player in cytokine-induced signalling. Leukemia. 1997;11:181-184.

48. Liu L, Damen JE, Hughes MR, Babic I, Jirik FR, Krystal G. The Src homology 2 (SH2) domain of SH2-containing inositol phosphatase (SHIP) is essential for tyrosine phosphorylation of SHIP, its association with Shc, and its induction of apoptosis. J Biol Chem. 1997;272:8983-8988.

49. Tu Z, Ninos JM, Ma Z, et al. Embryonic and hematopoietic stem cells express a novel SH2-containing inositol 5'-phosphatase isoform that partners with the Grb2 adapter protein. Blood. 2001;98:2028-2038.

50. Lamkin TD, Walk SF, Liu L, Damen JE, Krystal G, Ravichandran KS. Shc interaction with Src homology 2 domain containing inositol phosphatase (SHIP) in vivo requires the Shc-phosphotyrosine binding domain and two specific phosphotyrosines on SHIP. J Biol Chem. 1997;272:10396-10401.

51. Lecoq-Lafon C, Verdier F, Fichelson S, et al. Erythropoietin induces the tyrosine phosphorylation of GAB1 and its association with SHC, SHP2, SHIP, and phosphatidylinositol 3-kinase. Blood. 1999;93:2578-2585.

52. Wolf I, Lucas DM, Algate PA, Rohrschneider LR. Cloning of the genomic locus of mouse SH2 containing inositol 5-phosphatase (SHIP) and a novel 110-kDa splice isoform, SHIPdelta. Genomics. 2000;69:104-112.

53. Lucas DM, Rohrschneider LR. A novel spliced form of SH2-containing inositol phosphatase is expressed during myeloid development. Blood. 1999;93:1922-1933.

54. Rohrschneider LR, Fuller JF, Wolf I, Liu Y, Lucas DM. Structure, function, and biology of SHIP proteins. Genes Dev. 2000;14:505-520.

55. Rohrschneider LR, Custodio JM, Anderson TA, Miller CP, Gu H. The intron 5/6 promoter region of the ship1 gene regulates expression in stem/progenitor cells of the mouse embryo. Dev Biol. 2005.

56. Burgering BM, Coffer PJ. Protein kinase B (c-Akt) in phosphatidylinositol-3-OH kinase signal transduction. Nature. 1995;376:599-602.

57. Franke TF, Yang SI, Chan TO, et al. The protein kinase encoded by the Akt proto-oncogene is a target of the PDGF-activated phosphatidylinositol 3-kinase. Cell. 1995;81:727-736.

58. Yao R, Cooper GM. Requirement for phosphatidylinositol-3 kinase in the prevention of apoptosis by nerve growth factor. Science. 1995;267:2003-2006.

59. Freeburn RW, Wright KL, Burgess SJ, Astoul E, Cantrell DA, Ward SG. Evidence that SHIP-1 contributes to phosphatidylinositol 3,4,5-trisphosphate metabolism in T lymphocytes and can regulate novel phosphoinositide 3-kinase effectors. J Immunol. 2002;169:5441-5450.

60. Carver DJ, Aman MJ, Ravichandran KS. SHIP inhibits Akt activation in B cells through regulation of Akt membrane localization. Blood. 2000;96:1449-1456.

61. Aman MJ, Lamkin TD, Okada H, Kurosaki T, Ravichandran KS. The inositol phosphatase SHIP inhibits Akt/PKB activation in B cells. J Biol Chem. 1998;273:33922-33928.

62. Bolland S, Pearse RN, Kurosaki T, Ravetch JV. SHIP modulates immune receptor responses by regulating membrane association of Btk. Immunity. 1998;8:509-516.

63. Scharenberg AM, El-Hillal O, Fruman DA, et al. Phosphatidylinositol-3,4,5-trisphosphate (PtdIns-3,4,5-P3)/Tec kinase-dependent calcium signaling pathway: a target for SHIP-mediated inhibitory signals. Embo J. 1998;17:1961-1972.

64. Luckhoff A, Clapham DE. Inositol 1,3,4,5-tetrakisphosphate activates an endothelial Ca(2+)-permeable channel. Nature. 1992;355:356-358.

65. Cullen PJ, Loomis-Husselbee J, Dawson AP, Irvine RF. Inositol 1,3,4,5-tetrakisphosphate and Ca2+ homoeostasis: the role of GAP1IP4BP. Biochem Soc Trans. 1997;25:991-996.

66. Huber M, Helgason CD, Damen JE, et al. The role of SHIP in growth factor induced signalling. Prog Biophys Mol Biol. 1999;71:423-434.

67. van der Geer P, Pawson T. The PTB domain: a new protein module implicated in signal transduction. Trends Biochem Sci. 1995;20:277-280.

68. Laminet AA, Apell G, Conroy L, Kavanaugh WM. Affinity, specificity, and kinetics of the interaction of the SHC phosphotyrosine binding domain with asparagine-X-X-phosphotyrosine motifs of growth factor receptors. J Biol Chem. 1996;271:264-269.

69. van der Geer P, Wiley S, Gish GD, et al. Identification of residues that control specific binding of the Shc phosphotyrosine-binding domain to phosphotyrosine sites. Proc Natl Acad Sci U S A. 1996;93:963-968.

70. Zhang S, Broxmeyer HE. p85 subunit of PI3 kinase does not bind to human Flt3 receptor, but associates with SHP2, SHIP, and a tyrosine-phosphorylated 100-kDa protein in Flt3 ligand-stimulated hematopoietic cells. Biochem Biophys Res Commun. 1999;254:440-445.

71. Gupta N, Scharenberg AM, Fruman DA, Cantley LC, Kinet JP, Long EO. The SH2 domain-containing inositol 5'-phosphatase (SHIP) recruits the p85 subunit of phosphoinositide 3-kinase during FcgammaRIIb1-mediated inhibition of B cell receptor signaling. J Biol Chem. 1999;274:7489-7494.

72. Kapeller R, Cantley LC. Phosphatidylinositol 3-kinase. Bioessays. 1994;16:565-576.

73. Alexandropoulos K, Cheng G, Baltimore D. Proline-rich sequences that bind to Src homology 3 domains with individual specificities. Proc Natl Acad Sci U S A. 1995;92:3110-3114.

74. Geier SJ, Algate PA, Carlberg K, et al. The human SHIP gene is differentially expressed in cell lineages of the bone marrow and blood. Blood. 1997;89:1876-1885.

75. Krystal G, Damen JE, Helgason CD, et al. SHIPs ahoy. Int J Biochem Cell Biol. 1999;31:1007-1010.

76. Horn S, Meyer J, Heukeshoven J, et al. The inositol 5-phosphatase SHIP is expressed as 145 and 135 kDa proteins in blood and bone marrow cells in vivo,

whereas carboxyl-truncated forms of SHIP are generated by proteolytic cleavage in vitro. Leukemia. 2001;15:112-120.

77. Pesesse X, Deleu S, De Smedt F, Drayer L, Erneux C. Identification of a second SH2-domain-containing protein closely related to the phosphatidylinositol polyphosphate 5-phosphatase SHIP. Biochem Biophys Res Commun. 1997;239:697-700.

78. Hejna JA, Saito H, Merkens LS, et al. Cloning and characterization of a human cDNA (INPPL1) sharing homology with inositol polyphosphate phosphatases. Genomics. 1995;29:285-287.

79. Liu Q, Dumont DJ. Molecular cloning and chromosomal localization in human and mouse of the SH2-containing inositol phosphatase, INPP5D (SHIP). Amgen EST Program. Genomics. 1997;39:109-112.

80. Wisniewski D, Strife A, Swendeman S, et al. A novel SH2-containing phosphatidylinositol 3,4,5-trisphosphate 5-phosphatase (SHIP2) is constitutively tyrosine phosphorylated and associated with src homologous and collagen gene (SHC) in chronic myelogenous leukemia progenitor cells. Blood. 1999;93:2707-2720.

81. Bruyns C, Pesesse X, Moreau C, Blero D, Erneux C. The two SH2-domain-containing inositol 5-phosphatases SHIP1 and SHIP2 are coexpressed in human T lymphocytes. Biol Chem. 1999;380:969-974.

82. Muraille E, Pesesse X, Kuntz C, Erneux C. Distribution of the src-homology-2-domain-containing inositol 5-phosphatase SHIP-2 in both non-haemopoietic and haemopoietic cells and possible involvement of SHIP-2 in negative signalling of B-cells. Biochem J. 1999;342 Pt 3:697-705.

83. Muraille E, Bruhns P, Pesesse X, Daeron M, Erneux C. The SH2 domain containing inositol 5-phosphatase SHIP2 associates to the immunoreceptor tyrosine-based inhibition motif of Fc gammaRIIB in B cells under negative signaling. Immunol Lett. 2000;72:7-15.

84. Ishihara H, Sasaoka T, Hori H, et al. Molecular cloning of rat SH2-containing inositol phosphatase 2 (SHIP2) and its role in the regulation of insulin signaling. Biochem Biophys Res Commun. 1999;260:265-272.

85. Sasaoka T, Hori H, Wada T, et al. SH2-containing inositol phosphatase 2 negatively regulates insulin-induced glycogen synthesis in L6 myotubes. Diabetologia. 2001;44:1258-1267.

86. Wada T, Sasaoka T, Funaki M, et al. Overexpression of SH2-containing inositol phosphatase 2 results in negative regulation of insulin-induced metabolic

actions in 3T3-L1 adipocytes via its 5'-phosphatase catalytic activity. Mol Cell Biol. 2001;21:1633-1646.

87. Blero D, De Smedt F, Pesesse X, et al. The SH2 domain containing inositol 5-phosphatase SHIP2 controls phosphatidylinositol 3,4,5-trisphosphate levels in CHO-IR cells stimulated by insulin. Biochem Biophys Res Commun. 2001;282:839-843.

88. Clement S, Krause U, Desmedt F, et al. The lipid phosphatase SHIP2 controls insulin sensitivity. Nature. 2001;409:92-97.

89. Marion E, Kaisaki PJ, Pouillon V, et al. The gene INPPL1, encoding the lipid phosphatase SHIP2, is a candidate for type 2 diabetes in rat and man. Diabetes. 2002;51:2012-2017.

90. Stambolic V, Suzuki A, de la Pompa JL, et al. Negative regulation of PKB/Akt-dependent cell survival by the tumor suppressor PTEN. Cell. 1998;95:29-39.

91. Li J, Yen C, Liaw D, et al. PTEN, a putative protein tyrosine phosphatase gene mutated in human brain, breast, and prostate cancer. Science. 1997;275:1943-1947.

92. Cantley LC, Neel BG. New insights into tumor suppression: PTEN suppresses tumor formation by restraining the phosphoinositide 3-kinase/AKT pathway. Proc Natl Acad Sci U S A. 1999;96:4240-4245.

93. Kishimoto H, Hamada K, Saunders M, et al. Physiological functions of Pten in mouse tissues. Cell Struct Funct. 2003;28:11-21.

94. Suzuki A, de la Pompa JL, Stambolic V, et al. High cancer susceptibility and embryonic lethality associated with mutation of the PTEN tumor suppressor gene in mice. Curr Biol. 1998;8:1169-1178.

95. Helgason CD, Damen JE, Rosten P, et al. Targeted disruption of SHIP leads to hemopoietic perturbations, lung pathology, and a shortened life span. Genes Dev. 1998;12:1610-1620.

96. Moody JL, Pereira CG, Magil A, Fritzler MJ, Jirik FR. Loss of a single allele of SHIP exacerbates the immunopathology of Pten heterozygous mice. Genes Immun. 2003;4:60-66.

97. Karlsson MC, Guinamard R, Bolland S, Sankala M, Steinman RM, Ravetch JV. Macrophages control the retention and trafficking of B lymphocytes in the splenic marginal zone. J Exp Med. 2003;198:333-340.

98. Liu Q, Shalaby F, Jones J, Bouchard D, Dumont DJ. The SH2-containing inositol polyphosphate 5-phosphatase, ship, is expressed during hematopoiesis and spermatogenesis. Blood. 1998;91:2753-2759.

99. Huber M, Helgason CD, Damen JE, Liu L, Humphries RK, Krystal G. The src homology 2-containing inositol phosphatase (SHIP) is the gatekeeper of mast cell degranulation. Proc Natl Acad Sci U S A. 1998;95:11330-11335.

100. Huber M, Helgason CD, Damen JE, et al. The role of the SRC homology 2-containing inositol 5'-phosphatase in Fc epsilon R1-induced signaling. Curr Top Microbiol Immunol. 1999;244:29-41.

101. Takeshita S, Namba N, Zhao JJ, et al. SHIP-deficient mice are severely osteoporotic due to increased numbers of hyper-resorptive osteoclasts. Nat Med. 2002;8:943-949.

102. Kuhn R, Schwenk F, Aguet M, Rajewsky K. Inducible gene targeting in mice. Science. 1995;269:1427-1429.

103. Oberdoerffer P, Otipoby KL, Maruyama M, Rajewsky K. Unidirectional Cre-mediated genetic inversion in mice using the mutant loxP pair lox66/lox71. Nucleic Acids Res. 2003;31:e140.

104. Muller AM, Medvinsky A, Strouboulis J, Grosveld F, Dzierzak E. Development of hematopoietic stem cell activity in the mouse embryo. Immunity. 1994;1:291-301.

105. Metcalf D, Moore AS, Shortman K. Adherence column and buoyant density separation of bone marrow stem cells and more differentiated cells. J Cell Physiol. 1971;78:441-450.

106. Durand C, Dzierzak E. Embryonic beginnings of adult hematopoietic stem cells. Haematologica. 2005;90:100-108.

107. Huang H, Auerbach R. Identification and characterization of hematopoietic stem cells from the yolk sac of the early mouse embryo. Proc Natl Acad Sci U S A. 1993;90:10110-10114.

108. Medvinsky AL, Samoylina NL, Muller AM, Dzierzak EA. An early pre-liver intraembryonic source of CFU-S in the developing mouse. Nature. 1993;364:64-67.

109. Godin IE, Garcia-Porrero JA, Coutinho A, Dieterlen-Lievre F, Marcos MA. Para-aortic splanchnopleura from early mouse embryos contains B1a cell progenitors. Nature. 1993;364:67-70.

110. Medvinsky A, Dzierzak E. Definitive hematopoiesis is autonomously initiated by the AGM region. Cell. 1996;86:897-906.

111. Miller CL, Eaves CJ. Expansion in vitro of adult murine hematopoietic stem cells with transplantable lympho-myeloid reconstituting ability. Proc Natl Acad Sci U S A. 1997;94:13648-13653.

112. Oostendorp RA, Audet J, Eaves CJ. High-resolution tracking of cell division suggests similar cell cycle kinetics of hematopoietic stem cells stimulated in vitro and in vivo. Blood. 2000;95:855-862.

113. Yonemura Y, Ku H, Lyman SD, Ogawa M. In vitro expansion of hematopoietic progenitors and maintenance of stem cells: comparison between FLT3/FLK-2 ligand and KIT ligand. Blood. 1997;89:1915-1921.

114. Bryder D, Jacobsen SE. Interleukin-3 supports expansion of long-term multilineage repopulating activity after multiple stem cell divisions in vitro. Blood. 2000;96:1748-1755.

115. Hasumura M, Imada C, Nawa K. Expression change of Flk-2/Flt-3 on murine hematopoietic stem cells in an activating state. Exp Hematol. 2003;31:1331-1337.

116. Ku H, Yonemura Y, Kaushansky K, Ogawa M. Thrombopoietin, the ligand for the Mpl receptor, synergizes with steel factor and other early acting cytokines in supporting proliferation of primitive hematopoietic progenitors of mice. Blood. 1996;87:4544-4551.

117. Sitnicka E, Lin N, Priestley GV, et al. The effect of thrombopoietin on the proliferation and differentiation of murine hematopoietic stem cells. Blood. 1996;87:4998-5005.

118. Petzer AL, Zandstra PW, Piret JM, Eaves CJ. Differential cytokine effects on primitive (CD34+CD38-) human hematopoietic cells: novel responses to Flt3-ligand and thrombopoietin. J Exp Med. 1996;183:2551-2558.

119. Kobayashi M, Laver JH, Kato T, Miyazaki H, Ogawa M. Thrombopoietin supports proliferation of human primitive hematopoietic cells in synergy with steel factor and/or interleukin-3. Blood. 1996;88:429-436.

120. Young JC, Bruno E, Luens KM, Wu S, Backer M, Murray LJ. Thrombopoietin stimulates megakaryocytopoiesis, myelopoiesis, and expansion of CD34+ progenitor cells from single CD34+Thy-1+Lin- primitive progenitor cells. Blood. 1996;88:1619-1631.

121. Rasko JE, O'Flaherty E, Begley CG. Mpl ligand (MGDF) alone and in combination with stem cell factor (SCF) promotes proliferation and survival of human megakaryocyte, erythroid and granulocyte/macrophage progenitors. Stem Cells. 1997;15:33-42.

122. Ohmizono Y, Sakabe H, Kimura T, et al. Thrombopoietin augments ex vivo expansion of human cord blood-derived hematopoietic progenitors in combination with stem cell factor and flt3 ligand. Leukemia. 1997;11:524-530.

123. Ramsfjell V, Borge OJ, Veiby OP, et al. Thrombopoietin, but not erythropoietin, directly stimulates multilineage growth of primitive murine bone marrow progenitor cells in synergy with early acting cytokines: distinct interactions with the ligands for c-kit and FLT3. Blood. 1996;88:4481-4492.

124. Piacibello W, Sanavio F, Garetto L, et al. Extensive amplification and self-renewal of human primitive hematopoietic stem cells from cord blood. Blood. 1997;89:2644-2653.

125. Ramsfjell V, Borge OJ, Cui L, Jacobsen SE. Thrombopoietin directly and potently stimulates multilineage growth and progenitor cell expansion from primitive (CD34+ CD38-) human bone marrow progenitor cells: distinct and key interactions with the ligands for c-kit and flt3, and inhibitory effects of TGF-beta and TNF-alpha. J Immunol. 1997;158:5169-5177.

126. Borge OJ, Ramsfjell V, Cui L, Jacobsen SE. Ability of early acting cytokines to directly promote survival and suppress apoptosis of human primitive CD34+CD38- bone marrow cells with multilineage potential at the single-cell level: key role of thrombopoietin. Blood. 1997;90:2282-2292.

127. Yagi M, Ritchie KA, Sitnicka E, Storey C, Roth GJ, Bartelmez S. Sustained ex vivo expansion of hematopoietic stem cells mediated by thrombopoietin. Proc Natl Acad Sci U S A. 1999;96:8126-8131.

128. Snoeck HW, Weekx S, Moulijn A, et al. Tumor necrosis factor alpha is a potent synergistic factor for the proliferation of primitive human hematopoietic progenitor cells and induces resistance to transforming growth factor beta but not to interferon gamma. J Exp Med. 1996;183:705-710.

129. Adams GB, Chabner KT, Foxall RB, et al. Heterologous cells cooperate to augment stem cell migration, homing, and engraftment. Blood. 2003;101:45-51.

130. Eto T, Winkler I, Purton LE, Levesque JP. Contrasting effects of P-selectin and E-selectin on the differentiation of murine hematopoietic progenitor cells. Exp Hematol. 2005;33:232-242.

131. Gong JK. Endosteal marrow: a rich source of hematopoietic stem cells. Science. 1978;199:1443-1445.

132. Calvi LM, Adams GB, Weibrecht KW, et al. Osteoblastic cells regulate the haematopoietic stem cell niche. Nature. 2003;425:841-846.

133. Zhang J, Niu C, Ye L, et al. Identification of the haematopoietic stem cell niche and control of the niche size. Nature. 2003;425:836-841.

134. Visnjic D, Kalajzic Z, Rowe DW, Katavic V, Lorenzo J, Aguila HL. Hematopoiesis is severely altered in mice with an induced osteoblast deficiency. Blood. 2004;103:3258-3264.

135. Moore MA. Cytokine and chemokine networks influencing stem cell proliferation, differentiation, and marrow homing. J Cell Biochem Suppl. 2002;38:29-38.

136. Vuillet-Gaugler MH, Breton-Gorius J, Vainchenker W, et al. Loss of attachment to fibronectin with terminal human erythroid differentiation. Blood. 1990;75:865-873.

137. Yoder MC, Williams DA. Matrix molecule interactions with hematopoietic stem cells. Exp Hematol. 1995;23:961-967.

138. Lewinsohn DM, Nagler A, Ginzton N, Greenberg P, Butcher EC. Hematopoietic progenitor cell expression of the H-CAM (CD44) homing-associated adhesion molecule. Blood. 1990;75:589-595.

139. Gu YC, Kortesmaa J, Tryggvason K, et al. Laminin isoform-specific promotion of adhesion and migration of human bone marrow progenitor cells. Blood. 2003;101:877-885.

140. Verfaillie CM, McCarthy JB, McGlave PB. Differentiation of primitive human multipotent hematopoietic progenitors into single lineage clonogenic progenitors is accompanied by alterations in their interaction with fibronectin. J Exp Med. 1991;174:693-703.

141. Simmons PJ, Masinovsky B, Longenecker BM, Berenson R, Torok-Storb B, Gallatin WM. Vascular cell adhesion molecule-1 expressed by bone marrow stromal cells mediates the binding of hematopoietic progenitor cells. Blood. 1992;80:388-395.

142. Teixido J, Hemler ME, Greenberger JS, Anklesaria P. Role of beta 1 and beta 2 integrins in the adhesion of human CD34hi stem cells to bone marrow stroma. J Clin Invest. 1992;90:358-367.

143. Frenette PS, Denis CV, Weiss L, et al. P-Selectin glycoprotein ligand 1 (PSGL-1) is expressed on platelets and can mediate platelet-endothelial interactions in vivo. J Exp Med. 2000;191:1413-1422.

144. Katayama Y, Hidalgo A, Furie BC, Vestweber D, Furie B, Frenette PS. PSGL-1 participates in E-selectin-mediated progenitor homing to bone marrow: evidence for cooperation between E-selectin ligands and alpha4 integrin. Blood. 2003;102:2060-2067.

145. Chigaev A, Zwartz G, Graves SW, et al. Alpha4beta1 integrin affinity changes govern cell adhesion. J Biol Chem. 2003;278:38174-38182.

146. Becker PS, Nilsson SK, Li Z, et al. Adhesion receptor expression by hematopoietic cell lines and murine progenitors: modulation by cytokines and cell cycle status. Exp Hematol. 1999;27:533-541.

147. Cerny J, Dooner M, McAuliffe C, et al. Homing of purified murine lymphohematopoietic stem cells: a cytokine-induced defect. J Hematother Stem Cell Res. 2002;11:913-922.

148. Scott LM, Priestley GV, Papayannopoulou T. Deletion of alpha4 integrins from adult hematopoietic cells reveals roles in homeostasis, regeneration, and homing. Mol Cell Biol. 2003;23:9349-9360.

149. Aiuti A, Webb IJ, Bleul C, Springer T, Gutierrez-Ramos JC. The chemokine SDF-1 is a chemoattractant for human CD34+ hematopoietic progenitor cells and provides a new mechanism to explain the mobilization of CD34+ progenitors to peripheral blood. J Exp Med. 1997;185:111-120.

150. Hattori K, Heissig B, Rafii S. The regulation of hematopoietic stem cell and progenitor mobilization by chemokine SDF-1. Leuk Lymphoma. 2003;44:575-582.

151. Peled A, Petit I, Kollet O, et al. Dependence of human stem cell engraftment and repopulation of NOD/SCID mice on CXCR4. Science. 1999;283:845-848.

152. Kim CH, Hangoc G, Cooper S, et al. Altered responsiveness to chemokines due to targeted disruption of SHIP. J Clin Invest. 1999;104:1751-1759.

153. Rottapel R, Reedijk M, Williams DE, et al. The Steel/W transduction pathway: kit autophosphorylation and its association with a unique subset of cytoplasmic signaling proteins is induced by the Steel factor. Mol Cell Biol. 1991;11:3043-3051.

154. Vicente-Manzanares M, Rey M, Jones DR, et al. Involvement of phosphatidylinositol 3-kinase in stromal cell-derived factor-1 alpha-induced lymphocyte polarization and chemotaxis. J Immunol. 1999;163:4001-4012.

155. Craddock BL, Welham MJ. Interleukin-3 induces association of the protein-tyrosine phosphatase SHP2 and phosphatidylinositol 3-kinase with a 100-kDa tyrosine-phosphorylated protein in hemopoietic cells. J Biol Chem. 1997;272:29281-29289.

156. Helgason CD, Antonchuk J, Bodner C, Humphries RK. Homeostasis and regeneration of the hematopoietic stem cell pool are altered in SHIP-deficient mice. Blood. 2003;102:3541-3547.

157. Ma Q, Jones D, Springer TA. The chemokine receptor CXCR4 is required for the retention of B lineage and granulocytic precursors within the bone marrow microenvironment. Immunity. 1999;10:463-471.

158. Ulyanova T, Scott LM, Priestley GV, et al. VCAM-1 expression in adult hematopoietic and nonhematopoietic cells is controlled by tissue-inductive signals and reflects their developmental origin. Blood. 2005;106:86-94.

159. Morrison SJ, Weissman IL. The long-term repopulating subset of hematopoietic stem cells is deterministic and isolatable by phenotype. Immunity. 1994;1:661-673.

160. Christensen JL, Weissman IL. Flk-2 is a marker in hematopoietic stem cell differentiation: a simple method to isolate long-term stem cells. Proc Natl Acad Sci U S A. 2001;98:14541-14546.

161. Spangrude GJ, Brooks DM. Phenotypic analysis of mouse hematopoietic stem cells shows a Thy-1-negative subset. Blood. 1992;80:1957-1964.

162. Kiel MJ, Yilmaz OH, Iwashita T, Yilmaz OH, Terhorst C, Morrison SJ. SLAM Family Receptors Distinguish Hematopoietic Stem and Progenitor Cells and Reveal Endothelial Niches for Stem Cells. Cell. 2005;121:1109-1121.

163. Goodell MA, Brose K, Paradis G, Conner AS, Mulligan RC. Isolation and functional properties of murine hematopoietic stem cells that are replicating in vivo. J Exp Med. 1996;183:1797-1806.

164. Zhou S, Schuetz JD, Bunting KD, et al. The ABC transporter Bcrp1/ABCG2 is expressed in a wide variety of stem cells and is a molecular determinant of the side-population phenotype. Nat Med. 2001;7:1028-1034.

165. Fleming WH, Alpern EJ, Uchida N, Ikuta K, Spangrude GJ, Weissman IL. Functional heterogeneity is associated with the cell cycle status of murine hematopoietic stem cells. J Cell Biol. 1993;122:897-902.

166. Peters SO, Kittler EL, Ramshaw HS, Quesenberry PJ. Murine marrow cells expanded in culture with IL-3, IL-6, IL-11, and SCF acquire an engraftment defect in normal hosts. Exp Hematol. 1995;23:461-469.

167. Lambert JF, Liu M, Colvin GA, et al. Marrow stem cells shift gene expression and engraftment phenotype with cell cycle transit. J Exp Med. 2003;197:1563-1572.

168. Venezia TA, Merchant AA, Ramos CA, et al. Molecular signatures of proliferation and quiescence in hematopoietic stem cells. PLoS Biol. 2004;2:e301.

169. Harrison DE. Competitive repopulation: a new assay for long-term stem cell functional capacity. Blood. 1980;55:77-81.

170. Nichogiannopoulou A, Trevisan M, Neben S, Friedrich C, Georgopoulos K. Defects in hemopoietic stem cell activity in Ikaros mutant mice. J Exp Med. 1999;190:1201-1214.

171. Helgason CD, Kalberer CP, Damen JE, et al. A dual role for Src homology 2 domain-containing inositol-5-phosphatase (SHIP) in immunity: aberrant development and enhanced function of b lymphocytes in ship -/- mice. J Exp Med. 2000;191:781-794.

172. Rolink AG, Nutt SL, Melchers F, Busslinger M. Long-term in vivo reconstitution of T-cell development by Pax5-deficient B-cell progenitors. Nature. 1999;401:603-606.

173. Domen J, Cheshier SH, Weissman IL. The role of apoptosis in the regulation of hematopoietic stem cells: Overexpression of Bcl-2 increases both their number and repopulation potential. J Exp Med. 2000;191:253-264.

174. Randall TD, Weissman IL. Phenotypic and functional changes induced at the clonal level in hematopoietic stem cells after 5-fluorouracil treatment. Blood. 1997;89:3596-3606.

175. Doyonnas R, Nielsen JS, Chelliah S, et al. Podocalyxin is a CD34-related marker of murine hematopoietic stem cells and embryonic erythroid cells. Blood. 2005;105:4170-4178.

176. Vermeulen M, Le Pesteur F, Gagnerault MC, Mary JY, Sainteny F, Lepault F. Role of adhesion molecules in the homing and mobilization of murine hematopoietic stem and progenitor cells. Blood. 1998;92:894-900.

177. Budnik A, Grewe M, Gyufko K, Krutmann J. Analysis of the production of soluble ICAM-1 molecules by human cells. Exp Hematol. 1996;24:352-359.

178. Meager A, Bird C, Mire-Sluis A. Assays for measuring soluble cellular adhesion molecules and soluble cytokine receptors. J Immunol Methods. 1996;191:97-112.

179. Lobb RR, Chi-Rosso G, Leone DR, et al. Expression and functional characterization of a soluble form of endothelial-leukocyte adhesion molecule 1. J Immunol. 1991;147:124-129.

180. Rothlein R, Mainolfi EA, Czajkowski M, Marlin SD. A form of circulating ICAM-1 in human serum. J Immunol. 1991;147:3788-3793.

181. Ara T, Tokoyoda K, Sugiyama T, Egawa T, Kawabata K, Nagasawa T. Long-term hematopoietic stem cells require stromal cell-derived factor-1 for colonizing bone marrow during ontogeny. Immunity. 2003;19:257-267.

182. Geissler EN, Ryan MA, Housman DE. The dominant-white spotting (W) locus of the mouse encodes the c-kit proto-oncogene. Cell. 1988;55:185-192.

183. Cappellini A, Tabellini G, Zweyer M, et al. The phosphoinositide 3-kinase/Akt pathway regulates cell cycle progression of HL60 human leukemia cells through cytoplasmic relocalization of the cyclin-dependent kinase inhibitor p27(Kip1) and control of cyclin D1 expression. Leukemia. 2003;17:2157-2167.

184. Solar GP, Kerr WG, Zeigler FC, et al. Role of c-mpl in early hematopoiesis. Blood. 1998;92:4-10.

185. Wright DE, Bowman EP, Wagers AJ, Butcher EC, Weissman IL. Hematopoietic stem cells are uniquely selective in their migratory response to chemokines. J Exp Med. 2002;195:1145-1154.

186. Neipp M, Zorina T, Domenick MA, Exner BG, Ildstad ST. Effect of FLT3 ligand and granulocyte colony-stimulating factor on expansion and mobilization of facilitating cells and hematopoietic stem cells in mice: kinetics and repopulating potential. Blood. 1998;92:3177-3188.

187. Ikuta K, Ingolia DE, Friedman J, Heimfeld S, Weissman IL. Mouse hematopoietic stem cells and the interaction of c-kit receptor and steel factor. Int J Cell Cloning. 1991;9:451-460.

188. Papayannopoulou T, Craddock C, Nakamoto B, Priestley GV, Wolf NS. The VLA4/VCAM-1 adhesion pathway defines contrasting mechanisms of lodgement of transplanted murine hemopoietic progenitors between bone marrow and spleen. Proc Natl Acad Sci U S A. 1995;92:9647-9651.

189. Peled A, Kollet O, Ponomaryov T, et al. The chemokine SDF-1 activates the integrins LFA-1, VLA-4, and VLA-5 on immature human CD34(+) cells: role in transendothelial/stromal migration and engraftment of NOD/SCID mice. Blood. 2000;95:3289-3296.

190. Szilvassy SJ, Humphries RK, Lansdorp PM, Eaves AC, Eaves CJ. Quantitative assay for totipotent reconstituting hematopoietic stem cells by a competitive repopulation strategy. Proc Natl Acad Sci U S A. 1990;87:8736-8740.

191. Kaushansky K. The molecular mechanisms that control thrombopoiesis. J Clin Invest. 2005;115:3339-3347.

192. Wendling F. Thrombopoietin: its role from early hematopoiesis to platelet production. Haematologica. 1999;84:158-166.

193. Carrington PA, Hill RJ, Stenberg PE, et al. Multiple in vivo effects of interleukin-3 and interleukin-6 on murine megakaryocytopoiesis. Blood. 1991;77:34-41.

194. Yonemura Y, Kawakita M, Masuda T, Fujimoto K, Kato K, Takatsuki K. Synergistic effects of interleukin 3 and interleukin 11 on murine megakaryopoiesis in serum-free culture. Exp Hematol. 1992;20:1011-1016.

195. Quesniaux VF. Interleukin 11. Leuk Lymphoma. 1994;14:241-249.

196. Sasaki H, Hirabayashi Y, Ishibashi T, et al. Effects of erythropoietin, IL-3, IL-6 and LIF on a murine megakaryoblastic cell line: growth enhancement and expression of receptor mRNAs. Leuk Res. 1995;19:95-102.

197. Yang FC, Tsuji K, Oda A, et al. Differential effects of human granulocyte colony-stimulating factor (hG-CSF) and thrombopoietin on megakaryopoiesis and platelet function in hG-CSF receptor-transgenic mice. Blood. 1999;94:950-958.

198. Hamada T, Mohle R, Hesselgesser J, et al. Transendothelial migration of megakaryocytes in response to stromal cell-derived factor 1 (SDF-1) enhances platelet formation. J Exp Med. 1998;188:539-548.

199. Wang JF, Liu ZY, Groopman JE. The alpha-chemokine receptor CXCR4 is expressed on the megakaryocytic lineage from progenitor to platelets and modulates migration and adhesion. Blood. 1998;92:756-764.

200. Avecilla ST, Hattori K, Heissig B, et al. Chemokine-mediated interaction of hematopoietic progenitors with the bone marrow vascular niche is required for thrombopoiesis. Nat Med. 2004;10:64-71.

201. Cserhati I, Kelemen E. Acute prolonged thrombocytosis in mice induced by thrombocythaemic sera; a possible human thrombopoietin; a preliminary communication. Acta Med Acad Sci Hung. 1958;11:473-475.

202. Cserhati I, Tanos B, Kelemen E. [Acute prolonged thrombocytosis in mice induced by the serum of patients having thrombocythemia; postulated human thrombopoietin.]. Orv Hetil. 1958;99:540-541.

203. Kelemen E, Cserhati I, Tanos B. Demonstration and some properties of human thrombopoietin in thrombocythaemic sera. Acta Haematol. 1958;20:350-355.

204. Bartley TD, Bogenberger J, Hunt P, et al. Identification and cloning of a megakaryocyte growth and development factor that is a ligand for the cytokine receptor Mpl. Cell. 1994;77:1117-1124.

205. de Sauvage FJ, Hass PE, Spencer SD, et al. Stimulation of megakaryocytopoiesis and thrombopoiesis by the c-Mpl ligand. Nature. 1994;369:533-538.

206. Gurney AL, Carver-Moore K, de Sauvage FJ, Moore MW. Thrombocytopenia in c-mpl-deficient mice. Science. 1994;265:1445-1447.

207. Kaushansky K, Lok S, Holly RD, et al. Promotion of megakaryocyte progenitor expansion and differentiation by the c-Mpl ligand thrombopoietin. Nature. 1994;369:568-571.

208. Lok S, Foster DC. The structure, biology and potential therapeutic applications of recombinant thrombopoietin. Stem Cells. 1994;12:586-598.

209. Lok S, Kaushansky K, Holly RD, et al. Cloning and expression of murine thrombopoietin cDNA and stimulation of platelet production in vivo. Nature. 1994;369:565-568.

210. Wendling F, Maraskovsky E, Debili N, et al. cMpl ligand is a humoral regulator of megakaryocytopoiesis. Nature. 1994;369:571-574.

211. Brodsky WY, Uryvaeva IV. Cell polyploidy: its relation to tissue growth and function. Int Rev Cytol. 1977;50:275-332.

212. Hancock V, Martin JF, Lelchuk R. The relationship between human megakaryocyte nuclear DNA content and gene expression. Br J Haematol. 1993;85:692-697.

213. Winkelmann M, Pfitzer P, Schneider W. Significance of polyploidy in megakaryocytes and other cells in health and tumor disease. Klin Wochenschr. 1987;65:1115-1131.

214. Italiano JE, Jr., Lecine P, Shivdasani RA, Hartwig JH. Blood platelets are assembled principally at the ends of proplatelet processes produced by differentiated megakaryocytes. J Cell Biol. 1999;147:1299-1312.

215. Hartwig J, Italiano J, Jr. The birth of the platelet. J Thromb Haemost. 2003;1:1580-1586.

216. Kaushansky K. Thrombopoietin. N Engl J Med. 1998;339:746-754.

217. Avraham H, Price DJ. Regulation of megakaryocytopoiesis and platelet production by tyrosine kinases and tyrosine phosphatases. Methods. 1999;17:250-264.

218. Souyri M, Vigon I, Penciolelli JF, Heard JM, Tambourin P, Wendling F. A putative truncated cytokine receptor gene transduced by the myeloproliferative leukemia virus immortalizes hematopoietic progenitors. Cell. 1990;63:1137-1147.

219. Vigon I, Mornon JP, Cocault L, et al. Molecular cloning and characterization of MPL, the human homolog of the v-mpl oncogene: identification of a member of the hematopoietic growth factor receptor superfamily. Proc Natl Acad Sci U S A. 1992;89:5640-5644.

220. Stoffel R, Wiestner A, Skoda RC. Thrombopoietin in thrombocytopenic mice: evidence against regulation at the mRNA level and for a direct regulatory role of platelets. Blood. 1996;87:567-573.

221. McCarty JM, Sprugel KH, Fox NE, Sabath DE, Kaushansky K. Murine thrombopoietin mRNA levels are modulated by platelet count. Blood. 1995;86:3668-3675.

222. Harker LA, Finch CA. Thrombokinetics in man. J Clin Invest. 1969;48:963-974.

223. Kaushansky K, Lin N, Grossmann A, Humes J, Sprugel KH, Broudy VC. Thrombopoietin expands erythroid, granulocyte-macrophage, and megakaryocytic progenitor cells in normal and myelosuppressed mice. Exp Hematol. 1996;24:265-269.

224. Carver-Moore K, Broxmeyer HE, Luoh SM, et al. Low levels of erythroid and myeloid progenitors in thrombopoietin-and c-mpl-deficient mice. Blood. 1996;88:803-808.

225. Alexander WS, Roberts AW, Nicola NA, Li R, Metcalf D. Deficiencies in progenitor cells of multiple hematopoietic lineages and defective megakaryocytopoiesis in mice lacking the thrombopoietic receptor c-Mpl. Blood. 1996;87:2162-2170.

226. Kimura S, Roberts AW, Metcalf D, Alexander WS. Hematopoietic stem cell deficiencies in mice lacking c-Mpl, the receptor for thrombopoietin. Proc Natl Acad Sci U S A. 1998;95:1195-1200.

227. Ninos JM, Jefferies LC, Cogle CR, Kerr WG. The thrombopoietin receptor, c-mpl, is a selective surface marker for human hematopoietic stem cells. J Transl Med. 2006;4:9.

228. Bunting S, Widmer R, Lipari T, et al. Normal platelets and megakaryocytes are produced in vivo in the absence of thrombopoietin. Blood. 1997;90:3423-3429.

229. Kaushansky K. Thrombopoietin: the primary regulator of platelet production. Blood. 1995;86:419-431.

230. Hattori K, Heissig B, Tashiro K, et al. Plasma elevation of stromal cell-derived factor-1 induces mobilization of mature and immature hematopoietic progenitor and stem cells. Blood. 2001;97:3354-3360.

231. Perez LE, Alpdogan O, Shieh JH, et al. Increased plasma levels of stromal-derived factor-1 (SDF-1/CXCL12) enhance human thrombopoiesis and mobilize human colony-forming cells (CFC) in NOD/SCID mice. Exp Hematol. 2004;32:300-307.

232. Kaushansky K, Fox N, Lin NL, Liles WC. Lineage-specific growth factors can compensate for stem and progenitor cell deficiencies at the postprogenitor cell level: an analysis of doubly TPO- and G-CSF receptor-deficient mice. Blood. 2002;99:3573-3578.

233. Drachman JG, Miyakawa Y, Luthi JN, et al. Studies with chimeric Mpl/JAK2 receptors indicate that both JAK2 and the membrane-proximal domain of Mpl are required for cellular proliferation. J Biol Chem. 2002;277:23544-23553.

234. Miyakawa Y, Drachman JG, Gallis B, Kaushansky A, Kaushansky K. A structure-function analysis of serine/threonine phosphorylation of the thrombopoietin receptor, c-Mpl. J Biol Chem. 2000;275:32214-32219.

235. Geddis AE, Fox NE, Kaushansky K. Phosphatidylinositol 3-kinase is necessary but not sufficient for thrombopoietin-induced proliferation in engineered Mpl-bearing cell lines as well as in primary megakaryocytic progenitors. J Biol Chem. 2001;276:34473-34479.

236. Santini V, Scappini B, Grossi A, et al. Lyn kinase is activated following thrombopoietin stimulation of the megakaryocytic cell line B1647. Haematologica. 2002;87:1242-1247.

237. Kojima H, Shinagawa A, Shimizu S, et al. Role of phosphatidylinositol-3 kinase and its association with Gab1 in thrombopoietin-mediated up-regulation of platelet function. Exp Hematol. 2001;29:616-622.

238. Drachman JG, Sabath DF, Fox NE, Kaushansky K. Thrombopoietin signal transduction in purified murine megakaryocytes. Blood. 1997;89:483-492.

239. Gurney AL, Wong SC, Henzel WJ, de Sauvage FJ. Distinct regions of c-Mpl cytoplasmic domain are coupled to the JAK-STAT signal transduction pathway and Shc phosphorylation. Proc Natl Acad Sci U S A. 1995;92:5292-5296.

240. Sasaki K, Odai H, Hanazono Y, et al. TPO/c-mpl ligand induces tyrosine phosphorylation of multiple cellular proteins including proto-oncogene products, Vav and c-Cbl, and Ras signaling molecules. Biochem Biophys Res Commun. 1995;216:338-347.

241. Huber M, Helgason CD, Scheid MP, Duronio V, Humphries RK, Krystal G. Targeted disruption of SHIP leads to Steel factor-induced degranulation of mast cells. Embo J. 1998;17:7311-7319.

242. Malbec O, Fridman WH, Daeron M. Negative regulation of c-kit-mediated cell proliferation by Fc gamma RIIB. J Immunol. 1999;162:4424-4429.

243. Tong W, Lodish HF. Lnk inhibits Tpo-mpl signaling and Tpo-mediated megakaryocytopoiesis. J Exp Med. 2004;200:569-580.

244. Lannutti BJ, Minear J, Blake N, Drachman JG. Increased megakaryocytopoiesis in Lyn-deficient mice. Oncogene. 2006.

245. Hodohara K, Fujii N, Yamamoto N, Kaushansky K. Stromal cell-derived factor-1 (SDF-1) acts together with thrombopoietin to enhance the development of megakaryocytic progenitor cells (CFU-MK). Blood. 2000;95:769-775.

246. Desponts C, Hazen AL, Paraiso KH, Kerr WG. SHIP-deficiency enhances HSC proliferation and survival but compromises homing and repopulation. Blood. 2006.

247. Kaser A, Brandacher G, Steurer W, et al. Interleukin-6 stimulates thrombopoiesis through thrombopoietin: role in inflammatory thrombocytosis. Blood. 2001;98:2720-2725.

248. Fielder PJ, Gurney AL, Stefanich E, et al. Regulation of thrombopoietin levels by c-mpl-mediated binding to platelets. Blood. 1996;87:2154-2161.

249. Kuter DJ, Rosenberg RD. Regulation of megakaryocyte ploidy in vivo in the rat. Blood. 1990;75:74-81.

250. Fibbe WE, Heemskerk DP, Laterveer L, et al. Accelerated reconstitution of platelets and erythrocytes after syngeneic transplantation of bone marrow cells derived from thrombopoietin pretreated donor mice. Blood. 1995;86:3308-3313.

251. Hartwig JH, Kung S, Kovacsovics T, et al. D3 phosphoinositides and outside-in integrin signaling by glycoprotein IIb-IIIa mediate platelet actin assembly and filopodial extension induced by phorbol 12-myristate 13-acetate. J Biol Chem. 1996;271:32986-32993.

252. Kovacsovics TJ, Bachelot C, Toker A, et al. Phosphoinositide 3-kinase inhibition spares actin assembly in activating platelets but reverses platelet aggregation. J Biol Chem. 1995;270:11358-11366.

253. Giuriato S, Payrastre B, Drayer AL, et al. Tyrosine phosphorylation and relocation of SHIP are integrin-mediated in thrombin-stimulated human blood platelets. J Biol Chem. 1997;272:26857-26863.

254. Moody JL, Xu L, Helgason CD, Jirik FR. Anemia, thrombocytopenia, leukocytosis, extramedullary hematopoiesis, and impaired progenitor function in Pten+/-SHIP-/- mice: a novel model of myelodysplasia. Blood. 2004;103:4503-4510.

255. Kiessling R, Klein E, Wigzell H. "Natural" killer cells in the mouse. I. Cytotoxic cells with specificity for mouse Moloney leukemia cells. Specificity and distribution according to genotype. Eur J Immunol. 1975;5:112-117.

256. Kiessling R, Klein E, Pross H, Wigzell H. "Natural" killer cells in the mouse. II. Cytotoxic cells with specificity for mouse Moloney leukemia cells. Characteristics of the killer cell. Eur J Immunol. 1975;5:117-121.

257. Herberman RB, Nunn ME, Lavrin DH. Natural cytotoxic reactivity of mouse lymphoid cells against syngeneic acid allogeneic tumors. I. Distribution of reactivity and specificity. Int J Cancer. 1975;16:216-229.

258. Colucci F, Caligiuri MA, Di Santo JP. What does it take to make a natural killer? Nat Rev Immunol. 2003;3:413-425.

259. Spits H, Lanier LL, Phillips JH. Development of human T and natural killer cells. Blood. 1995;85:2654-2670.

260. Lauwerys BR, Garot N, Renauld JC, Houssiau FA. Cytokine production and killer activity of NK/T-NK cells derived with IL-2, IL-15, or the combination of IL-12 and IL-18. J Immunol. 2000;165:1847-1853.

261. Street SE, Trapani JA, MacGregor D, Smyth MJ. Suppression of lymphoma and epithelial malignancies effected by interferon gamma. J Exp Med. 2002;196:129-134.

262. Djeu JY, Stocks N, Zoon K, Stanton GJ, Timonen T, Herberman RB. Positive self regulation of cytotoxicity in human natural killer cells by production of interferon upon exposure to influenza and herpes viruses. J Exp Med. 1982;156:1222-1234.

263. Stetson DB, Mohrs M, Reinhardt RL, et al. Constitutive cytokine mRNAs mark natural killer (NK) and NK T cells poised for rapid effector function. J Exp Med. 2003;198:1069-1076.

264. Zompi S, Colucci F. Anatomy of a murder--signal transduction pathways leading to activation of natural killer cells. Immunol Lett. 2005;97:31-39.

265. Screpanti V, Wallin RP, Ljunggren HG, Grandien A. A central role for death receptor-mediated apoptosis in the rejection of tumors by NK cells. J Immunol. 2001;167:2068-2073.

266. Clement MV, Haddad P, Soulie A, et al. Involvement of granzyme B and perforin gene expression in the lytic potential of human natural killer cells. Res Immunol. 1990;141:477-489.

267. Zychlinsky A, Joag S, Liu CC, Young JD. Cytotoxic mechanisms of murine lymphokine-activated killer cells: functional and biochemical characterization of homogeneous populations of spleen LAK cells. Cell Immunol. 1990;126:377-390.

268. Kagi D, Ledermann B, Burki K, et al. Cytotoxicity mediated by T cells and natural killer cells is greatly impaired in perforin-deficient mice. Nature. 1994;369:31-37.

269. Eriksson M, Leitz G, Fallman E, et al. Inhibitory receptors alter natural killer cell interactions with target cells yet allow simultaneous killing of susceptible targets. J Exp Med. 1999;190:1005-1012.

270. Lanier LL. Natural killer cells: from no receptors to too many. Immunity. 1997;6:371-378.

271. Stahls A, Liwszyc GE, Couture C, Mustelin T, Andersson LC. Triggering of human natural killer cells through CD16 induces tyrosine phosphorylation of the p72syk kinase. Eur J Immunol. 1994;24:2491-2496.

272. Clements JL, Yang B, Ross-Barta SE, et al. Requirement for the leukocyte-specific adapter protein SLP-76 for normal T cell development. Science. 1998;281:416-419.

273. Vivier E, da Silva AJ, Ackerly M, Levine H, Rudd CE, Anderson P. Association of a 70-kDa tyrosine phosphoprotein with the CD16: zeta: gamma complex expressed in human natural killer cells. Eur J Immunol. 1993;23:1872-1876.

274. Jevremovic D, Billadeau DD, Schoon RA, et al. Cutting edge: a role for the adaptor protein LAT in human NK cell-mediated cytotoxicity. J Immunol. 1999;162:2453-2456.

275. Galandrini R, Palmieri G, Piccoli M, Frati L, Santoni A. CD16-mediated p21ras activation is associated with Shc and p36 tyrosine phosphorylation and their binding with Grb2 in human natural killer cells. J Exp Med. 1996;183:179-186.

276. Umehara H, Huang JY, Kono T, et al. Involvement of protein tyrosine kinase p72syk and phosphatidylinositol 3-kinase in CD2-mediated granular exocytosis in the natural killer cell line, NK3.3. J Immunol. 1997;159:1200-1207.

277. Jiang K, Zhong B, Gilvary DL, et al. Pivotal role of phosphoinositide-3 kinase in regulation of cytotoxicity in natural killer cells. Nat Immunol. 2000;1:419-425.

278. Azzoni L, Kamoun M, Salcedo TW, Kanakaraj P, Perussia B. Stimulation of Fc gamma RIIIA results in phospholipase C-gamma 1 tyrosine phosphorylation and p56lck activation. J Exp Med. 1992;176:1745-1750.

279. Tassi I, Presti R, Kim S, Yokoyama WM, Gilfillan S, Colonna M. Phospholipase C-gamma 2 is a critical signaling mediator for murine NK cell activating receptors. J Immunol. 2005;175:749-754.

280. Caraux A, Kim N, Bell SE, et al. Phospholipase C-gamma2 is essential for NK cell cytotoxicity and innate immunity to malignant and virally infected cells. Blood. 2006;107:994-1002.

281. Colucci F, Schweighoffer E, Tomasello E, et al. Natural cytotoxicity uncoupled from the Syk and ZAP-70 intracellular kinases. Nat Immunol. 2002;3:288-294.

282. Yokoyama WM, Ryan JC, Hunter JJ, Smith HR, Stark M, Seaman WE. cDNA cloning of mouse NKR-P1 and genetic linkage with LY-49. Identification of a natural killer cell gene complex on mouse chromosome 6. J Immunol. 1991;147:3229-3236.

283. Ziegler SF, Levin SD, Johnson L, et al. The mouse CD69 gene. Structure, expression, and mapping to the NK gene complex. J Immunol. 1994;152:1228-1236.

284. Morse HC, 3rd. Genetic nomenclature for loci controlling surface antigens of mouse hemopoietic cells. J Immunol. 1992;149:3129-3134.

285. Ryan JC, Turck J, Niemi EC, Yokoyama WM, Seaman WE. Molecular cloning of the NK1.1 antigen, a member of the NKR-P1 family of natural killer cell activation molecules. J Immunol. 1992;149:1631-1635.

286. Karlhofer FM, Yokoyama WM. Stimulation of murine natural killer (NK) cells by a monoclonal antibody specific for the NK1.1 antigen. IL-2-activated NK cells possess additional specific stimulation pathways. J Immunol. 1991;146:3662-3673.

287. Dimasi N, Biassoni R. Structural and functional aspects of the Ly49 natural killer cell receptors. Immunol Cell Biol. 2005;83:1-8.

288. Smith HR, Heusel JW, Mehta IK, et al. Recognition of a virus-encoded ligand by a natural killer cell activation receptor. Proc Natl Acad Sci U S A. 2002;99:8826-8831.

289. Arase H, Mocarski ES, Campbell AE, Hill AB, Lanier LL. Direct recognition of cytomegalovirus by activating and inhibitory NK cell receptors. Science. 2002;296:1323-1326.

290. Lanier LL, Corliss BC, Wu J, Leong C, Phillips JH. Immunoreceptor DAP12 bearing a tyrosine-based activation motif is involved in activating NK cells. Nature. 1998;391:703-707.

291. Anderson P, Caligiuri M, Ritz J, Schlossman SF. CD3-negative natural killer cells express zeta TCR as part of a novel molecular complex. Nature. 1989;341:159-162.

292. Wu J, Song Y, Bakker AB, et al. An activating immunoreceptor complex formed by NKG2D and DAP10. Science. 1999;285:730-732.

293. Wilson MJ, Lindquist JA, Trowsdale J. DAP12 and KAP10 (DAP10)-novel transmembrane adapter proteins of the CD3zeta family. Immunol Res. 2000;22:21-42.

294. Hibbs ML, Selvaraj P, Carpen O, et al. Mechanisms for regulating expression of membrane isoforms of Fc gamma RIII (CD16). Science. 1989;246:1608-1611.

295. Lanier LL, Kipps TJ, Phillips JH. Functional properties of a unique subset of cytotoxic CD3+ T lymphocytes that express Fc receptors for IgG (CD16/Leu-11 antigen). J Exp Med. 1985;162:2089-2106.

296. McVicar DW, Taylor LS, Gosselin P, et al. DAP12-mediated signal transduction in natural killer cells. A dominant role for the Syk protein-tyrosine kinase. J Biol Chem. 1998;273:32934-32942.

297. Mason LH, Willette-Brown J, Anderson SK, et al. Characterization of an associated 16-kDa tyrosine phosphoprotein required for Ly-49D signal transduction. J Immunol. 1998;160:4148-4152.

298. Yokoyama WM, Kehn PJ, Cohen DI, Shevach EM. Chromosomal location of the Ly-49 (A1, YE1/48) multigene family. Genetic association with the NK 1.1 antigen. J Immunol. 1990;145:2353-2358.

299. Rajagopalan S, Winter CC, Wagtmann N, Long EO. The Ig-related killer cell inhibitory receptor binds zinc and requires zinc for recognition of HLA-C on target cells. J Immunol. 1995;155:4143-4146.

300. Vely F, Olcese L, Blery M, Vivier E. Function of killer cell inhibitory receptors for MHC class I molecules. Immunol Lett. 1996;54:145-150.

301. Vely F, Olivero S, Olcese L, et al. Differential association of phosphatases with hematopoietic co-receptors bearing immunoreceptor tyrosine-based inhibition motifs. Eur J Immunol. 1997;27:1994-2000.

302. Makrigiannis AP, Gosselin P, Mason LH, et al. Cloning and characterization of a novel activating Ly49 closely related to Ly49A. J Immunol. 1999;163:4931-4938.

303. Hanke T, Raulet DH. Cumulative inhibition of NK cells and T cells resulting from engagement of multiple inhibitory Ly49 receptors. J Immunol. 2001;166:3002-3007.

304. Ravetch JV, Lanier LL. Immune inhibitory receptors. Science. 2000;290:84-89.

305. Amigorena S, Bonnerot C, Drake JR, et al. Cytoplasmic domain heterogeneity and functions of IgG Fc receptors in B lymphocytes. Science. 1992;256:1808-1812.

306. Muta T, Kurosaki T, Misulovin Z, Sanchez M, Nussenzweig MC, Ravetch JV. A 13-amino-acid motif in the cytoplasmic domain of Fc gamma RIIB modulates B-cell receptor signalling. Nature. 1994;369:340.

307. D'Ambrosio D, Hippen KL, Minskoff SA, et al. Recruitment and activation of PTP1C in negative regulation of antigen receptor signaling by Fc gamma RIIB1. Science. 1995;268:293-297.

308. Mason LH, Gosselin P, Anderson SK, Fogler WE, Ortaldo JR, McVicar DW. Differential tyrosine phosphorylation of inhibitory versus activating Ly-49 receptor proteins and their recruitment of SHP-1 phosphatase. J Immunol. 1997;159:4187-4196.

309. Lanier LL. NK cell receptors. Annu Rev Immunol. 1998;16:359-393.

310. Binstadt BA, Brumbaugh KM, Dick CJ, et al. Sequential involvement of Lck and SHP-1 with MHC-recognizing receptors on NK cells inhibits FcR-initiated tyrosine kinase activation. Immunity. 1996;5:629-638.

311. Karre K, Ljunggren HG, Piontek G, Kiessling R. Selective rejection of H-2-deficient lymphoma variants suggests alternative immune defence strategy. Nature. 1986;319:675-678.

312. Hoglund P, Ohlen C, Carbone E, et al. Recognition of beta 2-microglobulin-negative (beta 2m-) T-cell blasts by natural killer cells from normal but not from beta 2m- mice: nonresponsiveness controlled by beta 2m- bone marrow in chimeric mice. Proc Natl Acad Sci U S A. 1991;88:10332-10336.

313. Bix M, Liao NS, Zijlstra M, Loring J, Jaenisch R, Raulet D. Rejection of class I MHC-deficient haemopoietic cells by irradiated MHC-matched mice. Nature. 1991;349:329-331.

314. Lanier LL. NK cell recognition. Annu Rev Immunol. 2005;23:225-274.

315. Kim S, Iizuka K, Kang HS, et al. In vivo developmental stages in murine natural killer cell maturation. Nat Immunol. 2002;3:523-528.

316. Raulet DH. Development and tolerance of natural killer cells. Curr Opin Immunol. 1999;11:129-134.

317. Hanke T, Takizawa H, McMahon CW, et al. Direct assessment of MHC class I binding by seven Ly49 inhibitory NK cell receptors. Immunity. 1999;11:67-77.

318. Michaelsson J, Achour A, Salcedo M, et al. Visualization of inhibitory Ly49 receptor specificity with soluble major histocompatibility complex class I tetramers. Eur J Immunol. 2000;30:300-307.

319. Brawand P, Lemonnier FA, MacDonald HR, Cerottini JC, Held W. Transgenic expression of Ly49A on T cells impairs a specific antitumor response. J Immunol. 2000;165:1871-1876.

320. Zajac AJ, Vance RE, Held W, et al. Impaired anti-viral T cell responses due to expression of the Ly49A inhibitory receptor. J Immunol. 1999;163:5526-5534.

321. Franke TF, Kaplan DR, Cantley LC. PI3K: downstream AKTion blocks apoptosis. Cell. 1997;88:435-437.

322. Franke TF, Kaplan DR, Cantley LC, Toker A. Direct regulation of the Akt proto-oncogene product by phosphatidylinositol-3,4-bisphosphate. Science. 1997;275:665-668.

323. Nisitani S, Satterthwaite AB, Akashi K, Weissman IL, Witte ON, Wahl MI. Posttranscriptional regulation of Bruton's tyrosine kinase expression in antigen receptor-stimulated splenic B cells. Proc Natl Acad Sci U S A. 2000;97:2737-2742.

324. Marti F, Xu CW, Selvakumar A, Brent R, Dupont B, King PD. LCK-phosphorylated human killer cell-inhibitory receptors recruit and activate phosphatidylinositol 3-kinase. Proc Natl Acad Sci U S A. 1998;95:11810-11815.

325. Nakamura MC, Niemi EC, Fisher MJ, Shultz LD, Seaman WE, Ryan JC. Mouse Ly-49A interrupts early signaling events in natural killer cell cytotoxicity and functionally associates with the SHP-1 tyrosine phosphatase. J Exp Med. 1997;185:673-684.

326. Smith KM, Wu J, Bakker AB, Phillips JH, Lanier LL. Ly-49D and Ly-49H associate with mouse DAP12 and form activating receptors. J Immunol. 1998;161:7-10.

327. Lowin-Kropf B, Held W. Positive impact of inhibitory Ly49 receptor-MHC class I interaction on NK cell development. J Immunol. 2000;165:91-95.

328. Lian RH, Chin RK, Nemeth HE, Libby SL, Fu YX, Kumar V. A role for lymphotoxin in the acquisition of Ly49 receptors during NK cell development. Eur J Immunol. 2004;34:2699-2707.

329. Trotta R, Parihar R, Yu J, et al. Differential expression of SHIP1 in CD56bright and CD56dim NK cells provides a molecular basis for distinct functional responses to monokine costimulation. Blood. 2005;105:3011-3018.

330. Anderson SK. Transcriptional regulation of NK cell receptors. Curr Top Microbiol Immunol. 2006;298:59-75.

331. Saleh A, Davies GE, Pascal V, et al. Identification of probabilistic transcriptional switches in the Ly49 gene cluster: a eukaryotic mechanism for selective gene activation. Immunity. 2004;21:55-66.

332. Marshall AJ, Niiro H, Yun TJ, Clark EA. Regulation of B-cell activation and differentiation by the phosphatidylinositol 3-kinase and phospholipase Cgamma pathway. Immunol Rev. 2000;176:30-46.

333. Evans MJ, Kaufman MH. Establishment in culture of pluripotential cells from mouse embryos. Nature. 1981;292:154-156.

334. Martin GR. Isolation of a pluripotent cell line from early mouse embryos cultured in medium conditioned by teratocarcinoma stem cells. Proc Natl Acad Sci U S A. 1981;78:7634-7638.

335. Brook FA, Gardner RL. The origin and efficient derivation of embryonic stem cells in the mouse. Proc Natl Acad Sci U S A. 1997;94:5709-5712.

336. Beddington RS, Robertson EJ. An assessment of the developmental potential of embryonic stem cells in the midgestation mouse embryo. Development. 1989;105:733-737.

337. Burdon T, Smith A, Savatier P. Signalling, cell cycle and pluripotency in embryonic stem cells. Trends Cell Biol. 2002;12:432-438.

338. Smith AG, Hooper ML. Buffalo rat liver cells produce a diffusible activity which inhibits the differentiation of murine embryonal carcinoma and embryonic stem cells. Dev Biol. 1987;121:1-9.

339. Williams RL, Hilton DJ, Pease S, et al. Myeloid leukaemia inhibitory factor maintains the developmental potential of embryonic stem cells. Nature. 1988;336:684-687.

340. Smith AG, Heath JK, Donaldson DD, et al. Inhibition of pluripotential embryonic stem cell differentiation by purified polypeptides. Nature. 1988;336:688-690.

341. Ying QL, Nichols J, Chambers I, Smith A. BMP induction of Id proteins suppresses differentiation and sustains embryonic stem cell self-renewal in collaboration with STAT3. Cell. 2003;115:281-292.

342. Qi X, Li TG, Hao J, et al. BMP4 supports self-renewal of embryonic stem cells by inhibiting mitogen-activated protein kinase pathways. Proc Natl Acad Sci U S A. 2004;101:6027-6032.

343. Hirano T, Nakajima K, Hibi M. Signaling mechanisms through gp130: a model of the cytokine system. Cytokine Growth Factor Rev. 1997;8:241-252.

344. Hibi M, Murakami M, Saito M, Hirano T, Taga T, Kishimoto T. Molecular cloning and expression of an IL-6 signal transducer, gp130. Cell. 1990;63:1149-1157.

345. Gearing DP, Comeau MR, Friend DJ, et al. The IL-6 signal transducer, gp130: an oncostatin M receptor and affinity converter for the LIF receptor. Science. 1992;255:1434-1437.

346. Burdon T, Chambers I, Stracey C, Niwa H, Smith A. Signaling mechanisms regulating self-renewal and differentiation of pluripotent embryonic stem cells. Cells Tissues Organs. 1999;165:131-143.

347. Burdon T, Stracey C, Chambers I, Nichols J, Smith A. Suppression of SHP-2 and ERK signalling promotes self-renewal of mouse embryonic stem cells. Dev Biol. 1999;210:30-43.

348. Kristensen DM, Kalisz M, Nielsen JH. Cytokine signalling in embryonic stem cells. APMIS. 2005;113:756-772.

349. Niwa H, Burdon T, Chambers I, Smith A. Self-renewal of pluripotent embryonic stem cells is mediated via activation of STAT3. Genes Dev. 1998;12:2048-2060.

350. Paling NR, Wheadon H, Bone HK, Welham MJ. Regulation of embryonic stem cell self-renewal by phosphoinositide 3-kinase-dependent signaling. J Biol Chem. 2004;279:48063-48070.

351. Schuringa JJ, van der Schaaf S, Vellenga E, Eggen BJ, Kruijer W. LIF-induced STAT3 signaling in murine versus human embryonal carcinoma (EC) cells. Exp Cell Res. 2002;274:119-129.

352. Qu CK, Feng GS. Shp-2 has a positive regulatory role in ES cell differentiation and proliferation. Oncogene. 1998;17:433-439.

353. Chan RJ, Johnson SA, Li Y, Yoder MC, Feng GS. A definitive role of Shp-2 tyrosine phosphatase in mediating embryonic stem cell differentiation and hematopoiesis. Blood. 2003;102:2074-2080.

354. Zhong Z, Wen Z, Darnell JE, Jr. Stat3: a STAT family member activated by tyrosine phosphorylation in response to epidermal growth factor and interleukin-6. Science. 1994;264:95-98.

355. Boulton TG, Zhong Z, Wen Z, Darnell JE, Jr., Stahl N, Yancopoulos GD. STAT3 activation by cytokines utilizing gp130 and related transducers involves a secondary modification requiring an H7-sensitive kinase. Proc Natl Acad Sci U S A. 1995;92:6915-6919.

356. Stahl N, Farruggella TJ, Boulton TG, Zhong Z, Darnell JE, Jr., Yancopoulos GD. Choice of STATs and other substrates specified by modular tyrosine-based motifs in cytokine receptors. Science. 1995;267:1349-1353.

357. Ernst M, Novak U, Nicholson SE, Layton JE, Dunn AR. The carboxyl-terminal domains of gp130-related cytokine receptors are necessary for suppressing embryonic stem cell differentiation. Involvement of STAT3. J Biol Chem. 1999;274:9729-9737.

358. Matsuda T, Nakamura T, Nakao K, et al. STAT3 activation is sufficient to maintain an undifferentiated state of mouse embryonic stem cells. Embo J. 1999;18:4261-4269.

359. Kolch W. Meaningful relationships: the regulation of the Ras/Raf/MEK/ERK pathway by protein interactions. Biochem J. 2000;351 Pt 2:289-305.

360. Nakaoka Y, Nishida K, Fujio Y, et al. Activation of gp130 transduces hypertrophic signal through interaction of scaffolding/docking protein Gab1 with tyrosine phosphatase SHP2 in cardiomyocytes. Circ Res. 2003;93:221-229.

361. Hibi M, Hirano T. Gab-family adapter molecules in signal transduction of cytokine and growth factor receptors, and T and B cell antigen receptors. Leuk Lymphoma. 2000;37:299-307.

362. Watanabe S, Umehara H, Murayama K, Okabe M, Kimura T, Nakano T. Activation of Akt signaling is sufficient to maintain pluripotency in mouse and primate embryonic stem cells. Oncogene. 2006.

363. Deuter-Reinhard M, Apell G, Pot D, Klippel A, Williams LT, Kavanaugh WM. SIP/SHIP inhibits Xenopus oocyte maturation induced by insulin and phosphatidylinositol 3-kinase. Mol Cell Biol. 1997;17:2559-2565.

364. Sun H, Lesche R, Li DM, et al. PTEN modulates cell cycle progression and cell survival by regulating phosphatidylinositol 3,4,5,-trisphosphate and Akt/protein kinase B signaling pathway. Proc Natl Acad Sci U S A. 1999;96:6199-6204.

365. Sly LM, Rauh MJ, Kalesnikoff J, Buchse T, Krystal G. SHIP, SHIP2, and PTEN activities are regulated in vivo by modulation of their protein levels: SHIP is up-regulated in macrophages and mast cells by lipopolysaccharide. Exp Hematol. 2003;31:1170-1181.

366. Keller G. Embryonic stem cell differentiation: emergence of a new era in biology and medicine. Genes Dev. 2005;19:1129-1155.

367. Yoshida K, Chambers I, Nichols J, et al. Maintenance of the pluripotential phenotype of embryonic stem cells through direct activation of gp130 signalling pathways. Mech Dev. 1994;45:163-171.

368. Davis S, Aldrich TH, Stahl N, et al. LIFR beta and gp130 as heterodimerizing signal transducers of the tripartite CNTF receptor. Science. 1993;260:1805-1808.

369. Maehama T, Dixon JE. The tumor suppressor, PTEN/MMAC1, dephosphorylates the lipid second messenger, phosphatidylinositol 3,4,5-trisphosphate. J Biol Chem. 1998;273:13375-13378.

370. Erneux C, Govaerts C, Communi D, Pesesse X. The diversity and possible functions of the inositol polyphosphate 5-phosphatases. Biochim Biophys Acta. 1998;1436:185-199.

371. Pesesse X, Moreau C, Drayer AL, Woscholski R, Parker P, Erneux C. The SH2 domain containing inositol 5-phosphatase SHIP2 displays phosphatidylinositol 3,4,5-trisphosphate and inositol 1,3,4,5-tetrakisphosphate 5-phosphatase activity. FEBS Lett. 1998;437:301-303.

372. Crowley MT, Harmer SL, DeFranco AL. Activation-induced association of a 145-kDa tyrosine-phosphorylated protein with Shc and Syk in B lymphocytes and macrophages. J Biol Chem. 1996;271:1145-1152.

373. Kiener PA, Lioubin MN, Rohrschneider LR, Ledbetter JA, Nadler SG, Diegel ML. Co-ligation of the antigen and Fc receptors gives rise to the selective modulation of intracellular signaling in B cells. Regulation of the association of phosphatidylinositol 3-kinase and inositol 5'-phosphatase with the antigen receptor complex. J Biol Chem. 1997;272:3838-3844.

374. Harmer SL, DeFranco AL. The src homology domain 2-containing inositol phosphatase SHIP forms a ternary complex with Shc and Grb2 in antigen receptor-stimulated B lymphocytes. J Biol Chem. 1999;274:12183-12191.

375. Reiske HR, Kao SC, Cary LA, Guan JL, Lai JF, Chen HC. Requirement of phosphatidylinositol 3-kinase in focal adhesion kinase-promoted cell migration. J Biol Chem. 1999;274:12361-12366.

376. Geiger H, True JM, de Haan G, Van Zant G. Age- and stage-specific regulation patterns in the hematopoietic stem cell hierarchy. Blood. 2001;98:2966-2972.

377. de Haan G, Van Zant G. Dynamic changes in mouse hematopoietic stem cell numbers during aging. Blood. 1999;93:3294-3301.

378. Morrison SJ, Wandycz AM, Akashi K, Globerson A, Weissman IL. The aging of hematopoietic stem cells. Nat Med. 1996;2:1011-1016.

379. Chen J, Astle CM, Harrison DE. Genetic regulation of primitive hematopoietic stem cell senescence. Exp Hematol. 2000;28:442-450.

380. Sudo K, Ema H, Morita Y, Nakauchi H. Age-associated characteristics of murine hematopoietic stem cells. J Exp Med. 2000;192:1273-1280.

381. Muller-Sieburg CE, Cho RH, Karlsson L, Huang JF, Sieburg HB. Myeloid-biased hematopoietic stem cells have extensive self-renewal capacity but generate diminished lymphoid progeny with impaired IL-7 responsiveness. Blood. 2004;103:4111-4118.

382. Muller-Sieburg CE, Cho RH, Thoman M, Adkins B, Sieburg HB. Deterministic regulation of hematopoietic stem cell self-renewal and differentiation. Blood. 2002;100:1302-1309.

383. Henckaerts E, Langer JC, Orenstein J, Snoeck HW. The positive regulatory effect of TGF-beta2 on primitive murine hemopoietic stem and progenitor cells is dependent on age, genetic background, and serum factors. J Immunol. 2004;173:2486-2493.

384. Luo JM, Liu ZL, Hao HL, Wang FX, Dong ZR, Ohno R. Mutation analysis of SHIP gene in acute leukemia. Zhongguo Shi Yan Xue Ye Xue Za Zhi. 2004;12:420-426.

ABOUT THE AUTHOR

Caroline Desponts received a Bachelor of Science in Agriculture with a Major in Microbiology from McGill University. There, she developed her interest for research under the guidance of Drs. Brian T Driscoll and David Zadworny. She then joined an internship program at Merck Frosst Center for Therapeutic Research. There, she worked under the guidance of Dr. Axel Ducret at the development of 2-D gel electrophoresis method for the study of the effect of drug treatment on protein phosphorylation. She then worked with Dr. Ernest Asante-Appiah at the discovery of drug binding site to ensure specific inhibition of target proteins. Her contribution to different studies at this center led to four publications. Caroline then joined the Interdisciplinary PhD program in Cellular and Molecular Biology at the University of South Florida. There, she developed an interest for stem cell research and decided to pursue her graduate studies under the guidance of William G. Kerr Ph.D. While working at the H. Lee Moffitt Cancer Center and Research Institute, Caroline contributed to several studies, which led to the publication of five papers.

End Page